



UNIVERSITÀ
DEGLI STUDI
DI PADOVA



TÉCNICO
LISBOA



UNIVERSITÀ DEGLI STUDI DI NAPOLI
FEDERICO II

Università degli Studi di Padova
Centro Ricerche Fusione (CRF)

Universidade de Lisboa
Instituto Superior Técnico (IST)

Università degli Studi di Napoli Federico II

JOINT RESEARCH DOCTORATE IN FUSION SCIENCE AND ENGINEERING
Cycle XXXI

ASSESSMENT OF THE ECONOMICS OF FUSION ENERGY
AS A KEY ELEMENT OF A FUTURE SUSTAINABLE
ENERGY MIX

Coordinator: Prof. Paolo Bettini

Supervisor: Eng. Chiara Bustreo

Co-Supervisor: Prof. Paolo Bettini

Ph.D. Student: Daniele Maggio

Padova, 30/11/2018

To my grandfather Arcangelo for his 100 years,
and to my family Mauro, Margherita and Chiara

Table of contents

Riassunto	1
Abstract	3
1 Introduction	5
1.1 Global energy demand.....	5
1.2 Research and thesis work	7
1.3 Fusion energy	8
1.4 The three types of confinement and the fusion machines	18
1.4.1 Gravitational confinement.....	18
1.4.2 Inertial confinement	18
1.4.3 Magnetic confinement.....	19
1.5 Iter project	24
1.5.1 The history.....	24
1.5.2 Working progress of the ITER project	27
1.6 DEMO – the engineering machine for study the future commercial reactor	29
2 FRESCO code	31
2.1 Geometric parameter	32
2.1.1 Dimension of the component surrounding the plasma	35
2.1.2 Toroidal Field Coil stress analysis	36
2.2 Plasma electromagnetic parameter	37
2.2.1 Central solenoid parameter.....	38
2.3 Operations phases for a fusion power plant	39
2.4 Central solenoid flux evaluation.....	40
2.5 Ramp-Up phase – the rise of the plasma current.....	41
2.6 Available flux and flat top period.....	44
2.7 Heating phase	45
2.8 Burning phase.....	47
2.9 Time for the vacuum vessel pump-down	48
2.10 Cycle time, ramp-down, and central solenoid charge time	48
2.11 Electricity production for a Fusion Power Plant	49
2.12 Economic assessment.....	51
2.13 Output section.....	53
2.14 FRESCO code – results.....	59

3	COMESE code	63
3.1	The new version of COMESE code – COMESE code C++	64
3.1.1	Files structure of the COMESE code C++	67
3.2	Input file – the scenario Input file	70
3.3	Input file – the Load and Generation profile source for the data	74
3.4	Load profile	77
3.5	How COMESE uses load profile of a reference year	80
3.6	European Load profiles	81
3.7	Generation profile from real data	85
3.7.1	Generation CSP with storage normalized profile for Italy	85
3.7.2	Generation PV profile for Italy	87
3.7.3	Generation Wind onshore profile for Italy	88
3.7.4	Generation Hydro run of river profile for Italy	89
3.7.5	Comparison of Generation normalized profile for Italy	90
3.7.6	Example of scaled Generation profile	91
3.8	Generation profiles for technology with different capacity factor	92
3.9	Generation profiles for European Country	94
3.9.1	European photovoltaic generation normalized profiles	94
3.9.2	European Wind onshore generation - normalized profiles	96
3.9.3	European Wind offshore generation - normalized profiles	98
3.10	Load and generation profile comparison for United Kingdom in different years	99
3.10.1	Comparison of Load normalized profile for United Kingdom	100
3.10.2	Comparison of Photovoltaic generation normalized profile for United Kingdom	100
3.10.3	Comparison of Wind onshore generation normalized profile for United Kingdom	100
3.10.4	Comparison of Wind offshore generation normalized profile for United Kingdom	101
3.11	Generation profile from assumption – Fusion power plant profile	101
3.12	Input file – the power plant technology data	103
3.13	Input file – the storage technology data	107
3.14	Storage system model	109
3.14.1	Charging and discharging process	110
3.14.2	Optimization method for the discharge process	110
3.14.3	Storage optimization method with activation of dispatchable technologies	111
3.15	Optimized flexible technology activation.	112
3.15.1	Common activation routine - CMOD	113

3.15.2	Power – hour deficit routine - PHDEF	114
3.15.3	Trapezoidal activation - TRP.....	115
3.16	Curtailement.....	117
3.17	Demand and generation.....	118
3.18	LCOTE and SLCOTE	120
3.19	LCOTE calculation: extra cost due to the battery storage system.....	121
3.20	Future improvement for COMESE code C++.....	123
4	Simulation of European scenarios with COMESE.....	125
4.1	The economic analysis with COMESE code.....	128
4.2	Assessment of the economics of fusion technology.....	130
5	Conclusion.....	131
6	Reference.....	133

Riassunto

Per poter valutare, dal punto di vista economico, in quali condizioni la tecnologia da fusione può essere un elemento chiave di un sistema di generazione elettrica futuro, è indispensabile disporre di strumenti di calcolo adeguati, in grado di simulare in modo semplice un reattore a fusione calcolando il costo di generazione, un sistema energetico, composto da differenti centrali elettriche, e di valutare per il sistema il costo medio di generazione.

Il lavoro di tesi inizia con la presentazione del codice di calcolo FRESCO (Fusion REactor Simplified COst): un codice sviluppato in linguaggio C++ che mira a modellare in modo semplificato un reattore a fusione basato sulla configurazione tokamak. FRESCO permette di calcolare i parametri geometrici, fisici ed ingegneristici di una centrale a fusione e di effettuare un'analisi economica valutando il costo di generazione. Come lavoro sono presentati prima i miglioramenti introdotti in FRESCO, come il modello del sistema di pompaggio per la camera da vuoto del reattore e l'integrazione tra il codice FRESCO ed un programma di ottimizzazione basato sugli algoritmi genetici. Sarà poi descritto lo studio condotto per capire come gli intervalli operativi di un reattore a fusione possono influire sul costo di generazione, accompagnato dall'ottimizzazione di questi intervalli per ottenere il minimo costo di generazione.

Nella seconda parte della tesi è presentato nel dettaglio il codice di calcolo COMESE C++ (COsto MEDio del Sistema Elettrico): un codice realizzato durante il lavoro di tesi allo scopo di avere uno strumento per lo sviluppo di nuovi scenari energetici. In particolare scenari che possano evidenziare come la tecnologia della fusione nucleare possa fare parte del parco di generazione elettrica. Il codice di calcolo COMESE C++ utilizza i dati della domanda elettrica e della generazione di un Paese, assieme ai dati delle tecnologie e dei sistemi di accumulo, per poter simulare uno scenario energetico. Esso permette di valutare se la generazione ipotizzata riesce a soddisfare la domanda, e in quel caso calcola il costo medio di generazione dello scenario, avendo la possibilità di eseguire un'analisi stocastica basata sul metodo Monte Carlo, per tenere conto dell'incertezza sui parametri economici delle tecnologie di generazione.

Il codice COMESE C++ è stato utilizzato per definire due scenari energetici europei 100% rinnovabili: uno per il Nord Europa basato sulla tecnologia di generazione eolica e uno per il Sud Europa basato sulle tecnologie di generazione fotovoltaiche. Partendo da questi scenari di riferimento sono poi stati sviluppati nuovi scenari con la tecnologia da fusione, ed è stata fatta un'analisi per determinare il costo di investimento di centrali elettriche a fusione tale da rendere competitiva la tecnologia e ridurre il costo medio di generazione di uno scenario energetico.

Abstract

In order to be able to evaluate, from an economic point of view, under which conditions fusion technology can be a key element of a future electricity generation system, adequate calculation tools are needed to simulate a fusion reactor in a simple way and calculate the cost of electricity generated. Other tools are required to simulate an energy system, composed of different power plants, and to evaluate the system cost of electricity.

The thesis work begins with the presentation of the FRESCO code (Fusion REactor Simplified COst): a code developed in C ++ language with the aim to model in a simplified way a D-T fusion power plant based on the tokamak configuration. In FRESCO the power plant is studied from a technical and an economical point of view. It allows the users to calculate reactor parameters i.e. geometrical and physical dimension of the power plant, electromagnetic parameters of the machine, net electricity production, auxiliary energy needed, the operative cycle phases (especially for the pulsed configuration), and not last, the related capital cost and the cost of electricity. As part of the thesis work, the improvements introduced in FRESCO are presented first, such as the model of the reactor chamber vacuum pumping system, and the integration between the FRESCO code and an optimization program based on genetic algorithms. Then, the analysis of the effects of the duration of the operative phases in a pulsed power plant on the cost of electricity is presented.

In the second part of the thesis, the COMESE code (COsto MEDio del Sistema Elettrico, Average Cost of the Electric System) is described. The code developed as a part of the doctoral research activities, is used to develop and test energy scenarios. In particular, scenarios that can show how nuclear fusion technology can be part of the electricity generation park. The COMESE C ++ calculation code uses the electricity demand and generation data of a country, together with the data of the technologies and storage systems, in order to simulate an energy scenario. It allows to evaluate if the hypothesized generation succeeds in satisfying the demand. In that case, it calculates the levelized cost of timely electricity (LCOTE) for the scenario. It also offers the possibility to perform a stochastic analysis, based on the Monte Carlo method, in order to take into account the uncertainty on the economic parameters of generation technologies.

An application of the COMESE C ++ code is presented. Two fully renewable European energy scenarios, one for Northern Europe based on the wind generation technology and one for Southern Europe based on photovoltaic generation technologies, are studied and compared. Alternative scenarios including fusion technology were developed, in order to estimate which economic conditions (overnight cost) fusion power plants can be competitive and bring a benefit to the levelized cost of timely electricity of an energy scenario.

1 Introduction

In this chapter, after a description of world energy problems, it is introduced the research work and the objectives at the bases of the research and of the thesis work, then the key concepts of nuclear fusion as an energy source for the future are presented. Will be given an overview of the ITER project, and its objective: to verify from the point of view of physics the feasibility of the magnetic configuration for the future Tokamak fusion reactor. Magnetic configuration that will be used in the next DEMO, engineering machine, which starting from a physical configuration will allow the study of the first true fusion reactor prototype. At the end of the chapter the characteristics for the future commercial reactor will be described and the two ideas of continuous and pulsed power plant.

1.1 Global energy demand

The current world energy system faces now and it will faced in the next years a series of challenges constantly in evolution. The Young leader on Energy and Sustainability, YES group, a unique European organization led by young professional in energy and students working on energy subjects, has made an European survey on energy that it revealed like the force that will shape the future of energy is the climate change. The Mauna Loa Observatory in Hawaii registered in April 2017 a peak of concentration of carbon dioxide (CO₂) greater than the threshold of 410 ppm. The highest level reached in the last 800,000 years. In relation to the problem of climate change, the interest in renewable energy technologies has been constantly growing all over the world in the last years. New studies are constantly emerging, bearing witness to the global interest in the energy subject characterized by a rapid evolution.

The 2017 World Energy Outlook reports four “large-scale shift” that will be the key factors of the future energy development. One is the rapid deployment of the renewable technologies like photovoltaic and wind, accompanied to a decreasing on installation and generation costs. These aspects will lead to changes in the way of producing energy from all the nations of the world. From 2010 to now the photovoltaic cost is drop by 70%, wind technologies costs drop by 25% and batteries costs drop by 40%. This is accompanied with the increasing of the electricity penetration with respect to the primal energy consumption. In the international energy scenario it is clear the role of China whose decisions weighed by the growing energy demand will concretely shape the way of producing electricity. Political slogan for an "energy revolution" and a "fight against pollution" is spreading in China and the transition to a tertiary-based economic model is shifting the energy sector to a new direction which will influence the entire world energy system.

According to WEO 2017 the grow of the renewable energy will determine the progressive phase out of coal from electricity production, also in relation to the absence of developments in carbon capture storage technologies (CCS). The WEO 2017 describes that since 2000, the generation of coal electricity has grown by almost 900 gigawatts (GW), but the net additions expected from today to 2040 will be only 400 GW and many of these are plants already under construction. In parallel with renewable energies, the use of natural gas as a flexible energy source will grow, and energy efficiency measures will increase. Thanks to the development of energy efficiency technologies (low consumption light bulbs and LEDs, increase in the efficiency of household appliances), the energy efficiency measures have already been able to reduce the growth of energy requirements in the last

years. And it has allowed the developed countries to maintain their stable energy consumption for some years now.

The spread of renewable power plants characterized by irregular production requires the accumulation of energy and in the recent years there is a progressive increasing in funding for research in this field. At the same time the interest in the energy issue is so high for pushing the research for new energy sources able to sustain the economy and the life of the world in the future.

As regards to oil consumption the demand grows until the 2040, even if at a steady decline. From the point of view of fossil fuels, a key role will play the exploitation of the “shale gas” and the “tight oil” especially in the USA. The outlook for nuclear power has decreased compared to previous WEO forecasts. China continues to drive a gradual increase in nuclear fission power generation, and is expected to surpass the United States by 2030 to become the largest nuclear-based producer of electricity. From the point of view of the transport and vehicles the electric mobility is growing.

The European Union has adopted the Energy Roadmap 2050 with the intention to guide the European Countries in the field of the energy to reduce the greenhouse gas emission to 2050. The Energy Roadmap 2050 fixed to the 2050 a reduction by 80% of energy related greenhouse gas emission below 1990 levels. Goal that cannot be achieved without a 95% to 100% decarbonized power sector. For this purpose energy scenarios of all European countries are used to demonstrate possible solutions to be adopted.

In the field of research on alternative energy sources, Europe is active in the research for controlled thermonuclear fusion. A strategic energy source that can play a key role in the future generation of electricity, at European and global level.

With respect to the other sources of energy, the controlled thermonuclear fusion it is characterized by:

- High availability of uniformly distributed fuel throughout the planet. (Deuterium is in sea water, tritium can be obtained from lithium)
- No greenhouse gas emissions; the reaction products are helium (inert gas) and high energy neutrons that are used for tritium production.
- Reduced production of radioactive or activated materials; the tritium used in the reaction is radioactive but with a decay time of 12 years, the structures activated by the neutrons would have a decay of 100 years. Significantly lower times when compared to the decay time of the waste nuclear power plants (order of magnitude 100,000 years).
- High degree of intrinsic safety: the reaction is maintained from the outside and requires special conditions. Without these conditions the reactions end and the reactor switches off.
- No risk of proliferation for atomic weapons.
- It can replace the base power plant production currently covered by fossils and fission nuclear energy.

However the fusion power plant goal requires now significant investments in the research that can only be made at the public level to overcome many technological challenges (new materials, new measurement systems and diagnostics operating in extreme conditions, new technologies for heating the plasmas)

1.2 Research and thesis work

The activities presented in the thesis have been carried out within a research project on Fusion energy and energy scenarios. As explained in the previous paragraph, the world energy system will have to face increasingly pressing energy issues over the years linked to the problem of climate change. In particular, it will become increasingly important to look for an answer to the question: “How to produce energy in a sustainable way in the years to come?”. The research tool available to answer this question is based on energy scenarios, a set of hypotheses that aims to highlight a possible way to meet the energy needs in the next 10-20 years (short-term horizon) or even by the end of this century (long-term horizon).

That of energy scenarios is a wide subject of study, as there are many variables at stake in a sector that is constantly being updated. In this context they become fundamental the tools able to discern from all the energy scenarios those that can satisfy certain requirements. Like that of the lower generation cost described by the System Levelized Cost of Timely electricity SLCOTE.

The doctoral activities begun with an in-deep study of the fusion technology itself as a possible future Fusion Power Plant and the enhancement of the FRESKO code, (Fusion REactor Simplified COst), a code that models in a simplified way a D-T fusion power plant based on the tokamak model. With the intention to increase familiarity with this new technology from an economic point of view and to understand with what expedients it is possible to reduce the cost of generation in a hypothetical future power plant. Specifically, studies have been carried out to assess how the operational phase of a pulsed power plant can influence the cost of electricity.

Than moving from a single technology to the energy system, a wide activity has started on the implementation of computer tool for the development and analysis of energy scenarios. With the aim of setting up a flexible tool, because the subject of the energy sector is constantly in evolution, the COMESE, an excel spreadsheet used to perform energy systems simulations, has been converted in a much more flexible C++ code and then enhanced so to produce or simulate scenarios of any country, considering all the possible energy technologies and energy storage systems included.

With the upgraded COMESE C++ and the technical and economic assessments preformed with FRESKO, it will become concrete the possibility to study energy scenario with and without fusion, compare the different scenarios and study the best solution from the economic point of view.

1.3 Fusion energy

In order to understand the nuclear fusion reaction, a few key concepts are briefly recalled. From the concepts of atomic structure and mass defect, we move on to the definition of the two fissions and fusion nuclear processes, listing for the latter the main reactions and characteristics, confinement methods and some experiments currently in operation.

The atom consists of a nucleus of positive charge, on which most of the mass is concentrated, and of negatively charged electrons that orbit around it. The nucleus in turn is formed by nucleons: the protons positively charged and neutrons without charge, both of similar mass.

$$(1.1) \quad m_p \approx m_n = 1.67 \times 10^{-27} \text{ kg}$$

Every atom is naturally neutral: the charge of the protons is balanced by an equal charge born by the electrons of mass:

$$(1.2) \quad m_e = 9.11 \times 10^{-31} \text{ kg}$$

The charge possessed by a proton is equal and opposite to that of an electron and equal to the fundamental electric charge q .

$$(1.3) \quad q = 1.66 \times 10^{-19} \text{ C}$$

Every atom in nature is identified by the mass number A which indicates the number of nucleons in the nucleus, and the atomic number Z which indicates the number of nucleus protons. Experimentally it has been verified that there is a difference, call the mass defect, between the real mass $m_{atom_{REAL}}$ of an atom and the theoretical mass $m_{atom_{TH}}$ that can be determined as the sum of the masses of its components.

$$(1.4) \quad m_{atom_{TH}} = Z \times m_p + (A - Z) \times m_n$$

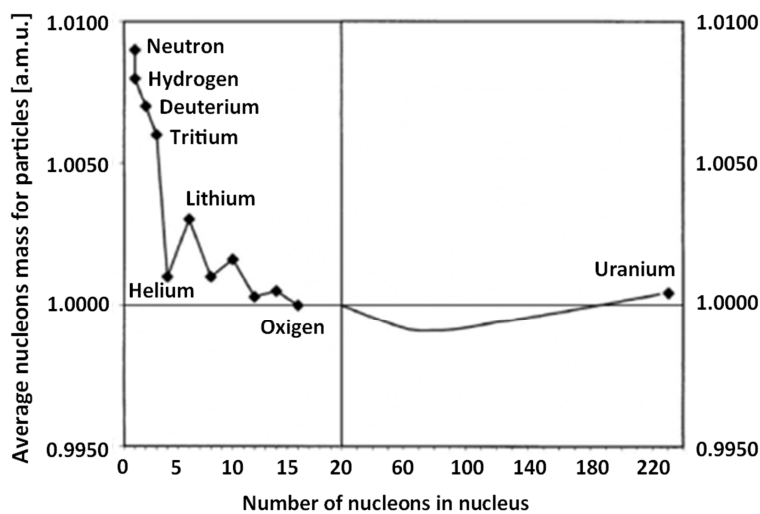


Figure 1-1: diagram that describes the average mass of the nuclides express in atomic mass unit for different atoms in function of there mass number. (Number of nucleons in nucleus)

This mass defect has been observed for all natural and artificial elements. Figure 1-1 summarizes for various elements the trend of the average mass of the theoretical nuclide of the atoms as a function of its mass number. Where the mass of the theoretical nuclide is obtained by dividing the real mass of the atom by the corresponding mass number and it is expressed in units of atomic mass ($1 \text{ amu} = 1.66 \times 10^{-27} \text{ kg}$).

$$(1.5) \quad m_{\text{nuclide}_{TH}} = \frac{m_{\text{atom}_{REAL}}}{Z \times m_p + (A - Z) \times m_n} [\text{amu}]$$

In Figure 1-1 we see that heavy atoms with many protons and neutrons in the nucleus have a lower average nuclide mass, while light atoms such as lithium or helium are higher. This difference in mass present for all natural and artificial atoms (equation 1.7) is explained with Einstein's mass energy equivalence:

$$(1.6) \quad E = m \cdot c^2$$

The loss of mass observed with the increase in the number of nuclides corresponds to the formation of strong nuclear bonds, which are able to keep the nucleus joined by winning the electrostatic repulsion forces.

$$(1.6) \quad \Delta m = [Z \cdot m_p + (A - Z) \cdot m_n] - m_{\text{real}} \text{ (mass defect)}$$

$$(1.7) \quad E_b = \Delta m \cdot c^2 = [Z \cdot m_p + (A - Z) \cdot m_n - m_{\text{real}}] \cdot c^2 [\text{J}] \text{ (binding energy)}$$

$$(1.8) \quad \frac{E_b}{A} = \frac{[Z \cdot m_p + (A - Z) \cdot m_n - m_{\text{real}}] \cdot c^2}{A} \left[\frac{\text{J}}{\text{nucleon}} \right] \text{ (binding energy per nucleon)}$$

Although the mass differences involved are small, the multiplicative constant $c^2 = 9 \cdot 10^{16} [\text{m}^2/\text{s}^2]$ is so high that the corresponding energy is a considerable amount. In order to highlight this fact, just think that: 1 gram of matter corresponds, according to the mass-energy equivalence, to $9 \cdot 10^{13} \text{ J}$ of energy, equivalent to the energy contained in about 2140 tons of oil.

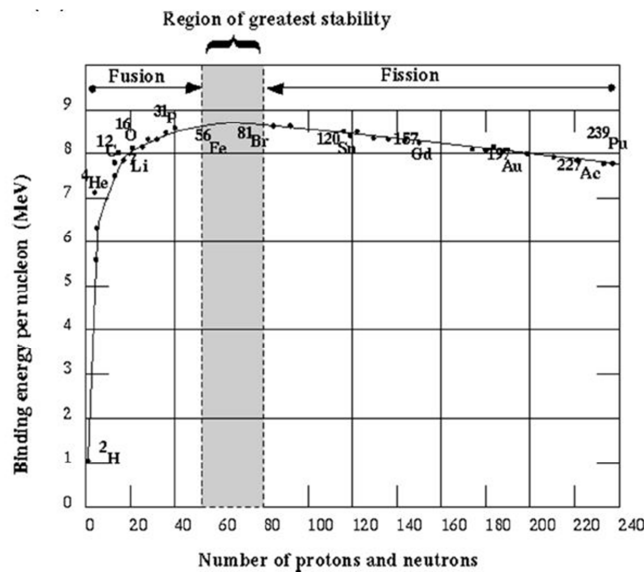
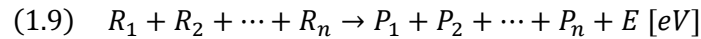


Figure 1-2: Binding energy per nucleon function of the mass number of the atoms

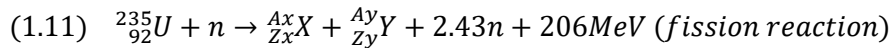
Figure 1-2 shows the trend of the average bond energy per nucleon (E_b/A [MeV/nucleons]) as a function of the corresponding mass number. The elements with a higher binding energy and therefore greater stability are placed at an intermediate atomic mass value around the atomic mass of the iron-nickel. Light or heavy atoms have weaker nuclear interactions than those of intermediate atoms, so it is easy to trigger nuclear reactions that yield more stable nuclei. This transition from light to heavy nuclei to stable intermediate nuclei is accompanied by a release of energy derived from the difference in mass between products and reagents. In general, by indicating with R the reactants and P the products a generic nuclear reaction can be represented with the following equations:



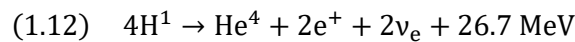
In which E, energy released by the reaction corresponds to:

$$(1.10) \quad E \equiv [(m_{R1} + m_{R2} + \dots + m_{Rn}) - (m_{P1} + m_{P2} + \dots + m_{Pn})] \cdot c^2 (\sim \text{MeV})$$

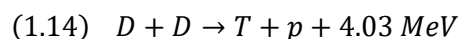
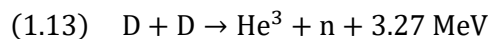
A first group of nuclear reactions that exploits the mass defect to obtain energy are those that divide, fission, heavy nuclei to obtain smaller nuclei than the initial nucleus. This process is exploited in nuclear fission reactors where a nucleus of uranium 235 is bombarded with a thermalized neutron ($T = 0.025\text{eV} = 290\text{K}$) producing fission products with a mass number between 70 and 170 and releasing on average 2.43 fast neutrons (exploited for the subsequent chain reaction) together with an average energy of 206 MeV, 0.88 MeV per nucleon of the initial uranium atom. This reaction uses as a "projectile particle" a neutron that doesn't need an high level of energy to approach the nucleus and fission it. Macroscopically, the energy released by a fission reaction corresponds to $84 \cdot 10^6 \text{ MJ} / \text{kg}$ of burning fuel. Around 106 times greater than the energy related to the calorific value of the diesel fuel equal to $40\text{MJ} / \text{kg}$.



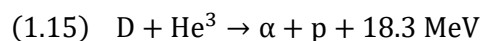
The second group of exothermic nuclear reactions join, "make a fusion", light nuclei to obtain heavier nuclei but with mass always less than the sum of the initial reactants. In general, the elements involved in this type of reaction are hydrogen isotopes (deuterium and tritium), helium and lithium. Example of a natural fusion reaction is the proton-proton cycle that occurs constantly in the sun, where hydrogen nuclei merge, releasing energy and producing helium and neutrons. Equation 1.12 shown the solar fusion reaction.



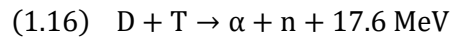
A first pair of fusion reactions that is of particular interest for artificial realization is that between Deuterium atoms:



Both reactions are equally likely to occur and constitute the optimal reaction for a future nuclear fusion reactor, involving non-radioactive elements available in large quantities. To these they are added the reaction of deuterium with the three isotope of helium.

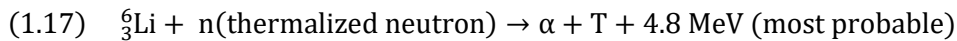


And the Deuterium Tritium (D-T) reaction with a 50% mixture of both gases.



Observing the reactions from the fuel point of view: deuterium is widely available in nature and is uniformly distributed, unlike uranium, rare and with mines strongly localized in a few countries. Deuterium is found in sea water in a concentration of 1 atom to 6700 of hydrogen (30g / ton of sea water). Based on current consumption, deuterium natural stock would be enough to run fusion reactors for a period of 2 billion years.

Tritium is not available in nature having a half-life of 12 years, but it can be obtained from fertilization reactions (equations 1.17 and 1.18) starting from lithium which is present in nature with two isotopes ${}^6\text{Li}$ (7.5%) and ${}^7\text{Li}$ (92.5%). The first one is the most useful isotope, because it reacts with thermalized neutrons and releases energy; unfortunately, it is the isotope with the less concentration in nature. In a future fusion reactor, the neutrons produced by the fusion reactions and coming out from the reactor, they will encounter a lithium blanket, and can sustain the fertilization reactions with lithium producing the tritium. Then, tritium will be extracted and used inside of the fusion power plant in a closed cycle, the fusion power plant will produce the fuel for its operation. It is estimated that the low-cost lithium reserved on earth would be sufficient (based on current energy consumption, and on the deuterium tritium reaction) for a period of 20,000 years. But this value will be lower than expected, because the lithium is also used for the batteries that are the principal antagonists in the use of lithium.



The third element He^3 is rare and, excluding the other fusion reactions, cannot be directly obtained. A great availability of He^3 would allow a much more energetic reaction of the D-T to be exploited. To better understand the amount of energy released by the fusion reactions, and the advantage of exploiting this energy source, in Table 1-1 all the fusion reactions are compared with the previous fission reaction. Nuclear fusion reactions release more energy than the fission reaction, particularly those between deuterium and helium 3 or tritium, nor release more than four times. This comparison can also be made on the bond energy curve as shown in Figure 1-3.

Table 1-1:Energy released from the principal fusion reaction.

Nuclear reaction	Energy			
	[MeV]	[MeV/nucleon]	10^6 [MJ/kg]	% respect the fission energy
Fission U_{235}	206	0.88	84	100
$D+D \rightarrow \text{He}^3+n$	3.27	0.82	78	93
$D+D \rightarrow T+p$	4.03	1.01	96	114
$D+ \text{He}^3 \rightarrow \alpha+p$	18.3	3.66	351	418
$D+ T \rightarrow \alpha+n$	17.6	3.52	338	402

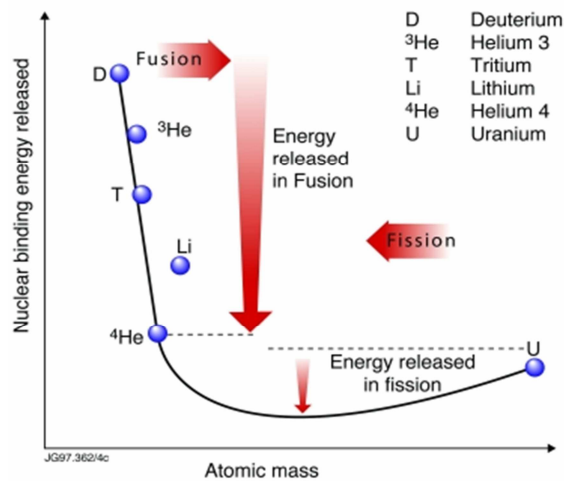


Figure 1-3: diagram that graphically shows the comparison in energetic terms between fusion and fission reaction

In order to make the nuclear fusion reactions happen, the nuclei of the particles involved in the reactions must be brought to a distance comparable with the nuclear diameter (order of magnitude $10^{-15}m$). At this distance the Colombian interactions between charged nuclei are so intense to reduce the probability of collision. This is the reason why the particles must be brought to high temperature, in that condition the particles have a speed high enough to be able to overcome the electrostatic repulsion and reach the region where the forces of strong nuclear attractions overcome repulsive Coulomb interactions, allowing the fusion of the two particles. According to the classical theory, the Colombian barrier is defined as the distance limit between the centers of the nuclei, after that the attractive nuclear interactions win the repulsive electronic ones. Note this distance indicate here as r_m it is possible to calculate the W energy that must have the particle to overcome the barrier:

$$(1.19) \quad W = \frac{Z_1 Z_2 e^2}{4\pi\epsilon_0 r_m} \text{ [eV]}$$

Where Z_1 and Z_2 indicate the atomic numbers of the particles involved, " e " is the elementary electric charge and r_m the Colombian barrier. For a Deuterium-Tritium reaction the two nuclei have the same atomic number, the Colombian barrier is of the order of $5 \cdot 10^{-15} m$ so the energy of the Coulomb barrier is $W = 288keV$. Knowing that $1eV$ corresponds to about $11600 K$, $288keV$ corresponds to about 3.4 billion K a temperature much higher than the temperature inside our sun (internal temperature of the sun $1.57 \cdot 10^7 K$).

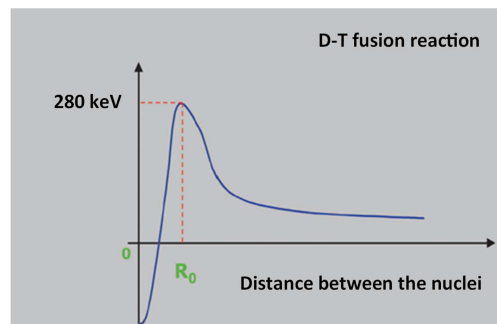


Figure 1-4: Electric potential energy of the particles function of the distance between the two nuclei and Coulomb barrier for a D-T fusion reaction

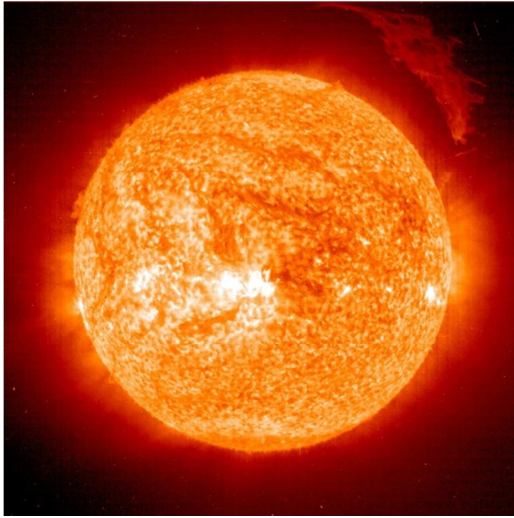


Figure 1-5: The sun

Table 1-2: Main data for the Sun

Main data for the Sun	
Surface	$6,0877 \times 10^{18} \text{ m}^2$
Volume	$1,4122 \times 10^{27} \text{ m}^3$
Mass	$1,9891 \times 10^{30} \text{ kg}$
Average density of the sun	$1,408 \times 10^3 \text{ kg/m}^3$
Average density of the nucleon	$1,5 \times 10^5 \text{ kg/m}^3$
Surface temperature	5777 K
Nuclear temperature	$\sim 1,57 \times 10^7 \text{ K}$
Gravity acceleration at the surface	274.0 m/s ² (27.94g)

In reality, to trigger the fusion reaction, it is not necessary a temperature of billions of degrees, the literature gives reference to 150 million K. To understand well what are the conditions for which the reaction occurs we must define the probability that two nuclei interact to give a fusion reaction. This is defined by the fusion cross section σ . If we consider a reaction between Deuterium and Tritium, and we assume that Tritium nucleus is the target and the Deuterium nucleus is the projectile equipped with a velocity v (as seen in Figure 1-6), the cross section can be seen as a circular surface centered in the target nucleus, if the deuterium atom passes through the surface, the fusion reaction takes place; if it goes out, the reaction does not occur. For nuclear fusions the cross section has a size of the order of magnitude of a nuclear diameter. In particular, it is measured in barn.

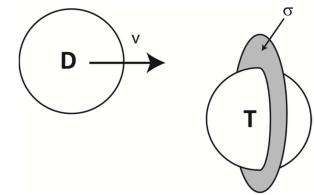


Figure 1-6: D-T collision, and cross section σ

$$(1.20) \quad 1 \text{ barn} = 10^{-28} \text{ m}^2$$

Figure 1-7 shows the trends of the fusion cross section for the main nuclear fusion reactions, the cross section is function of the kinetic energy of the particles involved. It should be noted that a correct evaluation of the fusion cross section must also take into account the quantum effects not considered by the classical theory. In particular this involves three effects:

- Even if a particle has an energy lower than the energy of the Coulomb barrier, it can still give rise to a fusion reaction, this effect is called tunnel effect.
- A particle with an energy higher than that of the Coulomb barrier may not give fusion reaction, due to the high velocity of the particles, the interaction time would not be sufficient to allow the reaction.
- Under certain conditions, the relative velocities of the particles are able to give rise to a resonance effect which increases the probability of a reaction.

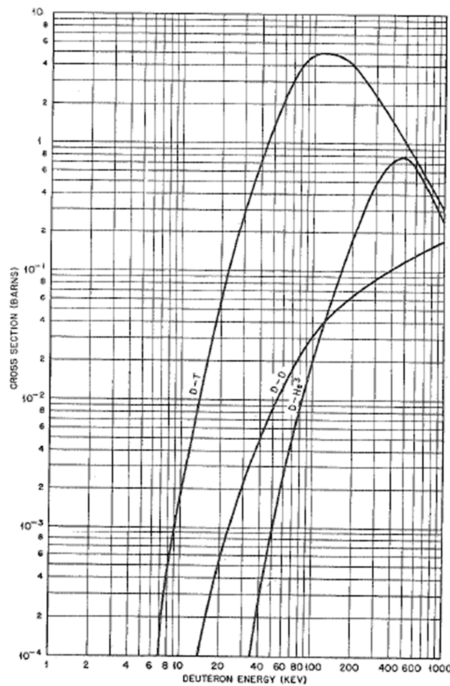


Figure 1-7: fusion cross section for the principal fusion reaction: D-T, D-D, D-He³

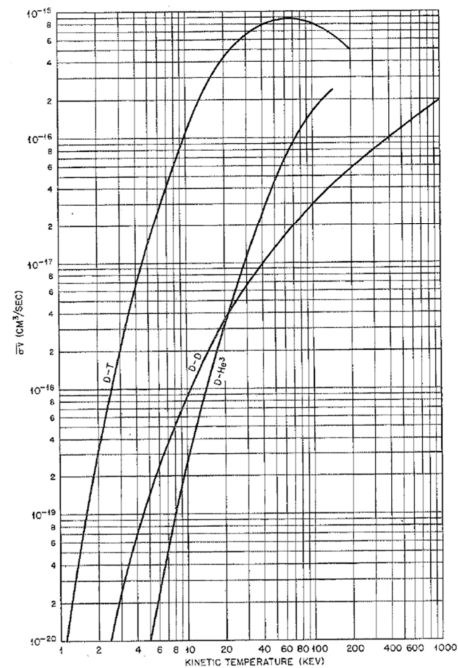


Figure 1-8: Trend of $\langle \sigma v \rangle$ for the principal fusion reaction: D-T, D-D, D-He³

Looking the diagram Figure 1-7 and considering the tunnel effect, it is possible to see that among of the three reactions, the "easiest" one to trigger is the reaction between Deuterium and Tritium. This reaction has a fusion cross section greater than the others for the same temperature.

The Deuterium-Tritium (D-T) is the reaction chosen for the first generation of fusion power plant. Although it involves the tritium that is a radioactive element not present in nature, it is the easiest to trigger and that allows to release a good amount of energy. The Deuterium-Helium³ (D-He³) reaction is not considered as a reaction useful for a fusion power plant because it is the more difficult to trigger and it uses He³ as fuel, element with a very low availability in nature. This does not exclude that it can still take place inside a deuterium reactor as a secondary reaction. Finally, the reaction between deuterium-deuterium, even if it does not constitute the immediate objective for a first generation of fusion power plant, it is the final objective for the second generation of fusion power plant. Since using only deuterium as fuel permits to eliminate tritium radioactive and increases the reserves of fuel, the reserve estimated for deuterium is higher than those of lithium. From here on, reference is made to the deuterium-tritium reaction. As it has been said in order to make the fusion happen, the reactants must be brought to high temperatures, i.e. they must have a high kinetic energy, and so being in the plasma state. Nor does it follow that the main objective of fusion research is to achieve a permanently confined plasma with the temperature and density characteristics suitable for the reaction. It is the condition that prevents the use of a traditional solid wall, because it is not able to contain a plasma that, with the simple contact, would lose the desired characteristics. Before describing in detail the structure of the machines that are based on this principle, we introduce the equation describing the thermonuclear power, the gain factor Q and the Lawson criterion and the triple product used to describe the optimal conditions to have the fusion reaction in a plasma.

It is possible to demonstrate, and for this we refer to the literature, that the thermonuclear power released by a fusion reaction can be evaluated with equation 1.21.

$$(1.21) \quad P_{th} = n_D n_T \langle \sigma v \rangle E_{th}$$

$$(1.22) \quad R_{12} = n_D n_T \langle \sigma v \rangle \text{ (reaction rate)}$$

Where with n_D and n_T are respectively the density of deuterium and tritium present in the mixture, $\langle \sigma v \rangle$ the weighted average on the distribution of velocity of the particles of the product between the fusion cross section and the particle velocity (see Figure 1-8 for the value), and with E_{th} the energy released by the single fusion reaction, which in the case of the D-T reaction is $E_{th} = 17.6 \text{ MeV}$. R_{12} , it indicates the reaction rate or how many reactions take place in a given volume of plasma. The maximum thermonuclear power is obtained when the mixture of the two fuels deuterium and tritium is at 50%, in these condition $n_D = n_T = \frac{1}{2}$, which allows to rewrite the equations 1.21 and 1.22 as:

$$(1.23) \quad P_{th} = \frac{1}{4} n^2 \langle \sigma v \rangle E_{th} = R_{12} E_{th}$$

$$(1.24) \quad R_{12} = \frac{1}{4} n^2 \langle \sigma v \rangle \text{ (reaction rate)}$$

The energy generated by the fusion reaction is contained in the kinetic energy of the fusion products, in the case of the deuterium tritium reaction in the alpha particles and in the neutrons. Observing that, the final energy and the momentum of the system after the fusion are greater than those of the reagents, and assuming that the released energy is distributed in the particles produced inversely proportional to the mass ($m_\alpha \cong 4m_n$), the energy can be divided as follows:

- E_α energy possessed by the α particle is 3.5 MeV
- E_n energy owned by the neutron is 14.1 MeV

and the total thermonuclear power results:

$$(1.25) \quad P_{th} = P_\alpha + P_n$$

$$(1.26) \quad P_\alpha = \frac{1}{4} n^2 \langle \sigma v \rangle E_\alpha$$

$$(1.27) \quad P_n = \frac{1}{4} n^2 \langle \sigma v \rangle E_n$$

Between the two products of the deuterium tritium reaction, only the alpha particle has the charge, while it is the neutron that carries the greatest amount of energy (about four-fifths). This plays a key role in the design of the future fusion power plant, and in particular of a reactor based on magnetic confinement. Of the total power produced by a thermonuclear reaction, if the magnetic fields are used to confine the plasma, only one-fifth of the total power produced can be captured by the magnetic fields and used to maintain the temperature of the reaction plasma. The remaining one comes out transported by the neutrons and can be exploited to obtain thermal energy which, through thermodynamic cycles, allows to obtain electric energy. Considering all the voices of power loss associated with the radiations emitted by a plasma, it can be shown that an external power supply is

necessary for maintaining the plasma at the temperature conditions required by the fusion. This external power indicated here as P_{ext} allows to define the gain factor Q (1.28), the ratio between the thermonuclear power released by the reaction and the power supplied from outside to trigger it.

$$(1.28) \quad Q = \frac{P_{th}}{P_{ext}}$$

Thanks to the gain factor, three operating conditions are identified:

- $Q = 1$ Breakeven: it indicates the condition in which the thermonuclear power equals the external power (only from the thermal point of view). This operating condition does not guarantee to have an equivalence of the electric power used and produced because it is not considered the efficiency.
- $Q \rightarrow \infty$ Ignition: all the power to maintain the plasma temperature in the fusion conditions is provided by the reaction itself. It is said that the reaction is self-sustaining.
- $Q > 1$ (*ES*: $Q \approx 10$) is the goal of the project of a fusion reactor: to have a surplus of power produced that allows to obtain an effective gain respectively to the external power given.

Considering the effects of yield η and starting from the hypotheses of:

- neglecting the confinement of the α particles, all the thermonuclear power exits the reactor;
- neglecting the losses due to synchrotron and line core radiation;
- do not supply any electrical power to the additional heating systems, and derive the power for maintaining the reaction directly from the thermonuclear power produced;

the following function is obtained:

$$(1.29) \quad n\tau_e = \frac{3kT}{\frac{\eta}{1-\eta} \frac{1}{4} \langle \sigma v \rangle E_{th} - b\sqrt{T}}$$

which binds three key parameters of a fusion plasma:

- n density of fuel particles
- T temperature, index of the kinetic energy possessed by the same particles
- τ_e energy confinement time, that is the time in which a plasma is able to maintain the absorbed energy.

In the equation 1.29, b is the coefficient describing the Bremsstrahlung radiation losses and k is the Boltzmann constant. Figure 1-9 shown the graph of the function 1.29, this function has a minimum value, the condition in which the power produced by the system equals the power supplied by external systems. This point is the so-called breakeven point.

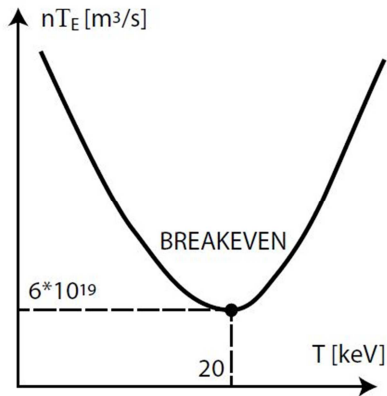


Figure 1-9: Q=1, Breakeven

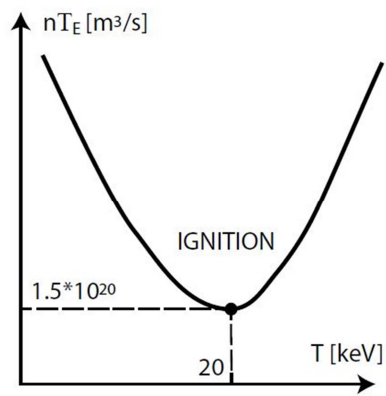


Figure 1-10: Ignition condition

If the same approach used for equation 1.29 is extended to the ignition condition, assuming that:

- only the alpha particles are confined to the system (neutrons exit to the system)
- no external power will be given to the reactor

It is possible to obtain a function equal to the previous one, but for the ignition condition:

$$(1.30) \quad n\tau_e = \frac{3kT}{\frac{1}{20} \langle \sigma v \rangle E_{th} - b\sqrt{T}}$$

Also the function 1.30 has a minimum, represented schematically in Figure 1-10, this point is the optimal point for obtaining the ignition of a plasma. From the values that describe this point:

- $T = 20 \text{ keV}$
- $n\tau_e = 1.5 \cdot 10^{20} \text{ m}^3/\text{s}$

The equation for the triple product is obtained:

$$(1.31) \quad n\tau_e T = 3 \cdot 10^{21} [\text{m}^{-3} \cdot \text{s} \cdot \text{keV}]$$

Given two of the three parameters, the triple product allows us to define the third one for the optimal conditions of ignition. So given two parameters, the third parameter to be determined is the goal that should be reached for having the best conditions of ignition.

1.4 The three types of confinement and the fusion machines

The scientific challenge of fusion is to make the nuclear reaction take place between deuterium and tritium, that is to succeed in confining a quantity of plasma with sufficient density, for a sufficiently long time and at a temperature able to trigger the fusion reaction ($T \approx 150$ million degrees). These three conditions (described in the triple product 1.31) require special confinement methods able to keep the plasma isolated from all the physical containment structures. In fact, any contact with the walls would result in the loss of the three desired characteristics and the shutdown of the machine. Three methods are currently known for effectively confining a high energy plasma:

- Gravitational confinement.
- Inertial confinement.
- Magnetic confinement.

1.4.1 Gravitational confinement

The first method of confinement, gravitational, is the one which occurs in all the stars. Here, the high mass (see Table 1-2) produces a gravitational field of great intensity, about 28 times the acceleration of gravity of the earth, which is able to effectively confine the plasma and to maintain the conditions of ignition that allow the nuclear fusion to support itself. This method is not physically feasible on earth because it cannot have a mass equal or superior to that of the sun, and for this reason, confinement methods are being studied that exploit alternative principles.

1.4.2 Inertial confinement

The first method that can be implemented is inertial confinement. Its origin comes from studies on the hydrogen bomb (H bomb), where the high temperatures generated by a nuclear fission bomb (driver) allow to obtain in an uncontrolled way the fusion reaction. With the inertial confinement studies, it is proposed to replace the H-bomb driver (the nuclear fission bomb) with a controlled device able to generate within a few nanoseconds a power of several hundreds millions of MW. Its impulsive operation, similar to an internal combustion engine, envisages having a capsule, Pellet (see Figure 1 15), containing a mixture of deuterium-tritium (fuel) coated with a material capable of quickly absorbing a high energy. During an operating cycle, the capsule is bombarded with a driver (energetic vector) able to provide a very high energy (high power lasers, concentrated X-ray beams, relativistic particle beams) of the Megajoule in few nanoseconds. This energy is absorbed by the capsule shell, which sublimates causing the implosion of the pellets and the increase in pressure and density of the fuel (n). In these extreme conditions the capsule heats up (T) in the central area (hot spot), where the ignition conditions are reached and the fusion reaction is triggered. This reaction then spreads outwards forming a thermonuclear wave that triggers other reactions, burning most of the fuel and releasing energy. The thermal energy produced is collected by a thermodynamic fluid and is used to operate in a specific thermodynamic cycle generating electricity. After being replaced the Pellet, the procedure is repeated. This confinement takes its name from the phenomenon of propagation and reaction that occurs at a higher speed than the inertia with which the gas of the capsule expands. Figure 1-11 shows the scheme of an inertial fusion machine (NIF), National Ignition Facility, of the Lawrence Livermore National Laboratory in California. Inertial fusion research is conducted at a national level by a few states, which are equipped with a nuclear arsenal, and have a close link with military research; many results are covered by secrecy and for this reason they are not supported by international research.

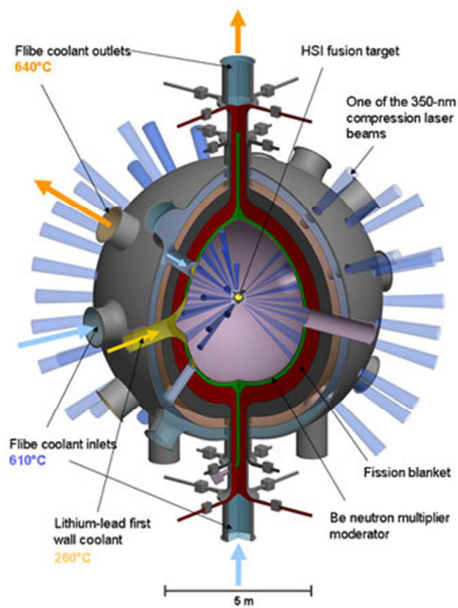


Figure 1-11: scheme of the NIF chamber, prototype of inertial fusion reactor.

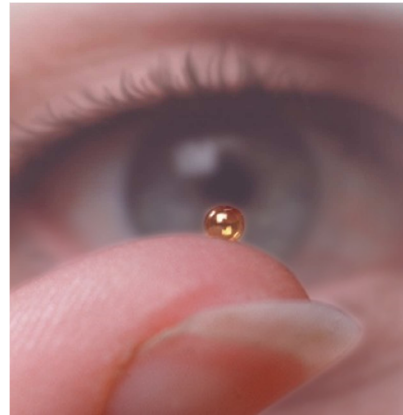


Figure 1-12: dimensions of the pellet used in an inertial fusion reactor.

1.4.3 Magnetic confinement

The concept / method on which the international interest is oriented is the magnetic confinement that sees its origin in studies on the motion of particles in electromagnetic fields. Given the extended Lorenz law (equation 1.32) and Newton's second law (equation 1.33), it can be demonstrated (refer to the specialized literature) that a particle moving in a uniform magnetic field, if it has a velocity component not parallel to the field, as a result of the same one, it will follow a helical path along the lines of the field. This principle is at the basis of magnetic confinement, in a vessel container in conditions of ultra-high vacuum, a plasma is produced which, thanks to the application of known magnetic fields of direction and intensity, is kept confined. The particles are obliged by the magnetic interactions to traverse internal trajectories to a closed magnetic surface.

$$(1.32) \quad F = qv \times B [N]$$

$$(1.33) \quad F = m \times a [N]$$

The first confining studies were conducted on magnetic mirror machines (Figure 1-13), formed by straight solenoids capable of generating uniform magnetic fields in a cylindrical region, and formed also by coils able to intensify them at the end, in order to confine the particles in the longitudinal direction by the so-called magnetic mirror effect. These machines effectively confine the particles in the transverse direction, but have considerable difficulty in confining them along the axial direction. The solution to this problem was to overcome by closing the solenoid to form a torus giving rise to the Tokamak, Russian acronym for "Toroidalny Kamera Makjna", machine with toroidal chamber (Figure 1-14). Tokamak is the most studied magnetic confinement configuration in the world; it derives from the studies on the fusion started in the Soviet Union in the late '50s, studies of which Europe and the so-called Western world remained in the dark until 1955, when they were announced in Geneva during the International Conference about the peaceful use of atomic energy.

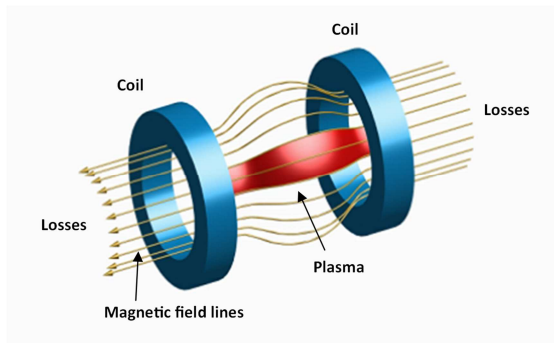


Figure 1-13: Magnetic mirror machine

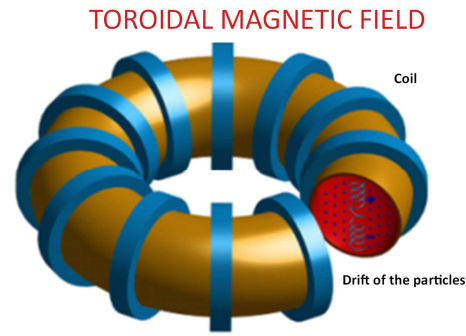


Figure 1-14: Toroidal solenoid

The Tokamak, as already mentioned can be seen as a solenoid wound to form a closed donut (Figure 1-14). It is formed by the vessel, the chamber where the plasma is produced and confined, and by the field coils that are placed around this structure. In general, the main coils on a Tokamak magnetic machine and the corresponding product fields (Figure 1-15) are:

- The toroidal coils forming the closed torus solenoid and producing the toroidal field (along the torus axis). This field corresponds to the field inside the donut, a field closed to form a circle along which the trajectories of the particles are screwed. Its function is to provide for the confinement of the particles.
- The poloidal coils located internally and externally to the toroidal structure have two tasks, to balance the toroidal forces that tend to take the plasma out of the donut configuration and to induce a current in the plasma core, the plasma current capable of generating the transverse poloidal field that surrounds the toroidal field lines and stabilizing the configuration. In particular the internal poloidal coils induce the plasma current, which behaves towards the plasma as a transformer (primary circuit - coils, secondary circuit - plasma), and together with the external pole coils contribute to produce a vertical field that actively balances the radial drift due to the toroidal forces that arise after closing the torus solenoid.

Depending on the desired configuration, additional coils are added, and these ones produce vertical or radial fields that provide both the balance of the plasma and the maintenance of an optimal shape. These coils are called coils for balance and form. The union of all the fields (screw-pinch configuration) generates the closed magnetic surface able to confine a fusion plasma.

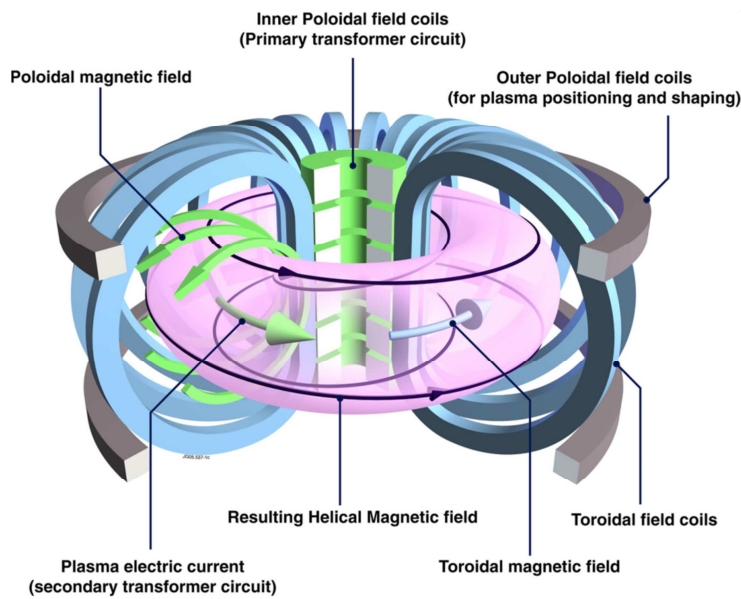


Figure 1-15: general scheme of a tokamak machine

An important characteristic of the Tokamak is its impulsive functioning. The poloidal coils that induce the plasma current are used as an inductance, and within them the magnetic energy is stored, then released and the plasma current is generated. This fact constitutes one of the limits of the machine, since it neither prevents continuous operation; a series of research aims to increase the duration of the impulse as much as possible in order to have an impulsive operation, but which lasts longer than one hour.

Given the intensity of the magnetic fields required, order of magnitude from 0.7 to 5-6T, in a Tokamak reactor all the coils are made of superconducting materials, which require temperatures close to absolute zero for their operation.

We also mention, in addition to the Tokamak, two other configurations for fusion machines, both based on magnetic confinement:

- The reverse field pinch (RFP) which is the magnetic confining configuration of the plasma studied for example with the RFX-mod machine (Figure 1-17) in Padua at the RFX consortium. A machine built to study the properties of plasma.
- The Stellarator, whose photo is shown in Figure 1-18, is a magnetic machine, which on condition of an increase in the system complexity and shape of the reels (overview diagram Figure 1-19, photo of a coil Figure 1-20), is able to realize the confinement field only thanks to external magnetic fields without the need for plasma current. The absence of plasma current allows this three-dimensional configuration to operate continuously.

Among the three types of machines in the tables: Table 1-3, Table 1-4 and Table 1-5 are given some of the main parameters. For another example of Tokamak quantities we can also refer to the ITER specifications listed in Table 1-6.

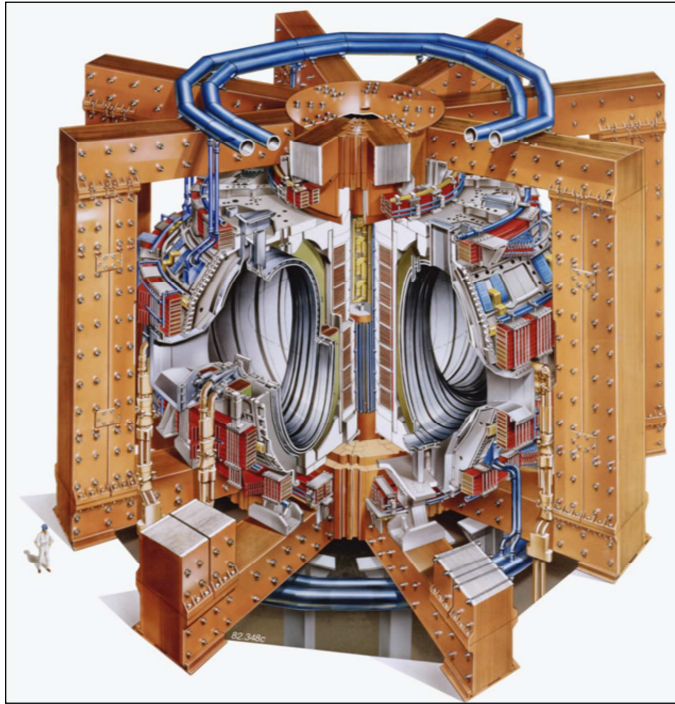


Figure 1-16: Joint European Torus – JET scheme (Tokamak)

Table 1-3: JET main parameters

Major radius	2.96 m
Minor radius	1.25 m
Maximum plasma current	4.80 MA
Maximum toroidal field, at the axis.	3.40 T
Pulse duration	20 – 40 s
Q in a Deuterium Tritium Plasma	0.90
Fusion Power	16 MW
Energy from fusion	22 MJ in 4 s

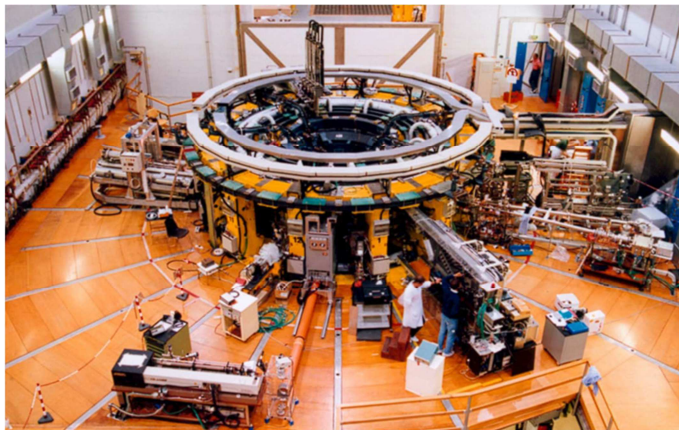


Figure 1-17: A photo of the RFX-mod experiment built at the RFX Consortium, Corso Stati Uniti 4, Padova. This machine studies the magnetic configuration known as Reverse field pinch-RFP.

Table 1-4: RFX-mod main parameters

Major radius	2.0 m
Minor radius	0.46 m
Maximum plasma current	2 MA
Maximum toroidal field	0.7 T
Pulse duration	0.5 s

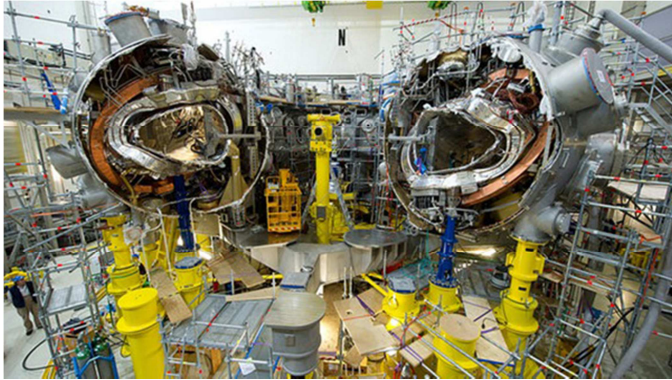


Figure 1-18: Photo of the experiment Wendelstein 7-X, stellarator studied at the Max-Plank Institute for Plasmaphysik, Greifswald. It is shown the complex structure of the coils.

Table 1-5: Wendelstein 7-X, main parameters

Major plasma radius	5.5 m
Minor plasma radius	0.53 m
Magnetic fields	3 T
Plasma volume	30 m ³
Pulse length	1800 s

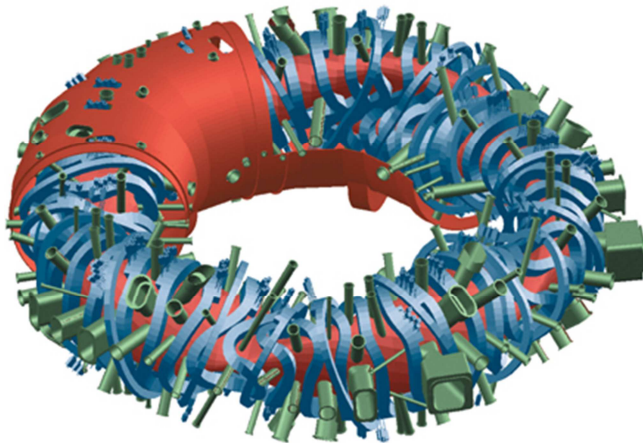


Figure 1-19: Internal scheme of the Wendelstein 7-X stellarator

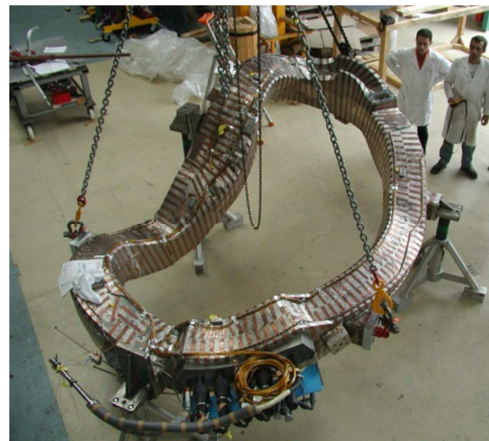


Figure 1-20: Photo of a deformed elliptical coil used in the Wendelstein 7-X stellarator

1.5 Iter project

ITER, acronym for International Thermonuclear Fusion Reactor or literally translated from the Latin "the way", is an international project that aims to demonstrate experimentally the feasibility of a fusion reactor of the Tokamak type. ITER is the result of years of international agreements, studies of numerous laboratories and experiments conducted on more than 200 Tokamak-type machines. Including the European JET machine, Joint European Torus (Figure 1-16), still operating in England and whose ITER is the successor. The time scale will see the first plasma of ITER in 2020, followed by the deuterium-tritium campaign for 2035.

1.5.1 The history

The history of ITER and the beginning of the international fusion research was placed in November 1985 at the "Superpower Summit", during the meeting between the then American president Ronald Reagan and the Supreme Soviet Secretary General Mikhail Gorbachev. The two world leaders, who met for the first time at the end of the Cold War, agreed to consider the energy of fusion an inexhaustible source of energy for the benefit of humanity ("an inexhaustible source of Energy for the benefit of mankind "). In the subsequent summit of Reykjavik (Iceland) on 11-12 October 1986 the agreement was reached between the European Union (Euratom), Japan, the Soviet Union and the USA to start the project of a large international research facility on fusion. So in April 1988 in Garching (Germany), at the Max Planck Institute for Plasmaphysik (IPP), 50 staff of professionals representing all the parties gathered to form the CDA - Conceptual Design Activities, with the aim of defining the technical characteristics of the project and the resources necessary for its realization. Under the guidance of the IAEA (International Atomic Energy Agency) the CDA met for six months a year until 1990. In the same year of the beginning of the work of the CDA, the latest version of Soviet tokamak the T-15 (heir of the first tokamak T-1 built in 1958) came into operation. On 9 November 1991 exactly ten years before the ITER project took the official lead, the JET reached for the first time the milestone of the fusion research, producing a thermonuclear fusion power between 1.5 and 2 MW. Internationally, it was announced that "a significant amount of power was obtained from a controlled fusion nuclear reaction. On this thrust, on July 21st 1992 in Washington DC (USA), on the basis of the specifications defined by the CDA, the work of the ITER-EDA (Engineering Design Activities) began. In three world locations: San Diego (USA), Garching (Germany), and Naka (Japan), the conceptual design of the experiment began. Canada and Kazakhstan are involved in the project respectively by Euratom and the Russian federation. In the meantime, new records are struck.

- December 1994, the TFTR (Tokamak Fusion Test Reactor) in Princeton (New Jersey), produces 16MW of Fusion Power.
- 1995 the TFTR always manages to produce a 510 million degree K plasma
- In 1997 the JT-60 (Japanese Tokamak) operating in Naka, improves the results obtained in thirty years of research by obtaining the best triple product conditions.
- In December of the same year, JET beat another three records producing 22MJ of fusion energy, 16MW of power in a single impulse, obtaining a power equal to 65% of that spent.

In Figure 1-32 the operating conditions reached over time are indicated for each machine. In 1998, six years after the beginning of the work of the ITER-EDA, the ITER council approves the final project of the experiment. Frightened by the cost, the United States decided to withdraw, and the San Diego site ends its activity. Despite this, the studies and research continue and in 2001 the new "ITER-FEAT" scheme was defined and approved: in addition to maintaining the majority of the previous program intact, measures aimed at containing costs were introduced. It is at this point that symbolically the

meaning of ITER as International Thermonuclear Experimental Reactor is associated with a deeper meaning, "the way". On January 10th 2003, China applied to enter the project. On January 30th 2003, the United States returned and six months later Korea asked to participate. ITER begins to take on an increasingly global character. In the same year the agreements for the search of the construction site begin. In February 2005, Euratom and Japan signed the Agreement for the Joint Implementation of the Broader Approach Activities in the Fusion Energy Research. An equal partnership between the European Union and Japan for coordinating the research to complement the ITER Project and to exploit the knowledge derived from ITER, with the aim to carry out new R&D and advanced technology development for the next-step device the DEMO machine. Engineering machine necessary for the study of the future fusion power plant. The agreed joint programme consists of three projects: the Engineering Validation and Engineering Design Activities for the International Fusion Materials Irradiation Facility (IFMIF/EVEDA), the International Fusion Energy Research Centre (IFERC), and the Satellite Tokamak Programme (STP) JT-60SA Project. In June 2005, after many negotiations, the official site for the construction of ITER, Cadarache in the south of France was chosen (Figure 1-22). Where the "Joint Work Site" was inaugurated on December 15th 2005. At the same time India also joins the project becoming the seventh participating partner. On November 21st, 2006 at the Élysée in Paris, the official agreement for the construction of ITER was signed by the seven participants, the European Union, the United States of America, the Russian Federation, Japan, China, Korea and India. The French President Jacques Chirac, the President of the European Commission José Manuel Barroso and 400 invited guests including the top representatives of ITER and member states of the European Union will be present at the signing.

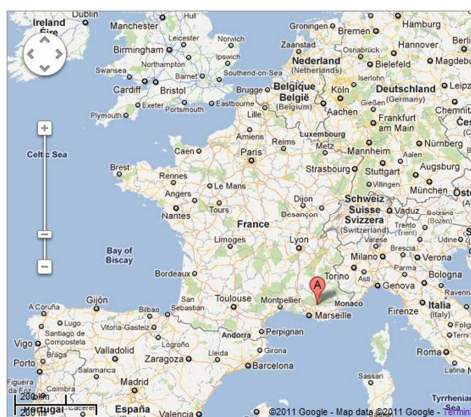


Figure 1-21: Geographical position of the ITER project construction site in Cadarache in the south of France.



Figure 1-22: site of construction of the ITER project in Cadarache in the south of France in September 2011

In January 2007, the work began in Cadarache with the preparation of 90 hectares of land. And in October of the same year the ITER Organization is officially announced to follow all the phases of study, planning, and construction. In the map in Figure 1-21 the geographical position of the site for ITER is indicated. Figure 1-22 show how the construction site was presented in September 2011. Figure 1-23 the construction progress the 25th of July 2018 seven year after. While in Figure 1-24 a reconstruction of how the site will be presented at the end of the works.



Figure 1-23: site of construction of the ITER project in Cadarache in the south of France 25 July 2018, ITER Organization/EJF Riche, <https://www.iter.org/album/Media/4%20-%20Aerial>



Figure 1-24: digital reconstruction of the ITER site

1.5.2 Working progress of the ITER project

From 2011 to 2018 the construction works continue, accompanied by design changes and numerous international agreements for the production of components and for transporting them. From Figure 1-25 to Figure 1-30 are shown some milestone reach during the construction progress photos taken from ITER Organization website to which you refer to see the latest photos, constantly updated.



Figure 1-25: February 2011, the excavation was completed for the construction of the antiseismic platform where to build the room of the Tokamak

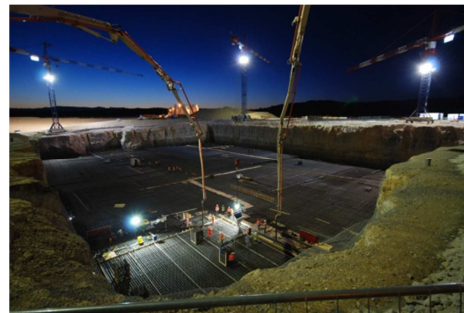


Figure 1-26: August 2011, the pouring for the foundations of the Tokamak building begins



Figure 1-27: December 2011, the first building of the complex, the plant for the on-site construction of the poloidal coils, is completed.



Figure 1-28: April 2012, completion of the antiseismic foundations of the Tokamak building



Figure 1-29: September 2012, completion of the ITER headquarters, a building of 20,500 square meters.



Figure 1-30: April-May 2015, state of construction of the Tokamak containment building

In Figure 1-32 the ITER Tokamak scheme is presented, while in Table 1-6 the main experimental quantities are given. ITER will not use the power produced by fusion reactions to produce electricity, its task will be to study the physics of the reactor and collect the data for the project of the future experiment and machine, which is why a considerable number of diagnostic systems are included in the project. To provide the external power necessary for the reaction, three neutral beam injectors

1.6 DEMO - the engineering machine for study the future commercial reactor

The final aim of all fusion research, and in particular of the ITER experiment, it is to acquire the necessary knowledge for the construction of a commercial reactor. The first experiment more similar to a reactor prototype will be DEMO, acronym for Demonstrative Reactor. This prototype, which is presented by a possible scheme Figure 1-33, it will have to run steadily or in a pulse condition and generate an electrical power of at least 1GW to be competitive with the other energy sources, and in any case it will not reach the ignition condition. The thermal power to maintain the plasma under operating conditions will result from the confinement of the alpha particles and the additional power supplied from the outside. The expected gain factor for the reactor should be around $Q = 30$ or higher.

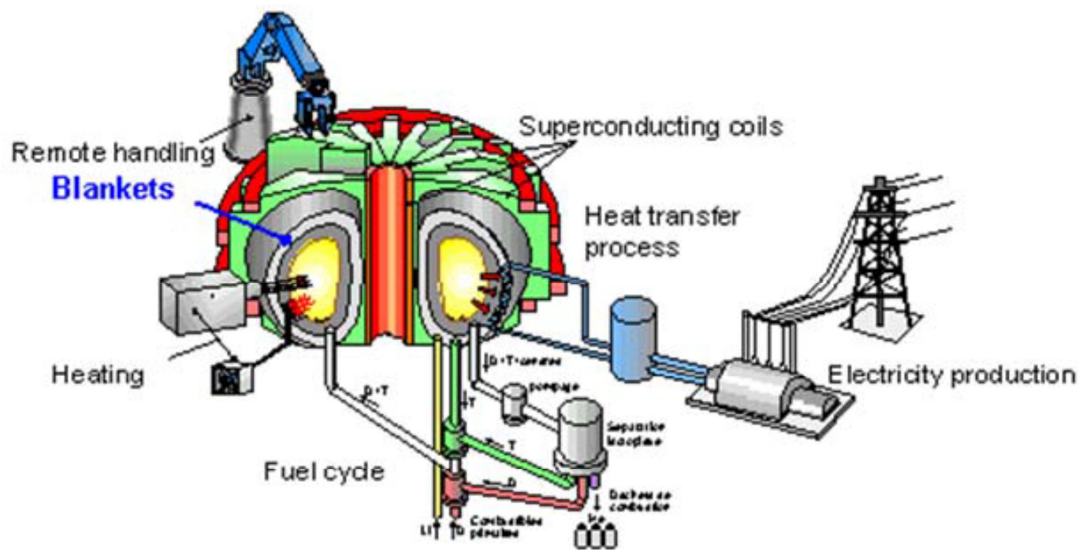


Figure 1-33: scheme of a prototype of fusion power plant

With the increase in power levels in DEMO, tests will be carried out on the life span of structural materials, and if necessary new substitute materials will be sought. In view of a continuous service, the procedures for the scheduled maintenance, and in particular the procedures for the robotized maintenance of the internal reactor chamber will also be tested. In ITER materials and devices will be tested for the first time, some of which will be an integral part of DEMO and will be added to the blanket and the electrical generation plant. In the blanket of DEMO, the special steel structure (Eurofer) surrounding the reaction chamber, they are present the ducts in which liquid lithium circulates with the task of absorbing high energy neutrons (80% energy thermonuclear produced) in escape from the plasma. The blanket in DEMO and in a future fusion power plant will perform two of the key functions for the fusion reactor:

- By absorbing the high energy neutrons, it will be able to accumulate thermal energy to be yielded to the thermodynamic fluid for the next phase of electrical generation.
- Absorbing neutrons will allow the lithium fertilization reactions to occur in the blanket with the production of new tritium to be used for the subsequent reaction.

Alongside the blanket there will be a complex system for the separation of tritium from lithium, for its purification and for sending it to the reaction chamber. The electrical generation plant will be of a conventional type substantially similar to that of a nuclear fission power plant. As regards to the

blanket modules for the production of tritium starting from lithium, the best solutions will be adopted in DEMO. Once the fusion power plant has been built, this will require a constant and planned maintenance similar to that carried out for a fission power plant, materials activated due to the neutron flux will have to be stored on site for a period of 50-100 years, after that they may be stored in an alternative warehouse. However, given the minimum radioactivity, they will not require the construction of long-term geological repositories, as required for nuclear fission waste. The hazards to the safety of the operation of the plant will be linked to the radioactivity of tritium and to the normal mechanical or electrical problems that a common thermoelectric power plant can know. Furthermore, in case of an accident, there is no problem of melting the core of the fission power plants, due to the very principle of operation of the fusion reactor, which does not have it.

2 FRESCO code

The FRESCO code (Fusion REactor Simplified COst), is a code written in C++ language with the aim to model in a simplified way a D-T fusion power plant base on the tokamak model. In FRESCO the power plant is studied from a technical and an economical point of view. Furthermore, it allows the users to calculate reactor parameters i.e. geometrical and physical dimension of the power plant, electromagnetic parameters of the machine, net electricity production, auxiliary energy needed, the operative cycle phases (especially for the pulse configuration), and not the last the related capital cost and the cost of electricity. With the last update, FRESCO code can be coupled with a Genetic Algorithm for optimization analysis. An example is the study carried out for the SOFT2016, where the cost of an hypothetic fusion power plant is optimized in function of the operational time (in case of a pulsed fusion power plant).

With FRESCO code it is possible to simulate steady-state and pulsed fusion reactor; it is also possible to change different component of the system an example is the tritium breeding blankets (HCPB or HCLL), and with a Monte Carlo routine, it is possible to perform a statistic analysis by varying parameters and the costs of the components of the system.

The data for a simulation with FRESCO code like geometric parameters, building materials, and the cost of all the technical solution and components come from the ITER experiment data at first. Other aspects, such as the tritium production inside the breeding blanket and the thermal to electricity conversion plant, are obtained from the technical description of the two power plant models presented in the European Fusion Power Plant Conceptual Study (PPCS). For Model B and Model AB are taken the two breeding blanket proposals included in the FRESCO simulation. Some other useful information can be obtained from the simulation made with another fusion code, like PROCESS code.

More than 2 thousands lines of the code can be divided in seven sections: the first one is the input data collection, followed by the calculation of the geometric parameter of the reactor, and the calculation of the electromagnetic parameter. The calculation of the thermal and electromagnetic flux and the operative time of the power plant are made in an unique section, in order to distinguish the two cases: one pulsed and one steady state model. The fifth section is demanded for the calculation of the cost of all the component of the reactor and the LCOE (Levelized Cost Of Electricity). Inside this part, there is the sixth section demand for the calculation of the electrical energy production. And finally, the last part for the output of the results. Input and output sections are strongly linked. In case of the optimization process with a Genetic Algorithm, in the last section it is created the resulted control file with the variables used in the genetic algorithm, in order to select the best simulation and generate the new input for the next generation.

The levelized cost of electricity (LCOE) is one of the most important information about a power plant, because thanks to this, it is possible to compare different technologies or different solutions over their economic life. And in a context of a sensitivity analysis or an optimization analysis, the LCOE can be the control value (control function) for an optimization.

In the next paragraphs, the sections here indicated are described, highlighting the new parts added in FRESCO code.

Compared to the previous version of the FRESKO code, one of the first improvements introduced has been the reorganization of the input parameters. This is a necessary operation, as some parameters were often doubled and defined in different areas of the program. These were then organized and collected in a single section of the program in order to be easily managed. The various input parameters will be presented during the explanation of the various sections of the FRESKO code.

The value of the input data are obtained from ITER experiment data, from the PPCS European model and from other studies made with other codes, for example PROCESS code.

2.1 Geometric parameter

The first geometric parameter calculated in FRESKO code is the plasma minor radius a , obtained by the fusion power (P_F , input datum) through an iterative process based on the equation 2.1.

$$(2.1) \quad P_F = \int_V \frac{(n_{DT}(r))^2}{4} \langle \sigma v \rangle \xi_{DT} dV$$

Fusion power, eq. 2.1, is function of the square of the fuel density function of the radial position (mix of deuterium and tritium) $n_{DT}(r)$, the average of the reactivity $\langle \sigma v \rangle$, the energy released by a single fusion reaction ξ_{DT} (for a deuterium-tritium reaction is $17.59 MeV$ equal to $2.81823 \cdot 10^{-21} J$) all integrate over the plasma volume.

Assuming equal deuterium and tritium density ($n_D = n_T$) the fuel density can be an input datum $n_{fuel} = n_{DT}$ or is calculated with the equation 2.3.

$$(2.2) \quad \frac{n_D + n_T}{n_e} = \frac{1}{Z - 1} \left(Z - Z_{eff} - 2(Z - 2) \frac{n_{He}}{n_e} \right)$$

$$(2.3) \quad n_{DT} = \frac{1}{2} n_e \left[\frac{1}{Z - 1} \left(Z - Z_{eff} - 2(Z - 2) \frac{n_{He}}{n_e} \right) \right]$$

where the electron density n_e , atomic mass number of impurity Z , atomic mass number of element of the plasma Z_{eff} , and the helium fraction (fixed to a 10% n_e) are all input datum. In the calculation is assumed a parabolic dependence of density, temperature and current to the radius, with the equation 2.4.

$$(2.4) \quad X(r) = X_0 \left(1 - \frac{r^2}{a^2} \right)^{\alpha_x}$$

X_0 is the value of the X at the magnetic axis. Temperature and density value at the magnetic axis are derived from the respective average value $\langle X \rangle$

$$(2.5) \quad X_0 = \langle X \rangle (1 + \alpha_x)$$

r is the radial coordinate of the concentric flux surface assuming the same elongation for each one ($0 < r < a$). The peaking factor of the equation α_x are input data for density α_n and temperature α_T , for the current is a function of the peaking factor of the temperature $\alpha_j = 3\alpha_T/2$.

Considered the H-mode operation, the equation 2.4 for the density profile becomes the equation 2.5 for $\frac{r}{a} < \rho_{ped n}$ and 2.6 for $\frac{r}{a} > \rho_{ped n}$, while the equation that describes the temperature profile is equation 2.9, in these equation is considered the data for pedestal and separatrix. With n_{ped} and n_{sep} are indicated respectively the density for the pedestal and for the separatrix, with T_{ped} the temperature for the pedestal region. $\rho_{ped n}$ and $\rho_{ped T}$ are the relative position for the pedestal region respect to the minor plasma radius a . $n_{DT}(0)$ plasma density in the core region is calculated with the equation 2.8 while T_0 is an input datum.

$$(2.5) \quad n_{DT}(r) = n_{ped} + (n_{DT}(0) - n_{ped}) \cdot \left(1 - \frac{(r/a)^2}{\rho_{ped n}^2}\right)^{\alpha_n} \quad \text{for } \frac{r}{a} < \rho_{ped n}$$

$$(2.6) \quad n_{DT}(r) = n_{ped} + (n_{ped} - n_{sep}) \cdot \left(\frac{(1 - r/a)}{(1 - \rho_{ped n})}\right) \quad \text{for } \frac{r}{a} > \rho_{ped n}$$

$$(2.7) \quad \rho_{ped n} = \frac{r_{ped n}}{a}$$

$$(2.8) \quad n_{DT}(0) = \frac{1}{3 \cdot \rho_{ped n}^2} \cdot \left[3n_{DT}(1 + \alpha_n) + n_{sep}(1 + \alpha_n)(-2 + \rho_{ped n} + \rho_{ped n}^2) - n_{ped} \left((1 + \alpha_n)(1 + \rho_{ped n}) + (\alpha_n - 2)\rho_{ped n}^2\right)\right]$$

$$(2.9) \quad T(r) = T_{ped} + (T_0 - T_{ped}) \cdot \left(1 - \frac{(r/a)^{t_B}}{(\rho_{ped T})^{t_B}}\right)^{\alpha_n}$$

$$(2.10) \quad \rho_{ped T} = \frac{r_{ped T}}{a}$$

In FRESKO code it is also defined the density weighted volume averaged plasma temperature $\langle T \rangle_{dw}$, with the equation 2.11.

$$(2.11) \quad \langle T \rangle_{dw} = T_0 \left(\frac{1 + \alpha_n}{1 + \alpha_n + \alpha_T}\right)$$

Remember that we assumed electron and ion temperature equal $T_e = T_i = T$. And α_n, α_T are input parameters which describe the parabolic profile.

Reactivity $\langle \sigma v \rangle$ is calculated by the Bosch and Hale formulation [29] with the equation

$$(2.12) \quad \langle \sigma v \rangle = C1\theta \sqrt{\frac{\xi}{m_r c^2 T(r)^3}} e^{-3\xi}$$

the plasma volume is expressed with the equation:

$$(2.13) \quad V = (2\pi R)(A_f \pi r^2 k)$$

$$(2.14) \quad dV = (2\pi A a)(2A_f \pi k r dr)$$

where R is the major radius of the torus, A is the aspect ratio given in input ($A = R/a$), k is a coefficient for the elongation of the section, and finally A_f is a correction factor representing the rate

between the elliptic section and the section's shape of the plasma. Replacing equation 2.14 in the fusion power equation 2.1, we can obtain this equation:

$$(2.15) \quad P_F = 4\pi^2 A a A_f k \xi_{DT} \int_0^a \frac{(n_{DT}(r))^2}{4} \langle \sigma v \rangle r dr$$

Defining R_0 the radial distance of the plasma centre from the major axis of the torus, Z_0 the vertical distance to the mid-plane of the torus, it is possible to represent the coordinate of the plasma boundaries with the next two equation. Where θ is the radial coordinate of a radial reference system place in the centre of the plasma poloidal section.

$$(2.16) \quad \begin{cases} R(\theta) = R_0 + a \cos(\theta + \delta \sin \theta) \\ Z(\theta) = Z_0 + ka \sin(\theta) \end{cases}$$

Therefore a fair approximation of the plasma poloidal section area is given by the sum of rectangles with base equal to $R(\theta + d\theta) - R(\theta)$ and height to $Z(\theta + \delta\theta)$. With this assumption is possible to rewritten the equation 2.15 in the equation 2.17

$$(2.17) \quad P_F = 4\pi^2 A A_f k \xi_{DT} a \sum_{r=0}^a \frac{(n_{DT}(r))^2}{4} \langle \sigma v \rangle r dr$$

The obtained formulation allows to integrate the equation with numerical methods, the only unknown variable is the minor radius a . The value of a is calculated through an iteration process. With the value of the minor radius a , it is possible to calculate the major radius R from the aspect ratio A , the poloidal section area S and the plasma volume V .

The average wall loading (W) ratio between the fusion power and the internal blanket surface is evaluated with the equation 2.20. Where it is assumed that the first wall surface S_{wall} coincides with the external plasma surface (no scrape of layer). With this approximation the average wall loading is overestimated. The plasma surface is calculated with the ARIES formulation 2.18

$$(2.18) \quad S_{wall} = S_{plasma} = (2\pi R) P_{plasma} = (2\pi R)(2\pi a S)$$

Where P_{plasma} is the plasma perimeter, S is the plasma shape factor (ratio of the plasma poloidal perimeter to the perimeter of a circular one with the same minor radius) calculated with the equation 2.19

$$(2.19) \quad S = \left(\frac{1 + k^2(1 + 2\delta^2 + 1.2\delta^3)}{2} \right)^{1/2}$$

Remember that k is the elongation factor and δ the triangulation factor.

$$(2.20) \quad W = \frac{0.8 \cdot P_f}{S_{wall}}$$

In the equation 2.20, " $0.8 \cdot P_f$ " is the energy released by the D-T reaction and associated to neutron particles.

2.1.1 Dimension of the component surrounding the plasma

The second part of the geometrical parameter section is dedicated to the dimensioning of the component surrounding the plasma. As we can see in the Figure 2-1, which represents the inner section of the machine, from the plasma wall we find: First wall, breeding blanket, high temperature shield (HTS), Low temperature shield (LTS), vacuum vessel (VV), Toroidal field coil and central solenoid coil(CS). Each one of these component has an appropriate thickness.

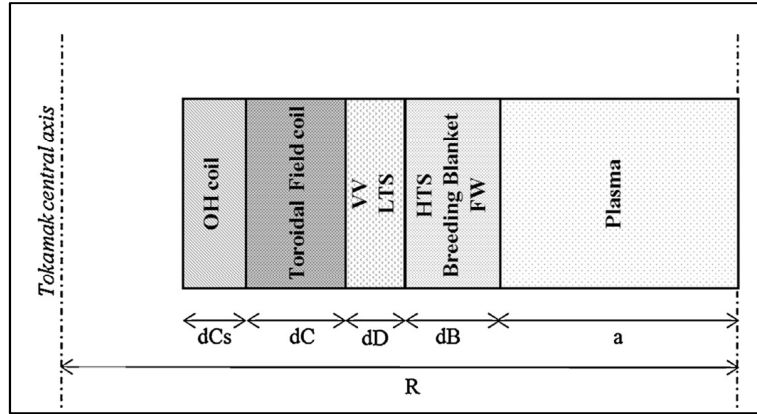


Figure 2-1: simplified representation of the inboard radial build of the machine. The blanket thickness, dB , is the sum of first wall thickness, breeding blanket and high temperature shield (HTS). While dD is the thickness of the vacuum vessel with the Low temperature shield (LTS) and dC the Toroidal field coil thickness. [27]

The blanket thickness dB , that includes also the first wall and the high temperature shield, depends on the choice of the breeding blanket technology. In FRESCO two are the possible choices: the first one is the Helium Cooled lithium led (HCLL), the second one is the Helium Cooled Pebble Bed (HCPB). In function of the power density of the first wall W and the technology, the FRESCO code calculates the appropriate thickness.

For the HCLL:

$$(2.21) \quad dB = breedingThickness + \left(0.781 \cdot \left(\frac{W}{1.84} \right) \right)$$

$$(2.22) \quad breedingThickness = 0.425 \cdot \left(multiplication \frac{factor}{1.18} \right)$$

For the HCPB:

$$(2.23) \quad dB = breedingThickness + \left(0.663 \cdot \left(\frac{W}{2.1261} \right) \right)$$

$$(2.24) \quad breedingThickness = 0.365 \cdot \left(multiplication \frac{factor}{1.39} \right)$$

For a specific simulation, the dB parameter can be also given as input datum. The vacuum vessel thickness dD , that includes also the low temperature shield, is an input datum of the simulation.

Toroidal field coil thickness dC is calculated from the previous vacuum vessel thickness dD and the value of the maximum magnetic field in the machine B_{tm} and the maximum current density acceptable for the conductors j_{cond} (for ITER experiment this value is set to 10 A/mm^2).

$$(2.25) \quad B_{t_0} = B_{tm} \frac{R - a - dB - dD}{R} = B_{tm} \frac{r_e}{R}$$

$$(2.26) \quad r_e = R - a - dB - dD$$

$$(2.27) \quad I_{tor} = \frac{2\pi R B_{t_0}}{\mu_0}$$

$$(2.28) \quad S_{TC} = \frac{I_{tor}}{j_{cond}} = \pi(r_e^2 - r_i^2)$$

$$(2.29) \quad r_i = \sqrt{r_e^2 - \frac{S_{TC}}{\pi}}$$

$$(2.30) \quad dC = r_e - r_i$$

The thickness of the central solenoid dCs is an input datum for the machine (set to 0.8m from the ITER design value).

Here, in FRESKO, at the end of the geometric section there is the first control of the geometry: if the internal building radius leads to an internal radius of the central solenoid below zero, an error occurred and the input data must be checked, especially the data linked to the plasma radius.

$$(2.31) \quad R_{CDi} = R_{CSe} - dC \text{ must be } > 0$$

2.1.2 Toroidal Field Coil stress analysis

The evaluation of the toroidal field coil stress analysis $\langle \sigma_{TFC} \rangle$ can be carried out at the end of the geometric section with the equation 2.32, where R_1 and R_2 , the distance of the inner and outer leg of the machine, are evaluated respectively with the equation 2.33 and 2.34, respecting the tokamak axis. The mechanical stress on toroidal field coil is used for the evaluation of the total number of cycles acceptable for a pulse power plant.

$$(2.32) \quad \langle \sigma_{TFC} \rangle = \frac{1}{4} \langle j_{cond} \rangle B_{tmax} R_1 \ln \frac{R_2}{R_1}$$

$$(2.33) \quad R_1 = R_{CSe} + \frac{dC}{2} = \left(R - a - dB - \frac{dC}{2} \right)$$

$$(2.34) \quad R_2 = R + a + dB + dD + \frac{dC}{2}$$

2.2 Plasma electromagnetic parameter

In this section the plasma electromagnetic parameter is totally defined: plasma inductance L_p , plasma resistivity (so the plasma resistance R_p) with the Spitzer formulation, the total plasma current and at the end of the section is evaluated the poloidal beta and compared with the Troyon limit. The plasma inductance L_p is calculated by the sum of the internal L_i and external inductance L_e . The internal inductance is evaluated from the inductance per unit length l_i with equation 2.36 function of the current density profile. External inductance L_e , see equation 2.38 is a function of the geometric parameter of the plasma.

$$(2.35) \quad L_p = L_i + L_e$$

$$(2.36) \quad l_i = \log(1.65 + 0.89 + \alpha_j) \left[\frac{H}{m} \right]$$

$$(2.37) \quad L_i = \frac{\mu_0}{4\pi} 2\pi R l_i [H]$$

$$(2.38) \quad L_e = \mu_0 R \left[\left(1 + \frac{a^2}{8R^2} \right) \ln \frac{8R}{a} + \frac{a^2}{24R^2} - 2 \right] [H]$$

(The whole quantity is determined with the same formula used in the Process code.) The plasma resistivity ρ_p is obtained by the Spitzer formulation equation 2.39 where Λ is evaluated with the equation 2.40.

$$(2.39) \quad \rho_p = Z_{eff} (1.65 * 10^{-9}) \frac{\ln \Lambda}{T_0^{3/2}} [\Omega m]$$

$$(2.40) \quad \Lambda = 37.8 - \ln \frac{\langle n_e \rangle^{1/2}}{\langle T_{dw} \rangle}$$

Assuming the plasma at a low temperature, like an ohmic conductor, the plasma resistance R_p is evaluated with equation 2.41 where $S_{plasma} = A_f \pi a^2 k$ is the plasma cross section area, and $\rho_p \gamma_{NC}$ the parallel resistivity. With the hypothesis that the variation of neoclassical resistivity enhancement factor γ_{NC} along the minus radius doesn't change, a constant value is taken and $\gamma_{NC} = 2.5$. Average value given by Wesson.

$$(2.41) \quad R_p = \rho_p \gamma_{NC} \frac{2\pi R}{S_{plasma}} [\Omega]$$

From the MHD safety factor at the 95% of the flux surface q_{95} given as input datum is now possible to compute the Plasma current with equation 2.42. derived from the Ampere's law.

$$(2.42) \quad I_p = \frac{\pi a^2 B_{t0}}{\mu_0 q_{cyl} R} \left(\frac{1 + k^2 (1 + 2\delta^2 + 1.2\delta^3)}{2} \right)^{1/2}$$

In the equation 2.42 we found the plasma shape factor function of the elongation coefficient k and triangularity coefficient δ , the cylindrical equivalent safety factor q_{cyl} obtained from equation 2.43 and function of the aspect ratio A .

$$(2.43) \quad q_{cyl} \cong q_{95} \frac{\left(1 - \frac{1}{A^2}\right)^2}{\left(1.17 - 0.65 \frac{1}{A}\right)}$$

The evaluation of the plasma current I_p enables the estimation of the poloidal beta with the equation 2.44, and the possibility to compare these value with the Troyon limits here indicates as β_n .

$$(2.44) \quad \beta_{pol} = \frac{nk_B T}{\frac{B_{t0}^2}{2\mu_0}}$$

$$(2.45) \quad \beta_{pol} < \beta_n \frac{I_p}{aB_{t0}}$$

2.2.1 Central solenoid parameter

In the electromagnetic parameters section, it is also evaluated the parameter of the central solenoid of the machine. The central solenoid inductance is evaluated from equation 2.46.

$$(2.46) \quad L_{CS} = \frac{\mu_0 N_t^2 (S_{CSi} + 0.5S_{dCS})}{h_{CS}}$$

Where N_t is the number of turning an input datum (with the reference of ITER value, the number of turns is fixed to 264.1 turns/m, ITER CS data $h_{CS} = 12.45 \text{ m}$ with 3288 turns), h_{CS} is the height of the central solenoid approximated as two times the value of the major radius (for ITER data $h_{CS}/R \cong 2$), S_{CSi} internal central solenoid area, S_{dCS} central solenoid annulus section. The current in the central solenoid is evaluated with the 2.47 where $B_{CSmax} = 13 \text{ T}$. Finally it is calculated the energy stored in the central solenoid inductance with equation 2.48.

$$(2.47) \quad I_{CS} = \frac{B_{CSmax} h_{CS}}{N_t \mu_0}$$

$$(2.48) \quad E_{CS} = \frac{1}{2} L_{CS} I_{CS}^2$$

2.3 Operations phases for a fusion power plant

The FRESCO code is conceived for economic assessments of simplified models of fusion power plant (FPP). FRESCO can consider two types of power plant operation scenarios: the pulse operation scenario, and the steady state operation scenarios. The selection between the two options is one of the input parameters. The approach used for modelling the operative cycle for a pulse power plant is described in Figure 2-2, where the operation cycle of the machine, τ_{cycle} , is split into two periods: the flat top phase τ_{FT} where in the reactor it happened the fusion reaction and it is produced the thermal energy, and the dwell time τ_{dwell} , where the reactor is prepared for the next pulse. In the FRESCO model, it is assumed that the thermal energy generated by fusion reactions during the burn phase is partly converted into electricity and partly stored in a thermal energy storage (TES), operating with molten salt (60% NaNO₃, 40% KNO₃). The FPP lifetime PP_{life} is set at the maximum of 60 years with a maximum number of operative cycles equal to $N_C = 2 \times 10^5$ cycles. The flat top phase τ_{FT} is composed by the plasma heating time τ_H where it is reached the burning condition and the burning time τ_{burn} . While in the dwell time occurs the Ramp-up, where the plasma current rise from zero to the nominal level, Ramp-down, where the plasma current goes to zero at the end of the pulse, and the operation for preparing the machine, like the pump down process for restoring the initial level of pressure, and the recharge of the central solenoid. So dwell time (τ_{dwell}) extends from the end of the burn until the beginning of the next heating phase. Since the central solenoid is charged while the vacuum vessel is pumped down, the two phases can partially or fully overlap. Thus the dwell time can be evaluated as:

$$(2.49) \quad \tau_{dwell} = \tau_{RU} + \max(\tau_{CS}, \tau_{pump}) + \tau_{RD}$$

While flat top time is:

$$(2.50) \quad \tau_{FT} = \tau_H + \tau_{burn}$$

Using the same notation of the Figure 2-2 the operational phases can be expressed as:

- $\tau_{RU} = t_1 - t_0$ Ramp-up time, where the current rises from zero to the nominal plasma current
- $\tau_H = t_1 - t_2$ Heating time, that is the time from the current flat top initiation to the burning time condition
- $\tau_{burn} = t_3 - t_2$ Burning time, where it happened the fusion reaction and it is produced the thermal energy
- $\tau_{RD} = t_4 - t_3$ is the Ramp-down time, where the pulse is ended, generally set equal to the Ramp-up time,
- τ_{CS} is the Charge time for the central solenoid,
- τ_{pump} is the time need for pump-down operation of the machine,

The cycle time of operation has a maximum value that depends on the maximum number of cycle over the power plant lifetime and the availability factor, that is a function of the blanket and divertor lifetime.

$$(2.51) \quad \tau_{cycleMAX} = \frac{n_{secYear} \cdot AF}{N_{cycleYear}}$$

Where $n_{secYear}$ is the number of second of one year, AF is the availability factor, and $N_{cycleYear}$ the number of cycle accepted for one year of operation:

$$(2.52) \quad N_{cycleYear} = \frac{N_C}{PP_{life}}$$

N_C is the total number of cycles accepted during the power plant lifetime PP_{life} .

The availability factor is calculated in FRESKO with an iteration routine, starting from the information of the total power plant lifetime PP_{life} , the lifetime of the divertor and the blanket that specified the number of a month after that the component must be substituted, and the duration of the operation for the substitution for the divertor and for the blanket. The routine uses, if specified, a Monte Carlo Routine for varying the life and substitution time. Then, it is simulated an hypothetic life of operation and it is evaluated the number of the substitution for each component, the month where the machine is stopped for maintenance and the correspond availability factor AF .

$$(2.53) \quad AF = \frac{\text{effective operation month}}{\text{total month of operation}}$$

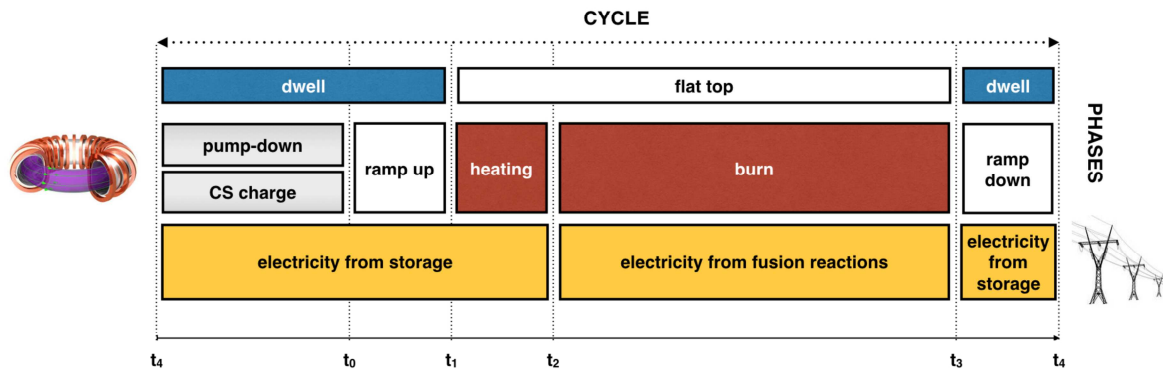


Figure 2-2: Operative cycle of a fusion power plant [125]

A different case is the steady state operation where the time for central solenoid recharge is set to one hour, only for the starting operation of the reactor. Because the sustaining of the plasma current in a steady state reactor is done with external heating and current drive systems.

In the next paragraph, it will be described for each phase here presented, how in FRESKO code the time of each phase is calculated, if it is not set as input, and how the flux balance and the thermal energy balance are evaluated, from which it depends the duration of each phase. It is also presented the improvement added to FRESKO code the routine for the evaluation of the pump-down process.

2.4 Central solenoid flux evaluation

In FRESKO code for the central solenoid operation, it is assumed the double swing operation. The magnetic field inside the central solenoid is a complete reversal from $+B_{CS}$ to $-B_{CS}$. The central solenoid flux ϕ_{CS} is calculated with equation 2.54.

$$(2.54) \quad \phi_{Cs} = 2 \cdot \pi \cdot BCS_{Max} \cdot \left(RCS_{Int}^2 + \frac{1}{2}(RCS_{Ext}^2 + RCS_{Int}^2) \right)$$

To the central solenoid flux it is then added the contribution of the vertical field ϕ_{VF} :

$$(2.55) \quad B_V = \frac{\mu_0 I_{tot}}{4\pi R} \left(\beta_{thp} + \frac{l_i}{2} - \frac{3}{2} + \log\left(\frac{8A}{k^2}\right) \right)$$

$$(2.56) \quad \phi_{VF} = \pi \cdot (R^2 - RCS_{Ext}^2) B_V$$

$$(2.57) \quad \phi_{Cs_{tot}} = \phi_{Cs} + \phi_{VF}$$

The flux produced by the central solenoid and the vertical field $\phi_{Cs_{tot}}$ is used in the ramp up phase for the rise of the current from zero to the nominal level ϕ_{RU} . The remaining one $\phi_{Available}$ can be used for sustaining the plasma current in the flat top phase. The calculation of these value are shown in chapter 2.6.

2.5 Ramp-Up phase – the rise of the plasma current

In the Ramp-up phase, the central solenoid operates as a primary of an hypothetic transformer and it induces in the gas fuel inside of the torus vessel, secondary of the hypothetic transformer, a current named the plasma current $i_p(t)$. At the beginning of the Ramp-up time t_0 the current is $i_p(t_0) = 0$, than it rises until it is reached the nominal value $i_p(t_1) = I_p$ at the time t_1 . The Ramp-up time is defined as:

$$(2.58) \quad \tau_{RU} = t_1 - t_0$$

The flux required for the Ramp-up rise of the current is calculated with the equation 2.59 and it is a function of the plasma inductance L_p , the plasma resistance $R_p[T(t)]$ function of the plasma temperature, and the variation of plasma current $i_p(t)$ function of time. The plasma temperature $T(t)$ is expressed in [keV] and it varies from 0 at t_0 to T_{ohm} at t_1 . T_{ohm} is the final temperature at the end of the Ramp-up phase result of the ohmic heating. The plasma can be seen as a conductor with a resistance $R_p[T(t)]$ crossed by the current $i_p(t)$, the resistivity of the plasma conductor is a function of the temperature and it decreases with it, as described by the Spitzer resistivity formulation 2.39. Acting as a conductor, the plasma can be heated by ohmic heating; however, since the resistivity decreases with the temperature, it can be heated only for few keV. In FRESCO T_{ohm} , not knowing a priori, it is calculated with an iterative process based on power balance equation 2.61.

$$(2.59) \quad \phi_{RU} = \int_{t_0}^{t_1} L_p \frac{di_p(t)}{dt} dt + \int_{t_0}^{t_1} R_p[T(t)] i_p(t) dt$$

As presented in equation 2.59, the Ramp-up flux is the sum of two integrals: the first one depends on the plasma inductance and the plasma current variation; the second one is a function of the resistance of the plasma. “Ejima formulation” gives an approximation of the second integral, the minimal resistive flux consumption [30].

$$(2.60) \quad C_{Ejima} \mu_0 R I_p = \int_{t_0}^{t_1} R_p[T(t)] i_p(t) dt$$

Where C_{Ejima} is the Ejima coefficient set to 0.3-0.45. FRESKO code uses the ‘‘Ejima formulation’’ for the evaluation and control of the Ramp-up time. With the new improvement, the Ramp-up time can be set as input parameter or can be calculated with the iteration routine. If Ramp-up time is set as input, the resistive contribution to the Ramp-up flux is evaluated directly with the integral, and the result is compared with the value given by ‘‘Ejima formulation’’. If the integral value is less than the reference, the routine returns a specific error code. Otherwise, when the Ramp-up time is not set as input with an iterative process, the value of the Ramp-up time is increased until the resistive flux equals the minimum flux consumption obtained by the ‘‘Ejima formulation’’. In the solution of equation 2.60 it is assumed a linearity dependence between the plasma temperature and the plasma current.

Also the ohmic temperature T_{ohm} is calculated in FRESKO code with an iterative process operating simultaneously with the routine for τ_{RU} . Starting with a first attempt value for $T_{ohm} = 1 \text{ keV}$, the routine increases the temperature until the power balance for the ramp up phase is satisfied. Equation 2.61 shows the plasma thermal power balance which must be verified for all the phase of the reactor, and equation 2.62 shows the extended version. The time derivative of the plasma energy W on the left side must be equal to the sum of the power losses P_{losses} and the heating power $P_{heating}$. In FRESKO the power losses are calculated as the sum of conductive losses P_{cond} and radiative losses P_{rad} . The radiative losses include the Bremsstrahlung losses P_{brem} and the synchrotron losses P_{sync} . While the heating power $P_{heating}$ is the sum of the ohmic power P_{Ohmic} , the alpha power P_{α} generated from the fusion reaction, and the external auxiliary power P_{aux} . The auxiliary heating power P_{aux} is assumed to be provided only by RF system for the Ramp-up time, and by RF systems and NBI systems for the flat top phase.

$$(2.61) \quad \frac{dW}{dt} = -P_{losses} + P_{heating}$$

$$(2.62) \quad \frac{dW}{dt} = -P_{cond} - P_{rad} + P_{\alpha} + P_{Ohmic} + P_{aux}$$

For the evaluation of the ohmic temperature T_{ohm} , it is assumed that the auxiliary heating P_{aux} provided by RF system in the Ramp-up is equal to the minimum power needed to reach the H-mode condition, the threshold power $P_{threshold}$. With the equation 2.64, the lower bound for the threshold power and with the equation 2.63 the upper bound are estimated. Where with n_{Ramp} is indicated, the plasma density at the end of the ramp up equal to $0.4n_{GW}$, n_{GW} is the greenwald density. The first value for the P_{aux} power is set as the average value of the two threshold limit equation 2.65.

$$(2.63) \quad P_{thresholdUP} = 0.0488e^{0.057}n_{ramp}^{0.717+0.035} + B_{T0}^{0.803+0.032} + S_{FW}^{0.941+0.019}$$

$$(2.64) \quad P_{thresholdLOW} = 0.0488e^{-0.057}n_{ramp}^{0.717-0.035} + B_{T0}^{0.803-0.032} + S_{FW}^{0.941-0.019}$$

$$(2.65) \quad P_{aux} = P_{threshold} = \frac{P_{thresholdUP} - P_{thresholdLOW}}{2}$$

For each value of T_{ohm} in the iteration, the resistivity of the plasma 2.66 and the corresponding ohmic power are calculated, equation 2.68 where g_{ohm} is a coefficient that is considered the profile for temperature and density.

$$(2.66) \quad \rho_{ohm} = Z_{eff}(1.65 \cdot 10^{-9}) \frac{\ln \Lambda}{T_{ohm}^{3/2}} [\Omega m]$$

$$(2.67) \quad \Lambda = 37.8 - \ln \frac{\langle n_{ramp} \rangle^{1/2}}{\langle T_{dw ohm} \rangle}$$

$$(2.68) \quad P_{ohm} = \rho_{ohm} \cdot [J_0 \cdot 10^6]^2 \cdot g_{ohmic} \cdot V \cdot 10^{-6} [MW]$$

$$(2.69) \quad g_{ohm} = \frac{1}{1 + 2 \cdot \alpha_n + \frac{\alpha_T}{2}}$$

The alpha power is calculated with an iterative process similar to the one use for the evaluation of the minus radius a . The equation for the fusion power (2.17) is specified for the alpha power. Where $\xi_\alpha = 3.52 MeV$ is the energy released by the alpha particles in a D-T fusion reaction. (Remember that $1 eV = 1.6022 \cdot 10^{-19} J$)

$$(2.70) \quad P_\alpha = 4\pi^2 AA_f k \xi_\alpha a \sum_{r=0}^a \frac{(n_{DT}(r))^2}{4} \langle \sigma v \rangle r dr$$

$$(2.71) \quad P_\alpha = \pi^2 R A_f k \xi_\alpha \sum_{r=0}^a (n_{DT}(r))^2 \langle \sigma v \rangle r dr$$

$$(2.72) \quad P_\alpha = \pi^2 R k A_f \xi_\alpha (1.6 \cdot 10^{-19}) P_{\alpha_sum} [MW]$$

$$(2.73) \quad P_{\alpha_sum} = \sum_{r=0}^a (n_{DT}(r))^2 \langle \sigma v \rangle r dr$$

The losses by radiation is evaluated as Bremsstrahlung losses with the equation 2.74, while the conduction losses are evaluated with the equation 2.76, where the plasma energy W is calculated with equation 2.77, and the confinement time is estimated with the formulation 2.78

$$(2.74) \quad P_{rad RU} = P_{brem} = (1.68 \cdot 10^{-2}) \left(\frac{n_{e0}}{10^{20}} \right)^2 Z_{eff} \left(\frac{T_{0 ohm}}{10} \right)^{0.5} g_{n2th} V$$

$$(2.75) \quad g_{n2th} = \frac{1}{1 + 2 \cdot \alpha_n + \frac{\alpha_T}{2}}$$

$$(2.76) \quad P_{cond RU} = \frac{W_{plasmaRU}}{\tau}$$

$$(2.77) \quad W_{plasmaRU} = (3 \cdot 1.6021 \cdot 10^{-22}) n_{Ramp} T_{dw ohm} V$$

$$(2.78) \quad \tau = 0.0562 \cdot I_P^{0.93} B_t^{0.15} P_{in}^{-0.69} \frac{\langle n_e \rangle^{0.41}}{10^{19}} M^{0.19} R^{1.97} \epsilon^{0.58} k^{0.78}$$

At the end they are calculated the total power produced in the Ramp-up phase $P_{prod\ RU}$, the total losses $P_{loss\ RU}$ and the plasma power $P_{plasma\ RU}$ at the end of the Ramp-up.

$$(2.79) \quad P_{prod\ RU} = P_{ohm\ RU} + P_{\alpha\ RU}$$

$$(2.80) \quad P_{loss\ RU} = P_{rad\ RU} + P_{cond\ RU}$$

$$(2.81) \quad P_{plasma\ RU} = \frac{W_{plasma\ RU}}{\tau_{RU}}$$

With that information, it is evaluated the parameter that controls the iteration process:

$$(2.82) \quad k_{iteration} = \left| \frac{P_{plasma\ RU}}{P_{prod\ RU} + P_{aux} - P_{loss\ RU}} \right|$$

The iteration process ends when $k_{iteration}$ becomes near one, in the interval of $[0.9 - 1.1]$. At the end of the iteration, it is evaluated the v_{raise} parameter that indicates the velocity for the rising for the current

$$(2.83) \quad v_{raise} = \frac{I_P}{\tau_{RU}}$$

If the value of v_{raise} is greater than the limit fixed and the auxiliary power is less than the upper limit for the threshold power, the initial value for the auxiliary power is increased and the iteration process is restarted with a new initial value.

2.6 Available flux and flat top period

Once it is calculate the Ramp-up time with the equation 2.59, it is evaluated the total flux required in the Ramp-up ϕ_{RU} , and from the knowledge of the flux produced by the central solenoid ϕ_{CStot} , it is calculated the available flux at the end of the Ramp-up ϕ_{Avail} equation 2.84. Where with ϕ_{CD_RU} it is indicated the possible flux generated by a current drive system in the Ramp-up phase, in the main case this quantity is equal to zero $\phi_{CD_RU} = 0$.

$$(2.84) \quad \phi_{Avail} = \phi_{CStot} + \phi_{CD_RU} - \phi_{RU}$$

If the available flux ϕ_{Avail} is negative, the code gives an error because the central solenoid flux is not able to sustain the Ramp-up phase, otherwise $\phi_{Avail} > 0$ FRESKO code distinguishes between the two possible types of operation, steady-state and pulse operation.

For the steady-state operation, the central solenoid has to be sized only for the production of the flux required for the current Ramp-up, an available flux greater than zero indicating that the central solenoid has been oversized. For this condition, the current contribution is calculated from the current drive system as a difference between the plasma current and the bootstrap current, given in input as a percentage of the plasma current.

$$(2.85) \quad I_{CD} = I_P - I_{BS}$$

For the pulsed operation, if the flat top time τ_{FT} is set as input, the routine evaluates the required flux for sustaining the current ϕ_{REQ} .

$$(2.86) \quad \phi_{REQ} = (I_P - I_{BS}) \cdot 10^6 R_P \tau_{FT}$$

And comparing the required flux ϕ_{REQ} with the available one ϕ_{Avail} , it distinguishes two possible pulse operations:

- $\phi_{REQ} < \phi_{Avail}$ we are in an inductive pulse operation mode, the available flux can sustain the plasma current for all the flat top period, the machine doesn't need an external current from current drive systems $I_{CD} = 0$, the inductive current is $I_i = I_P - I_{BS}$.
- $\phi_{REQ} > \phi_{Avail}$ we are in an hybrid pulse operation mode, the plasma current can be sustained partially with the available flux, but an external current drive system is needed for sustaining the current for all the flat top period. The available flux can sustain the current only for a time τ_{avail} .

$$(2.87) \quad I_i = \frac{\phi_{Avail}}{R_P \tau_{FT} 10^6}$$

$$(2.88) \quad I_{CD} = I_P - I_i - I_{BS}$$

$$(2.89) \quad \tau_{avail} = \frac{\phi_{Avail}}{R_P (I_P - I_{BS}) 10^6}$$

If the flat top time τ_{FT} has a negative value, i.e. it is not set as input, the routine calculates the flat top time with the assumption of an inductive mode operation. The current drive is set to zero $I_{CD} = 0$ and the inductive one is $I_i = I_P - I_{BS}$. Only the available flux is used for sustaining the current in the flat top operation so $\tau_{FT} = \tau_{avail}$.

$$(2.90) \quad \tau_{avail} = \tau_{FT} = \frac{\phi_{Avail}}{R_P (I_P - I_{BS}) 10^6}$$

2.7 Heating phase

The first phase that composes the flat top is the heating phase, where the plasma is heated and brought to the burning condition. In FRESCO the duration of the heating phase can be set as input or can be calculated from the thermal energy balance equation.

Known from the input file or from previously calculation, the principal parameters required for the fusion power plant operation i.e. the plasma temperature, the plasma temperature weighted over the density $\langle T_{dw} \rangle$, the density of the plasma, the efficiency ε and the plug efficiency η_{plug} of the current drive system, are possible to calculate for the heating phase the ohmic power with equation 2.91 and the alpha power with the same approach use for the Ramp-up phase, see chapter 2.5.

$$(2.91) \quad P_{ohm} = \rho_{ohm} \cdot \gamma_{NC} \cdot [J_0 \cdot 10^6]^2 \cdot g_{ohm} \cdot V \cdot 10^{-6} [MW]$$

The auxiliary power P_{aux} is set equal to the power coupled by the heating and the current drive systems $P_{coupHCD}$.

$$(2.92) \quad P_{aux} = P_{coupHCD} = P_{coupH} + P_{coupCD}$$

Initially the heating power is set to zero $P_{coupH} = 0$ so the auxiliary power is equal to the power coupled by the current drive systems $P_{aux} = P_{coupHCD} = P_{coupCD}$ calculated with the equation 2.94. But for the inductive operation where $P_{coupCD} = 0$, the heating power will be set to $P_{coupH} = 50 \text{ MW}$ considered the minimum heating power needed for a fusion power plant during the heating phase.

$$(2.93) \quad \gamma_{CD} = \frac{I_{CD} R n}{P_{coupCD}}$$

$$(2.94) \quad P_{coupCD} = \frac{I_{CD}}{\varepsilon}$$

$$(2.95) \quad \eta_{CD} = \eta_{plug} \varepsilon$$

The power produced in the heating phase is then equal to:

$$(2.96) \quad P_{prod H} = P_{ohm} + P_{\alpha} + P_{coupHCD}$$

Remember that for this calculation, the auxiliary power is equal to the heating and the current drive power.

$$(2.97) \quad P_{aux} = P_{coupHCD}$$

For evaluating the total power losses, it is calculated the Bremsstrahlung losses with the equation 2.74, the synchrotron losses with Trubnikov formulation 2.98 where ψ is function of the reflectivity.

$$(2.98) \quad P_{sync} = (6.214 \cdot 10^{-17}) n_e \langle T_{dw} \rangle B_{t_0}^2 \psi V$$

$$(2.99) \quad P_{rad} = P_{brem} + P_{sync}$$

And the conduction losses P_{cond} (2.100) are obtained from the plasma energy W_{plasma} equation 2.99 calculated for the temperature weighted over the density at the beginning of the burning phase equal to the temperature desired for the D-T fusion condition.

$$(2.99) \quad W_{plasma} = (3 \cdot 1.6021 \cdot 10^{-22}) n T_{dw} V$$

$$(2.100) \quad P_{cond} = P_{prod} - P_{rad}$$

$$(2.101) \quad \tau_{eH} = \frac{W_{plasma}}{P_{cond}}$$

$$(2.102) \quad P_{losses} = P_{rad} + P_{cond}$$

If the heating time is not set as input ($\tau_H < 0$) the program calculates the value with the equation 2.103

$$(2.103) \quad \tau_H = \frac{(W_{plasma} - W_{plasma \text{ RU}})}{P_{coupHCD}}$$

Otherwise ($\tau_H > 0$) the auxiliary power will be updated with equation 2.104

$$(2.104) \quad P_{aux} = \frac{(W_{plasma} - W_{plasma\ RU})}{\tau_H}$$

The new value for the auxiliary power is then compared to the power coupled with the current drive systems and if $P_{aux} < P_{coupCD}$ it is generated an error, else $P_{aux} > P_{coupCD}$ the routine corrects the power coupled by heating systems $P_{coupH} = P_{aux} - P_{coupCD}$ and updates the value of the power produced P_{prod} , the confinement time τ_e , the power loss by conduction P_{cond} and the total power loss P_{losses} .

2.8 Burning phase

For the burning phase, it is assumed that the confinement time is equal to the value calculated for the heating phase $\tau_{e\ Burn} = \tau_{eH}$. The power production is the sum of ohmic heating power P_{ohm} and alpha power P_α , the same value calculated for the heating phase, and the power coupled from current drive systems, assuming that the heating systems are turned off at the beginning of the burning phase.

$$(2.105) \quad P_{prod\ Burn} = P_{ohm} + P_\alpha + P_{coupCD}$$

While the power losses are the same calculated for the heating phase, for the burning phase it is calculated the net plasma heating power for the reactor P_{in} as difference between the power production and the losses.

$$(2.106) \quad P_{in} = P_{prod\ Burn} - P_{loss}$$

Finally, it is evaluated the real auxiliary power installed with the plug efficiency:

- For $I_{CD} > 0$ hybrid mode operation $\frac{P_{coupHCD}}{\eta_{plug}}$
- For $I_{CD} < 0$ inductive mode operation $\frac{P_{coupH}}{\eta_{plug}}$

The Q factor are evaluated both with the Helios formulation and the Process formulation as

$$(2.107) \quad Q_{Helios} = \frac{P_f \cdot 10^9}{(P_{ohm} + P_{coupHCD}) \cdot 10^6}$$

$$(2.108) \quad Q_{Process} = \frac{P_f \cdot 10^9}{(P_{coupH}) \cdot 10^6}$$

And it is calculated the H factor as the ratio of confinement time $\tau_{e\ Burn}$ and the value of $\tau_{IPB98(y,2)}$ calculated with the equation 2.109

$$(2.109) \quad \tau_{IPB98(y,2)} = 0.0562 \cdot I_P^{0.93} B_t^{0.15} P_{in}^{-0.69} \frac{(n_e)^{0.41}}{10^{19}} M^{0.19} R^{1.97} \varepsilon^{0.58} k^{0.78}$$

Where M [amu] is the atomic mass of the ions (2.5 amu), ε is the inverse of the aspect ratio A, I_P [MA] the plasma current, B_t [T] the toroidal magnetic field, n_e [m^{-3}] the electron density. The time duration for the burning time τ_{burn} is evaluated as the difference between the flat top duration τ_{FT} and the duration of the heating time τ_H .

$$(2.110) \quad \tau_{Burn} = \tau_{FT} - \tau_H$$

2.9 Time for the vacuum vessel pump-down

The time for the vacuum vessel (VV) pump-down process τ_{pump} extends from the end of the current pulse (t_4) until the beginning of the Ramp-up (t_0). In Figure 2-2 $\tau_{pump} = t_4 - t_0$. One of the improvements done in FRESCO code, and not presented in the first version of the code, is the new module for the evaluation of the pump-down time. In the pump-down phase the pressure and the vacuum condition of the vacuum vessel are restored to the pre-impulse condition. $p(t_0) = 5 \cdot 10^{-4}$ [Pa]. The pump-down model integrates numerically the equation 2.111 increasing t_4 for a fixed value of t_0 until the two terms of the equation 2.111 are equal with a tolerance of $toll = 10^{-7}$.

$$(2.111) \quad p(t_0) = \frac{K_1}{S} \left(\frac{e^{at_4}}{e^{at_0}} \right) + \frac{1}{e^{at_0}} \frac{K_1}{V} \int_{t_4}^{t_0} t^n e^{at} dt$$

where $V [m^3]$ is the volume of the vessel, $p(t_0) [mPa]$ is the pressure required at t_0 , $S [\frac{m^3}{s}]$ is the pumping speed, $a = \frac{S}{V}$, $K_1 = 9 Pa m^3/s$ is the outgassing rate of the vacuum vessel wall and $n = -0.73$ is the decay index. Equation 2.111 is obtained integrating in the time variable the pump-down differential equation (2.112).

$$(2.112) \quad V \cdot \frac{dP}{dt} + S \cdot P = K_1 t^n$$

2.10 Cycle time, ramp-down, and central solenoid charge time

Given as input or calculated in the appropriate routine, the Ramp-up time τ_{RU} , the flat top time τ_{FT} , the heating time τ_H and, with the new modules, the time for pump-down process τ_{PUMP} . The last two periods are immediately evaluated: the time for the ram-down phase τ_{RD} is set equal to the ramp-up process, the time for the central solenoid charging τ_{CS} is set to one hour for the steady state operation or, for the pulse operation, it is set equal to the pump-down time. Both the time for the ramp-up and the time for charging the central solenoid can be set as input value. Fixed the time for the central solenoid charge, it is calculated the grid power necessary for the charge process:

$$(2.113) \quad P_{grid} = \frac{E_{CS}}{\tau_{CS}} \cdot 10^{-6}$$

At the end it is evaluated the dwell time τ_{dwell} and the cycle time τ_{cycle} for the pulse operation

$$(2.114) \quad \tau_{dwell} = \tau_{RU} + \max(\tau_{CS}, \tau_{pump}) + \tau_{RD}$$

$$(2.115) \quad \tau_{cycle} = \tau_{dwell} + \tau_{FT}$$

$$(2.116) \quad \tau_{cycle} = \max(\tau_{CS}, \tau_{pump}) + \tau_{RU} + \tau_H + \tau_{Burn} + \tau_{RD}$$

The two phases for pumping down the vacuum chamber and for charging the solenoid are independent of each other so they can be partially or fully overlapped, then the dwell time is set equal to the maximum time between the two process. From τ_{cycle} and the effective life for the power plant, it is evaluated the total number for the cycle for the pulse operation in the lifetime

$$(2.117) \quad N_{cycleOperation} = \frac{n_{secYear} \cdot AF}{\tau_{cycle}}$$

If the number of cycle in the lifetime exceeds the maximum allowable number of cycle, FRESCO will generate an appropriate error code.

$$(2.118) \quad N_{cycleOperation} < N_{cycleMAX}$$

The amplitude for the stress on the structure is evaluated with the formulation:

$$(2.119) \quad \sigma = 0.5 \cdot E \cdot (C_P + C_E)$$

Where:

$$(2.120) \quad E = 200000 \text{ MPa}$$

$$(2.121) \quad C_P = 0.311 \cdot (N_{cycleYear} \cdot Year_{operation})^{0.516}$$

$$(2.122) \quad C_E = 0.0199 \cdot (N_{cycleYear} \cdot Year_{operation})^{0.0788}$$

2.11 Electricity production for a Fusion Power Plant

Knowing the fusion Power P_f as input value for the simulation and evaluating the auxiliary power for the heating and the current drive systems $P_{coupHCD}$, the next step in the FRESCO routine is the evaluation, both for the steady state and the pulse operation, of the total thermal energy produced in the reactor and the gross and net electrical power production for the fusion power plant. Alpha power and the Neutron power are calculated respectively with the equations 2.123 and 2.124, thermal power with equation 2.125 where it is assumed a multiplication factor for the neutron power due to the effect of the breeding blanket.

$$(2.123) \quad P_\alpha = 0.2 \cdot P_f \cdot 10^3 \text{ [MW]}$$

$$(2.124) \quad P_n = 0.8 \cdot P_f \cdot 10^3 \text{ [MW]}$$

$$(2.125) \quad P_{therm} = P_\alpha + M \cdot P_n + P_{coupHCD} \text{ [MW]}$$

Considering all the systems and the losses, it is also possible to evaluate the total thermal power for a steady state power plant with equation 2.126, where the coefficients are taken from the paper written by LI-PUMA, A., et al. (see reference [54])

$$(2.126) \quad P_{thermTOT} = 0.991 \cdot (P_\alpha + P_{ohm} + P_{coupHCD}) + 0.921(M \cdot P_n) + 0.91 \cdot P_{pump} \text{ [MW]}$$

For a pulse power plant due to the pulse generation, it is assumed that the power plant is equipped with a molten salt storage system, similar to the one used for the concentrating solar power technologies. Part of the thermal energy generated in the burning time is stored and used during the dwell and heating time for obtaining a continuous generation of energy. Assuming that the round trip efficiency for the thermal storage is $\eta_{TES} = 80\%$, the equivalent total thermal power can be calculated with the equation 2.127.

$$(2.127) \quad P_{thermTOT_{EQ}} = P_{thermTOT} \frac{\tau_{burn}}{\left(\frac{1}{\eta_{TES}}(\tau_{Dwell} + \tau_H) + \tau_{burn}\right)}$$

And it is possible to evaluate energy and power in input and output to the thermal storage system (TES):

$$(2.128) \quad P_{TES-IN} = (P_{thermTOT} - P_{thermTOT_{EQ}})$$

$$(2.129) \quad W_{IN} = P_{TES-IN} \cdot \tau_{burn}$$

$$(2.130) \quad P_{TES-OUT} = P_{thermTOT_{EQ}}$$

$$(2.131) \quad W_{OUT} = P_{TES-OUT} \cdot (\tau_{Dwell} + \tau_H)$$

The gross electric power for a steady state power plant is:

$$(2.132) \quad P_{Egross} = P_{thermTOT} \cdot \eta_{rankine}$$

And for the pulsed power plant is:

$$(2.133) \quad P_{e\ gross} = P_{thermTOT_{EQ}} \cdot \eta_{rankine}$$

Where with $\eta_{rankine}$ is indicated the efficiency of generation process based on a Rankine cycle. The auxiliary power for the pumping system is evaluated with equation 2.134 where $f_{pump\%} = 21.36\%$ is the fraction of the gross electric power used to energize the pumping systems, same approach used for the evaluation of the power for the cryogenic systems evaluated with equation 2.135 where $f_{cryo\%} = 0.07\%$ of the gross electric power. The value for $f_{pump\%}$ and $f_{cryo\%}$ are taken from [54].

$$(2.134) \quad P_{pump} = \frac{f_{pump\%}}{100} \cdot P_{e\ gross}$$

$$(2.135) \quad P_{cryo} = \frac{f_{cryo\%}}{100} \cdot P_{e\ gross}$$

The net electric power generated by the fusion power plant is:

$$(2.136) \quad P_{e\ net} = P_{e\ gross} - (P_{pump} + P_{cryo} + P_{aux})$$

The recirculation fraction is:

$$(2.137) \quad f_{recirc} = \frac{P_{e\ gross} - P_{e\ net}}{P_{e\ gross}}$$

The total efficiency and the energy generated in one year expressed in kilowatt-hour are evaluated respectively with equations:

$$(2.138) \quad \eta_{FPP} = \frac{P_{e\ net}}{(P_f \cdot 10^3)}$$

$$(2.139) \quad kWh_y = (P_{e\ net} \cdot 8760 \cdot AF) \cdot 10^3 [kWh]$$

2.12 Economic assessment

The cost of electricity of the fusion power plant has been calculated in FRESKO with the levelized cost of electricity (LCOE) specified for carbon free technologies as shown in the equation 2.140.

$$(2.140) \quad \text{LCOE} = \frac{\sum_{i=0}^{\text{PPlife}} (I_{t,i} + \text{O\&M}_{t,i} + F_{t,i} + D_{t,i})(1+r)^{-t}}{\sum_t E_t(1+r)^{-t}}$$

where t is the year in which the sale of production takes place, PPlife is the power plant economical lifetime, I_t is the power plant investment cost, O\&M_t the operation and maintenance costs, F_t the fuel cost, D_t the cost of decommissioning, E_t is the amount of electricity produced, all evaluated in year t . Finally $(1+r)^{-t}$ is the discount factor and r the real discount rate for year t (inflation is neglected). The investment cost I_t is the sum of the overnight cost plus the interest during constructions IDC function of the lead time and the debt-equity ratio.

$$(2.141) \quad \text{IDC}_{\text{FRESKO}} = 16.5\% \text{ of the overnight cost}$$

For the evaluation of each term of the equation 2.140 in FRESKO it is used a scaling cost approach. Starting from the cost of ITER components and the cost of the material, the costs of the power plant are calculated scaling it with appropriate geometrical scaling factors: GM linear scaling, GM^2 surface scaling, GM^3 volume scaling, with specific coefficient function of the components and with a learning factor indicate as FM set as input.

$$(2.142) \quad GM = \frac{R_{\text{machine}}}{R_{\text{ITER}}}$$

$$(2.143) \quad R_{\text{ITER}} = 6.2 [m]$$

The cost for the materials (i.e. eurofer, deuterium, tungsten,...) are set as input and are actualized using the actualization factor calculated from the actualization rate r_{actual} respect to the reference year y_{ref} , equation 2.144.

$$(2.144) \quad f_a = \left(1 + \frac{r_{\text{actual}}}{100}\right)^{(y_0 - y_{\text{ref}})}$$

$$(2.145) \quad \text{Cost}_{\text{material_ACTUAL}} = \text{Cost}_{\text{material_INPUT}} \cdot f_a$$

For a deep description of the evaluation of all the cost of the components referred to the specific paper [27], here in the table they are summarized the cost of all the ITER component referred to the year 2000 taken from [27], and for each cost in the third column they are indicated the coefficient use in the FRESKO code scaling process. With all the costs of the component, it is possible to evaluate the direct cost as the sum of costs of all the components, plus the assembling costs, the power supply, waste storage, and building costs. The indirect costs are evaluated in function of the direct one using the same approach of Process code. The overnight cost is the sum of direct and indirect cost. Investment cost is then equal to the overnight cost plus the interest on capitals. The fuel cost is evaluated from the years of operation, and it is the sum of the deuterium and the cost of the breeding blanket material. The operation and the maintenance cost is evaluated as the cost of personnel (30.36M€/y) plus the administration costs (7.46) and the replacement costs of divertor and blanket modules. The decommissioning cost are set as input and derived from the fission power plant experience.

Table 2-1: Cost of the component of the machine and scaling coefficient [27]

Component of the machine	ITER cost [M€]	Scaling coefficient
<i>Magnetic systems</i>		
Toroidal fields coils windings	149.6	GM^3
Poloidal field coil & correction coils	63.6	GM^3
Magnetic structure	215.3	$GM^3 \cdot \frac{\sigma_{ITER}}{\sigma_{MAX}}$
Central solenoid coil	39.8	$\frac{\phi_{CS}}{\phi_{CS ITER}} \cdot \frac{B_{CS}}{B_{CS ITER}}$
Conductor	454	$\frac{S_{TC}}{S_{TC ITER}}$
<i>Vacuum vessel</i>		
Main Vessel	198.2	GM^3
Port assembler	95.9	–
<i>Divertor</i>	97.2	GM
<i>H&CD</i>		
Neutral Beam Injector	122.8	$\left(\frac{Cost_{NBI}}{P_{NBI}}\right)_{ITER}$
Radio Frequency heating systems	99.1	$\left(\frac{Cost_{RF}}{P_{RF}}\right)_{ITER}$
<i>Vacuum pumping & fuelling systems</i>		
Vacuum pumping	32.4	GM^3
Fuelling systems	11.4	–
<i>Cryostat and cryodistribution</i>		
Cryostat	96.9	GM^3
Cryodistribution	113.7	GM^3
<i>Tritium plant</i>	46.8	GM^3
<i>Diagnostics</i>	150.9	0.5
<i>Remote handling</i>	78.1	–
<i>Machine assembly</i>		
Assembly operation	64.3	GM
Assembling tooling	54.2	–
<i>Power supply</i>		GM
<i>Buildings</i>	486.4	–

2.13 Output section

The output section collects all the instruction for the correct presentation of the result. Here it is presented an example of the output file obtained by a FRESCO code simulation. The FPP simulate is the DEMO1 study with PROCESS code in April 2015, an example of a pulsed fusion reactor. At the beginning of the file it is written the origin of the data, the mode and the blanket use for the simulation and it is given the COE of that power plant. Then grouped by typology, they are provided all the parameters that characterize the simulated reactor, both the input and the output parameters. Each parameter is accompanied with the name and the corresponding measurement unit in the international system.

DEMO1 April 2015 2016-07-11 15:02:26

Mode: PULSED (burn time: 2 [h])

Blanket: HCPB

COE (Euro 2000): 63.426 [ceuro/kWh]

*** check:63.426 ***

RADIAL BUILD

2.87	[m]	minor radius (a)
8.897	[m]	major radius (R)
3.1		aspect ratio (A)
39.59	[m ²]	poloidal section area
25.43	[m]	poloidal section perimeter
2213.2	[m ³]	plasma volume
1421.6	[m ²]	FW surface
1.1452	[MW/m ²]	wall loading
1.683	[m]	inner radius
0.8	[m]	CS thickness (input)
2.483	[m]	outer radius
0.64795	[m]	TFC thickness
0.5	[m]	VV thickness (input)
1.08	[m]	BLK thickness

ELECTROMEGNETIC PARAMETER

2.0512e-005	[H]	plasma inductance (Lp)
6.4592e-006	[H]	plasma internal inductance (Li)
1.1555	[H]	plasma internal normalized inductance (li)
15.627		ln Lambda
5.7373e-009	[ohm]	plasma resistance (Rp)
20.779	[MA]	plasma current (Itot)
7.231	[MA]	bootstrap current (Ibs)
119.21	[mV]	loop voltage (loop)
5.2484e-021	[1/m ³]	Greenwald density (nGW)
1.521		n/nG
1.3109	[%]	beta thermal
1.2791	[%]	beta total

12.32	[T]	max toroidal magnetic field (input) (Btm)
5.66	[T]	toroidal field on axis (Bt0)
6.99e+019	[1/m3]	fuel density
2.584		Zeff
CENTRAL SOLENOID		
1.683	[m]	inner radius (RcsInt)
2.483	[m]	outer radius (RcsExt)
0.8	[m]	thickness (input)
8.8985	[m2]	bore (ScsInt)
10.47	[m2]	corona circolare (Scorona)
17.866	[m]	height (h)
3943.7	[#]	number of turns (Nspire)
46.865	[kA]	CS conductor current (Ics)
184.82	[MAT]	total CS current
15.462	[H]	CS inductance (Lcs)
16.979	[GJ]	CS stored energy (Lcs)
Vs considerations(Mode HYBRID)		
358.76	[Vs]	Vs generated by CS
150.6	[Vs]	Vs generated by Vertical field (VsVF)
509.36	[Vs]	Vs available (VsCs+VsVF)
495.92	[Vs]	required during ramp up (VsRampUp)
69.701	[Vs]	resistive (14.055%), (minimum: 69.694Vs)
426.22	[Vs]	inductive (85.945%)
495.92	[Vs]	from CS and VF
0	[Vs]	from CD systems (VsContrib)
559.63	[Vs]	Vs required for fully inductive operation (VsReq)
13.441	[Vs]	Vs available during flat top (VsDisp)
172.92	[sec]	time for fully inductive operation
546.19	[Vs]	Vs missing
0.32538	[Ma]	inductive current
13.222	[MA]	non inductive current required (Icd)
63.634	[%]	Icd/Itot
RAMP UP PHASE		
0.72874	[MWt]	ohmic power (PohmRampUp)
15.378	[MWt]	alpha power (AlfaPowerRampUp)
182.57	[MW]t	auxiliary heating power from RF (RFstartH = Pthresh)
198.68	[MWt]	total power production (PprodottaRampUp+RFstartH)

37.428	[MWt]	Total radiation power losses (PradRampUp)
157.49	[MWt]	Transport loss power (PcondRampUp)
194.92	[MWt]	power loss (PpersaRampUp)
3.6442	[MWt]	plasma power (WplasmaRampUp/tRaise)
198.56	[MWt]	power losses + plasma power (PpersaRampUp+WplasmaRampUp/tRaise)
182.16	[MWt]	upper limit H-mode threshold power (Pthresh_up)
112.98	[MWt]	lower limit H-mode threshold power (Pthresh_low)
147.57	[MWt]	H-mode threshold power (Pthresh)
41.7	[sec]	current raise time (tRaise)
0.49829	[MA/sec]	rate of current raise (vRaise)
1.4	[keV]	plasma temperature at the end of ramp up (Tohm)
7.1847e+019	[1/m3]	density @end of ramp up (nRamp)
0.96491	[sec]	L-mode confinement time (tauIPBLmode)
HEATING PHASE		
198.68	[MWt]	power production at the end of Ramp Up (PprodottaRampUp+RFstartH)
194.92	[MWt]	power loss at the end of Ramp Up (PpersaRampUp)
628.56	[MWt]	power production at the end of Heating (Pprodotta)
628.56	[MWt]	power loss at the end of Heating (Ppersa)
10.842	[sec]	heating phase (tHeat)
BURN PHASE		
0.11293	[MWt]	ohmic power (Pohm)
408.07	[MWt]	alpha power (AlfaPower)
220.37	[MWt]	auxiliary heating power (PcoupHCD)
628.56	[MWt]	total power production (Pprodotta)
108.74	[MWt]	Bremsstrahlung radiation power losses (Pbrem)
13.918	[MWt]	Synchrotron radiation power losses (Psyncr)
122.66	[MWt]	Total radiation power losses (Prad)
505.9	[MWt]	Transport loss power (Pcond = Wplasma/tauE)
628.56	[MWt]	total power losses (Ppersa)
220.37	[MWt]	auxiliary power for CD (PcoupCD)
0	[MWt]	auxiliary power for heating only (PcoupH)
367.28	[MW]	total auxiliary power installed for H&CD (Paus)
505.9	[MWt]	net heating power (Pin)
2.4935	[sec]	confinement time (tauIPB98y2)
2.6619	[sec]	confinement time (TAU_E)
1.0675	[sec]	H factor (TAU_E/tauIPB98y2)
9.2296		Q factor (Helios approach)

9.2344 Q factor (PROCESS approach)

OPERATIVE CYCLE

7828.5	[sec]	Cycle (2.1746 [h])
41.7	[sec]	Ramp up time
10.842	[sec]	Heating time
7189.2	[sec]	Burn time
7200	[sec]	Flat top
27.8	[sec]	Plasma ramp down time
558.96	[sec]	CS recharge
558.96	[sec]	Time for pumping
628.46	[sec]	Dwell time
3276.4	[#]	Cycles/annum
1.9659e+005	[#]	Cycles/lifetime
2e+005	[#]	Cycles to failure
30.377	[MW]	Power from electric grid for CS recharge

AVAILABILITY

720	[months]	power plant life (mesiVita)
585.2	[months]	operative months (mesiEffFunz)
134.8	[months]	power plant stop (mesiComplFerma)
3.2	[years]	DV life
4.4799	[years]	BLK life
4.3	[months]	time for DV replacement
7.89	[months]	time for BLK replacement
15	[#]	number of DV substitutions (numSostDV)
10	[#]	number of BLK substitutions (numSostBLK)
2	[#]	number of simultaneous substitutions (numSostContemp)
27	[#]	number of stops (numFermate)
81.278	[%]	availability factor

Tensione di progetto a temperatura criogenica [MPa] = 409.65

Tensione media calcolata sulle TFC [MPa] = 205.31

PLANT POWER BALANCE

407	[MWt]	Alpha power
1921	[MWt]	Neutron power in blanket
220.37	[MWt]	Heating power coupled to plasma
2647.7	[MWt]	Total thermal power

264.87	[MWt]	Input power to TES
2382.9	[MWt]	Total thermal power equivalent
44 [%]		Thermal to electric efficiency
1048.5	[MW]	Gross electric power
223.95	[MW]	Pumping power
0.42615	[MW]	H&CD efficiency (gammaCD)
0.6 [MW]		H&CD plug efficiency (plug_eff)
367.29	[MW]	H&CD power (Icd/etaCD)
7.3392	[MW]	Auxiliary and cryogenic power
598.58	[MW]	Recirculating power
449.88	[MW]	Net electric power
57.091	[%]	recirculating fraction (pumping inclusio)
22.107	[%]	total efficiency

BLANKET VOLUMES AND COSTS

32.029	[m3]	FW volume
717.92	[m3]	volBlkBreed
31.849	[m3]	volBlkBackWall
297.76	[m3]	volHTS
33.937	[m3]	gap
438.89	[m3]	volLTS
370.68	[m3]	volManifold
591.26	[m3]	volEurofer
496.8	[m3]	volBe
110.56	[m3]	volLiSiO4
158	[m3]	volZrH
507.3	[Meuro]	costoTotEurofer
551.45	[Meuro]	costoTotBe
16.717	[Meuro]	costoTotLiSiO4
69.141	[Meuro]	costoTotZrH
1144.6	[Meuro]	TOT blanket cost (with learning factor)

POWER PLANT COSTS

442.19	[Meuro]	toroidal field coils
187.84	[Meuro]	poloidal field coils
54.889	[Meuro]	central solenoid
684.92	[Meuro]	TOT coils
400.6	[Meuro]	magnetic structure
565.81	[Meuro]	superconductors
1651.3	[Meuro]	TOT magnets
681.74	[Meuro]	vacuum vessel
1144.6	[Meuro]	blanket
139.49	[Meuro]	divertor

1141	[Meuro]	H&CD (heating and current drive)
75.461	[Meuro]	diagnostics
520.62	[Meuro]	cryostat
112.25	[Meuro]	fuel pumping
138.33	[Meuro]	tritium recirculating system
78.147	[Meuro]	remote handling
96.222	[Meuro]	TFC power supply
38.48	[Meuro]	PFC power supply
118.76	[Meuro]	electric generation systems (turbines)
394.05	[Meuro]	Electric systems
0	[Meuro]	Inductive storage system
528.76	[Meuro]	TOT electric systems
18.513	[Meuro]	thermal energy storage
57.287	[Meuro]	waste storage
146.55	[Meuro]	assembly
729.61	[Meuro]	civil
7282.4	[Meuro]	Total direct costs
1694.9	[Meuro]	Contingency
1409.1	[Meuro]	Owners costs
3104	[Meuro]	Indirect costs
10386	[Meuro]	Overnight cost
5103.9	[euro/kWt]	per unit of fusion power
23087	[euro/kW]	per unit of electric power
69.909	[%]	IDC
17647	[Meuro]	Investment cost (IDC included)
8.672	[euro/kWt]	per unit of fusion power
39.227	[euro/kW]	per unit of electric power
562.61	[euro/kWa]	O&M costs
13538	[Meuro]	BLK and DV replacement costs
63.426	[ceuro/kWh]	Cost of electricity in Euro 2000
524.39	[\$/MWh]	Cost of electricity in dollars 1990
87.55	[%]	investment
1.344	[%]	operation and maintenance
0.1442	[%]	fuel
10.962	[%]	BLK and DV replacements

2.14 FRESCO code – results

An application of the enhanced version of the Fresco code has presented at the SOFT 2016 conference with the title: “Economic assessment of different operational reactor cycle structures in a pulsed DEMO-like power plant”[125]

In this work the improvements introduced in the FRESCO code were used, especially the new modules for the evaluation of the pump-down time and the module for the coupling with the genetic algorithm, in order to perform an optimization study of the operative cycle of a pulsed power plant and to find an economic optimal solution. Since the operative cycle of a pulsed fusion power plant is composed by a sequence of phases, whose duration cannot be arbitrarily chosen, due to both technical and physical constraints, for each phase it has been set a range of acceptable value, where the genetic algorithm operates by changing randomly the parameters value order to find the optimal cost solution. The results of the study show that the solution region is populated by local minima. The absolute minimum is achieved when the phases composing the dwell time are minimized Figure 2-3. The absolute minimum is achieved when the phases composing the dwell time are minimized. In Table 2-2 it is summarized the relevant parameters for the DEMO-like pulsed power plant used in FRESCO, and in Table 2-3 the result of the optimization process with the genetic algorithm.

Table 2-2: Relevant parameters for the DEMO-like pulsed power plant modelling in FRESCO [125]

<i>Input to FRESCO code</i>	
Fusion power (MW)	2035
Electron temperature (keV)	13
Electron density (10^{19} m^{-3})	0.79
Pedestal	yes
Aspect ratio	3
Elongation, 95% surface	1.59
Triangularity, 95% surface	0.33
Safety factor at 95% flux surface	3
Effective charge	2.58
Bootstrap fraction (%)	34.8
H&CD wall-plug efficiency (%)	40
<i>FRESCO code output</i>	
Minor radius(m)	2.87
Major radius (m)	8.89
Average neutron wall loading (MW/m^2)	1.14
Plasma current (MA)	20
AF (%)*	80

Table 2-3: Results from optimization [125]

Results from optimization.

	Low cost	Medium cost	High cost
<i>Optimisation variables</i>			
τ_{CS} (s)	502	502	502
τ_{RU} (s)	200	200	200
τ_H (s)	7	8	10
τ_{burn} (s)	10692	7721	5690
τ_{RD} (s)	260	260	260
<i>Relevant parameters</i>			
Total cycle time	3 h 15'	2 h 25'	1 h 51'
τ_{FT} (s)	10699	7729	5700
τ_{dwell} (s)	962	962	962
Duty cycle	0.91	0.89	0.85
PP lifetime (y)	59	44	34
P_{CD} [MWth]	168	145	117
P_H [MWth]	0	0	0
Auxiliary power (MWe)	419	364	292
τ_E (s)	2.9	3.1	3.3
Q	12	14	17
Net electric power (MW)	375	390	290
COE (₁₉₉₀ EURcent/kWh)	73	83	102

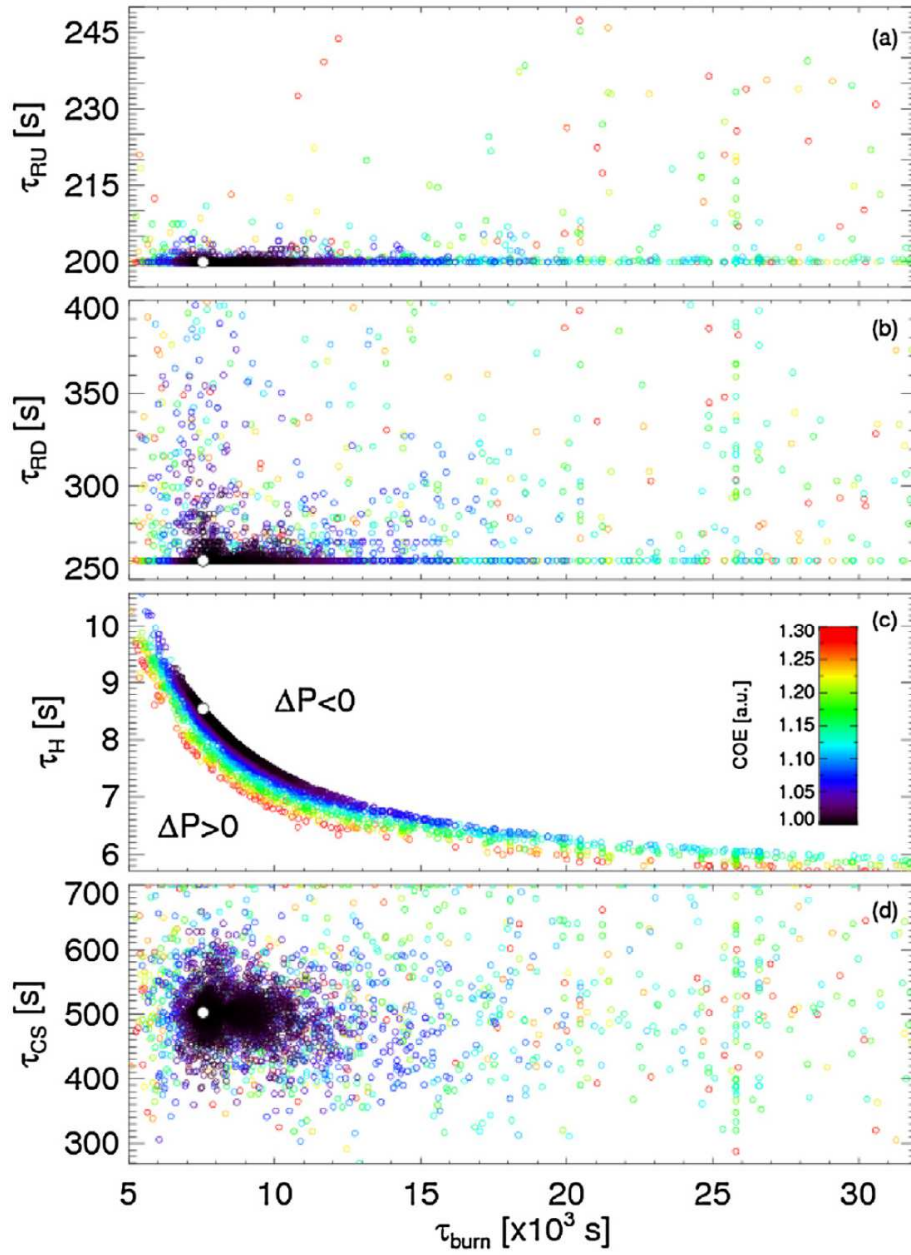


Figure 2-3: Relationship among τ_{burn} burn and the remaining optimization variables. The colour of the circles is a function of the COE. For the sake of clarity, only the solutions within 130% of the minimum COE are plotted (~6500 points). The white dot identifies the best case. In plot (c) ΔP is the additional power possibly required to raise the plasma temperature to burn conditions. [125]

3 COMESE code

The COMESE code (COsto MEDio del Sistema Elettrico, Average Cost of the Electric System), is a code developed at Consorzio RFX with the aim to have a computer tool able to verify energy scenarios presented in literature, and to develop, study and test the sustainability of new future energy scenarios. Originally, the first version of COMESE, here called COMESE-spreadsheet, it had been developed in my workgroup before the 2014, with the aim to investigate the Italian scenarios evolution up to 2050, with particular attention on renewable energy sources.

COMESE code-spreadsheet version featured a lot of limitation derived from the fact that it had been developed into a spreadsheet environment. The high number of worksheets that compose the COMESE-spreadsheet (eighteen worksheets) made it difficult to read and use. There wasn't a clear distinction of the input data from the calculation data and the output data. Formulas wasn't simple to read and it was difficult to modified because of the references linked with more than one worksheet. All of these issues converge in a rigidity to the subsequent improvement and result in more possibility of error in the use.

The doctoral activities encompassed the conversion and improvement of the COMESE code into a completely new version the COMESE code C++, a program written in a high level programming language. The choice of the C++ language was made for two reasons: firstly, the familiarity acquired during the study of FRESCO code, and secondly, the potential offered by the Object Oriented Programming, that permits to reuse portion of the code in a more easier way. The development of the code started from the beginning with the idea to create a modular code made of different section, class and methods, for having a program easy to use, control and maintain, and with the possibility to have a constant improvement for the next future.

COMESE code C++ like the previous one permits the study of new energy scenarios and to verify of their sustainability. The improvements added give the possibility to the users to simulate more scenarios in less time, they permit to verify if one scenario is able to satisfy the energy demand with an hourly resolution. The new COMESE code includes more powerful modules for managing an electric storage system, dispatchable technologies, and can do a Monte Carlo simulation for a stochastic analysis. COMESE code C++ includes the fusion technology as a possible power plant in future energy mix. The modular structure of the new COMESE code allows also to add in an easier way new power plant technologies, new storage system solutions, and to add new modules or to improve the existing ones without adapting the others to the new ones.

In this chapter it will be described the general structure of COMESE code C++, starting from how it works, then the structure of the program is presented, and finally, the sections of the program will be described in detail. The detailed description starts from the input files, than they will be described the modules that compose the central part of code, along with the description of the solutions adopted, and finally the output files will be presented with the main results of the simulation. For convenience in the next paragraph the word "COMESE code" will be referred to the new version "COMESE code C++".

3.1 The new version of COMESE code – COMESE code C++

COMESE code is a code for investigating possible future power system scenarios, the model adopting the assumption of a zero-dimensional network, i.e. transmission and distribution grids are not modelled in detail. All the generators, the storage systems and the loads are connected to the same node of the network. This is known as the copper plate assumption. The consequence of this assumption is that COMESE code do not calculate directly the grid cost of the network. The electric network cost is added as an additional cost at the end of the simulation.

The operation of the COMESE code can be divided in three main sections: a section for the preparation of the simulation with the creation of the folder for the results, and the loading of the input data (the scenario data and the load and generation profile), a section for the modelling of load, storage systems and power generation fleet. In these sections COMESE code meets the hourly demand profile with base power plants, must run power plants, the storage systems and finally the dispatchable power plants. The last section is for the economic assessment, where the cost of electricity is evaluated (COE) per each power plant, as well as the system Levelised Cost of Timely Electricity (LCOTE) and Monte Carlo simulations for the stochastic analysis of the LCOTE are performed. COMESE code can do a Monte Carlo Simulation with a maximum number of 1Msample - this limitation depends on the possibility to open the csv files of the result with a spreadsheet. But in principle the limit doesn't exist if the file is opened with more advance computer tools.

Figure 3-1 presents a flowchart that describes COMESE code operation. In grey boxes, they are presented the main input information used by COMESE code. In the white boxes the operations of the code. At the beginning COMESE code loads the scenario input file, where all the assumptions are collected for the energy scenario, i.e. the technology energy mix, the horizon year of the energy scenario, the total demand of electricity.

Then, the program loads the Load and Generation profile of the reference year for the must-run and special technologies. With the data of the scenario input file, the hourly data of the reference profile are scaled as a function of energy to obtain the Load and generation profiles over the time horizon. The new Load profile is taken as an objective, and in the second section of the COMESE code the program, like a dispatchable code, tries to distribute the generation of the power plants for meeting the Load.

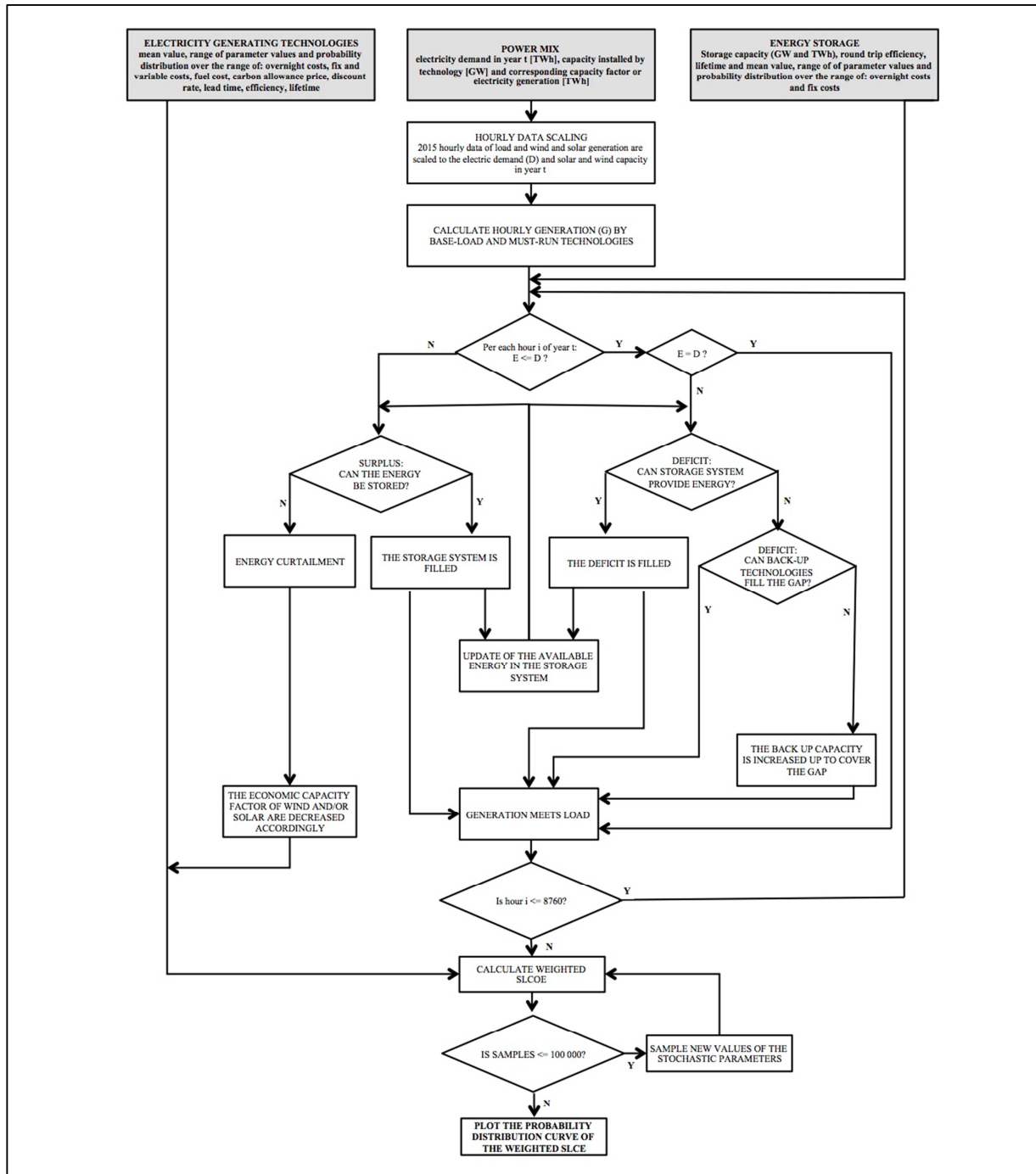


Figure 3-1: COMESE C++ flowchart.

In order to meet the Load, COMESE code activates at the beginning the base power plants with a constant generation profile, setting a power level equal to the average power over a year. The average power is calculated as the ratio of the energy generated by the base power plant, divided by the hours of one year. With this, it is assumed that a base power plant operates continuously for all the hours of the year, but with a power level lesser than the capacity installed and function of the capacity factor. Then COMESE code adds to the base generation the generation profiles of the must run technologies. At this point, COMESE code evaluates for each hour, where the generation exceeds the demand, the surplus condition, and where the generation remain under the demand, residual demand. It is obtained a vector for the hourly surplus and for the hourly residual demand.

Next step of COMESE code is the activation of the storage systems. COMESE code can activate one or more storage systems with a cascade mode, when the vector of the surplus and residual demand is scrolled by the routine: if it is found a surplus, the program will try to store the surplus in the first storage system; if this is full or it cannot receives more power in input because it reached the nominal one, the routine will store the energy in the first, and activate the second storage system for the remaining energy and so on. A similar procedure is used in the discharge, when a residual demand is found in one hour, the storage systems are activated in order for meeting the residual demand in function of the energy stored before and of the nominal power of the storage systems.

The energy storage activating procedure here is described in a simplified version, the discharge storage process has a more complex optimization routine which dialogues with the activation of dispatchable technologies. The routine controls hourly the input and output power from storage systems in order to reduce the capacity power installed for the dispatchable technologies. In the routine, it is assumed that in an electric system it is possible to have a prevision of the future Load of 3-4 days. For the description of the storage optimization methods, refer to the paragraph 3.14.

At this point COMESE code makes a second check of the surplus and residual demand, if the storage systems are too limited, it is possible that some energy cannot be stored, this energy will be curtailed. At the same time, it is possible that the residual demand was not fully met. COMESE code will pass now to the activation of the dispatchable technologies.

In function of the activation order specified in the scenario input file, COMESE code activates the dispatchable technologies. Important note: COMESE code does not increase automatically the energy level of all the dispatchable technologies fixed in the input data for the scenario, it only changes the capacity installed for some of them (specified in the input file), for covering the peak of power. At the end of the demand-generation calculation, it is possible that the generation cannot meet the Load, and the program returns a message of not feasible scenario. In this case, the code gives to the users all the information for correcting the initial input assumptions. The user will have then to decide how to correct the hypotheses of the input's scenario on the basis of the new information given by the simulation. This allows the verification of the sustainability of scenarios found for example in literature.

If at the end of the dispatchable activation routine there are surplus of generation, it is activated the curtailment routine, this routine cut the generation of the must-run technologies, some energy is thrown away, with the result of an increase COE of those technologies. All the energy generated in a scenario must be paid by the system including the curtailment.

The results of the COMESE code second section can be: the generation does not meet the Load, and the corrections on the scenario input assumptions are needed, or the generation meets the Load, and it is collected the information for the next economic analysis of the energy systems. I.e. The storage systems, if specified as unlimited in input, are fixed to the level for storing all the surplus, otherwise they are fixed to the input value, for all the technologies it is defined the real energy generated and the capacity installed.

At the beginning of the economic section, the last section of COMESE code, the program loads all the economic data for the technologies, and with the data obtained from the first load-generation analyses, it calculates for all the technologies the cost of electricity, then uses energy mix for evaluating the Levelized cost of timely electricity. The evaluation of the LCOTE is made weighting the COE of each technology with the energy used, and finally adding the additional cost of the storage system and the network. If in the simulation the Monte Carlo simulation is set with a number n of iterations, COMESE code iterates the evaluation of the COE of each technologies for n -times extracting the economic value from the interval of each parameter, and calculate n LCOTE for n systems. COMESE code returns as a result the deterministic value of the LCOTE, and a vector containing all the values of the Monte Carlo simulation. This vector can be elaborated in a post processing tools for obtaining the mode for LCOTE of the electric systems, and for plotting the probability distribution function of the LCOTE. An example of these analysis are given in chapter 4.

3.1.1 Files structure of the COMESE code C++

The COMESE code is made of around 20000 lines of code divided in 20 files. The main file named COMESE.cpp is composed by around 2600 lines of code that contain the heart of the program, which link together all the other files. The remaining 19 files are called “header file”. The header files can be grouped according to the function inside of the code.

The first group is the “Preparation files” that includes the instruction for creating the output result folders and the instruction for the simple command line interface, with which the user can set the names of the input file for the simulation. The secondo group is the Classes files (“Scenario.h”, “Storage.h”, “Technology.h”, “matriceDatiCarico.h”, “DatoMonteCarlo.h”). The Classes of the object oriented programming can be seen as the mould of the bricks that compose the COMESE code, in another way the classes is like a type of data (i.e. integer or double), but more advanced. They can store in an organized structure a lot of information and contain all the common functions, call methods, that can operate in the same type of data. The header file related to the calculus modules contain the instruction for the use of the dispatchable technologies, for the curtailment of the surplus energy, the evaluation of the interest on capital, the randomly extraction of a number from an interval. The last two groups of header file are the header file with all the auxiliary instruction, i.e. the routine for order a vector of data, and the header files containing the instruction for printing the results and prepare all the output tables.

Figure 3-2 presents the folder structure of the COMESE code C++. With the idea of making a clear distinction between the code files, input files and output files. In the main folder of COMESE code, three folders are presented: the folder “src” contain header files and the main file of the program; the input data folder contains the input data, and the output data folder contains the output data. Input and output files used in COMESE code are text file with the extension “.txt” and “.csv (MS-DOS)”. The csv text files were chosen for the output file, because they can be open and elaborate in an easier way with a spreadsheet.

COMESE code does not include graphical libraries, so all the post processing elaboration must be done with external codes. This aspect, with the idea to have a graphic user interface for the input data, it is one of the possible future improvements for the code.

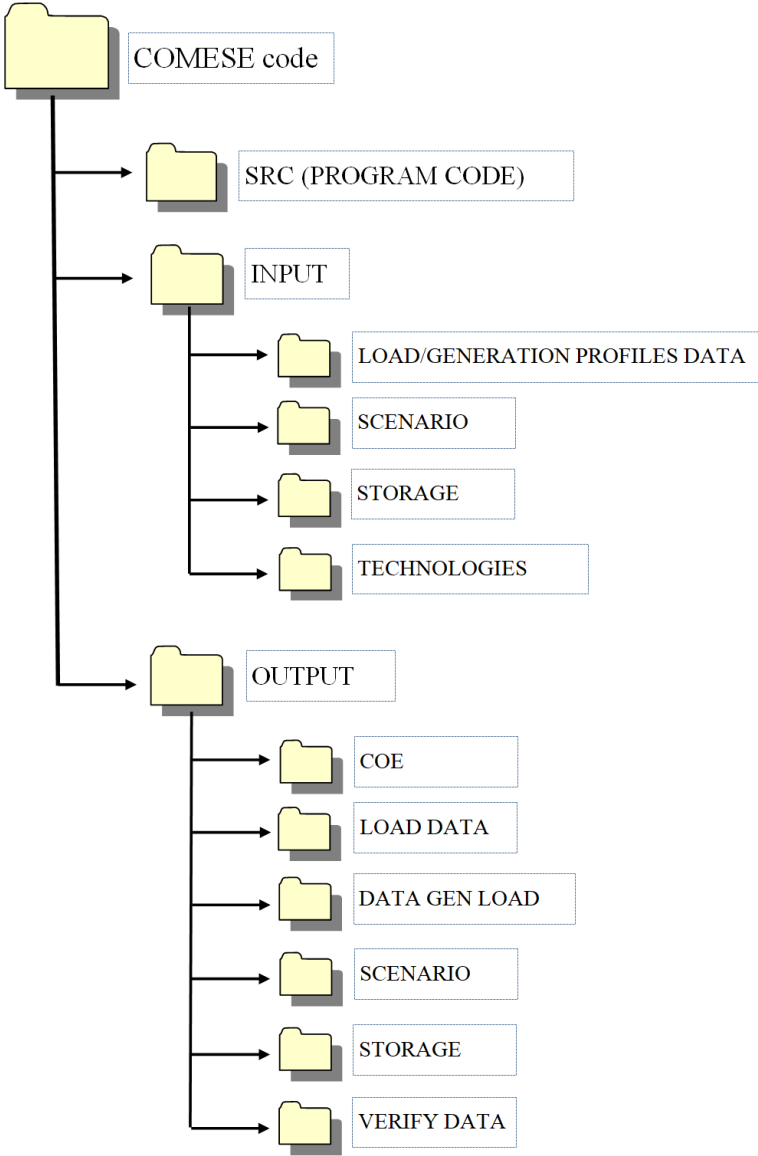


Figure 3-2: Folder structure of the COMESE code C++

In the input folder, there are four subfolders:

- Input Load Generation Data: contains all the Load and Generation profiles of must-run and special technologies used in the program for different years and countries.
- Input Scenarios: contains the input file that define a scenario.
- Input Storage: contains all the file defining the storage systems.
- Input technology: contains the input files for each technology, and one or more summary text files where it is written the list of technologies used for a simulation. The summary text file is

used as input of the COMESE code for indicating to the program which technology, present in the folder, must be loaded for the simulation.

The input files necessary for a simulation in COMESE code are:

- The scenario input file for the main assumption of the scenario.
- The Load profile, the reference profile of the demand of electricity from which COMESE code elaborates the Load profile for the simulation.
- The generation profiles, they are the generation profiles for the must run technologies and special technologies used for meeting the Load profile.
- The technology input files, containing all the information for the COE calculation for each technology.
- The storage input files, the ones with the economics and operative data for the storage systems
- The summary of the technologies used: list of the technologies input file used in the scenario simulation

All the input files are described in detail in the next paragraphs, where for each one it is given an example.

In the output file there are six subfolders:

- “Output COE”: it contains the result files of the LCOTE calculation and the data of the stochastic analysis.
- “Output Load Data”: it collects some of the intermediate data related to the simulation for meeting the total generation profile and the demand profile.
- “Output Data Gen Load”: it contains the intermediate tables printed at the end of the different sections for the filling of the load profile, and the final table that collects the results at the end of the section, when all the technologies have been activated.
- “Output Scenario”: it contains a summary of the scenario read as input, useful for the check of the reading information, and as a backup for reproducing the same result in a future simulation, and a summary of the scenario data before the economic calculations.
- “Output Storage”: it contains the matrices of data relate to the energy storage systems
- “Verify data”: in this folder it is located the file with all the message printed on the console, and for each technology and storage system, a text file with the voices of cost that compose the COE and the additional costs.

3.2 Input file - the scenario Input file

First input file for a scenario simulation in COMESE code is the scenario input file, this file containing the assumptions of the energy scenario. In Figure 3-3 is presented an example of the scenario input file. In this file, it is possible to find four zones highlighted in Figure 3-4. With A, B and C, it is marked the area of the data, with D the area for the comment, correspondent to the cells outside the rectangles. If something is written in the area D, it will be not read by the code; this is useful for leaving a comment inside of the input scenario data.

	A	B	C	D	E	F	G	H	I	J	
1	Scenario Name	Scenario_test									
2	Author	Daniele									
3	Creation data	ago-18									
4	Year time horizon	2080									
5	Reference year	2015									
6	Energy demand on the time horizon [TWh]	600									
7	Energy demand for reference year	-									
8	Annual growth rate [%]	-									
9	Parameters common to technologies	Base value	Mode	Min	Max	Distribution	Comment				
10	CO2 emissions cost [€/t]	0	-	-	-	-	Comment				
11	Discount rate [%]	0.05	-	-	-	-	Comment				
12	Import energy cost [€/kWh]	5	-	-	-	-	Comment				
13	Electric grid cost [€/kWh]	-	-	-	-	-	Comment				
14	Technologies used in the scenario	Share mix [%]	Energy [TWh]	Capacity installed [GW]	Equivalent hour of function [h]	Load factor [%]	Type of exerci	Order of intervention	Type of flexible activation	Comment	
15	Coal USC	0	0	0	0	100	Base		0	-	
16	Coal USC+CCS	0	0	0	0	100	Base		0	-	
17	Gas CCGT	0	0	0	0	0	Modulabile		3	PHDEF	
18	Gas CCGT+CCS	0	0	0	0	100	Modulabile		4	-	
19	Gas OCGT (back-up)	0	0	0	0	100	Modulabile		5	-	
20	Oil	0	0	0	0	0	Base		0	-	
21	Nuclear EPR	0	0	0	0	100	Base		0	-	
22	Nuclear SMR	0	0	0	0	100	Base		0	-	
23	Fusion	43.77961291	0	0	0	79.96575342	Intermittente		99	-	
24	Biogas (back-up)	0	0	0	0	100	Modulabile		6	-	
25	Biomass Waste	1.166666667	0	0	0	79.9086758	Base		0	-	
26	Bioenergy	3.154433794	0	0	0	62.78538813	Modulabile		2	PHDEF	
27	CSP with storage	0	0	0	0	45.66210046	Intermittente		61	-	
28	CSP without storage	0	0	0	0	100	Intermittente		20	-	
29	Wind onshore	7.283333333	0	0	0	21.68949772	Intermittente		81	-	
30	Wind offshore	0.666666667	0	0	0	22.83105023	Intermittente		82	-	
31	Floating Wind	0	0	0	0	100	Intermittente		83	-	
32	PV commercial roofs	17.93833333	0	0	0	13.69863014	Intermittente		71	-	
33	PV residential roofs	4.58	0	0	0	13.69863014	Intermittente		72	-	
34	PV utility scale (ground)	15.64833333	0	0	0	17.12328767	Intermittente		73	-	
35	Geothermal	1.314	0	0	0	90	Base		0	-	
36	Dam Hydro	5.226666667	0	0	0	27.96803653	Modulabile		1	TRP	
37	Hydro run of river	5.9	0	0	0	50.51369863	Intermittente		51	-	
38	Import	0	0	0	0	100	Base		0	-	
39	TOTAL	106.6580467	-	-	-	-	-		-	-	

Figure 3-3: Example of scenario input file “Scenario_test.csv”

1	Scenario Name	Scenario_test									
2	Author	Daniele									
3	Creation data	ago-18									
4	Year time horizon	2080									
5	Reference year	2015									
6	Energy demand on the time horizon [TWh]	600									
7	Energy demand for reference year	-									
8	Annual growth rate [%]	-									
9	Parameters common to technologies	Base value	Mode	Min	Max	Distribution	Comment				
10	CO2 emissions cost [€/t]	0	-	-	-	-	Comment				
11	Discount rate [%]	0.05	-	-	-	-	Comment				
12	Import energy cost [€/kWh]	5	-	-	-	-	Comment				
13	Electric grid cost [€/kWh]	-	-	-	-	-	Comment				
14	Technologies used in the scenario	Share mix [%]	Energy [TWh]	Capacity installed [GW]	Equivalent hour of function [h]	Load factor [%]	Type of exerci	Order of intervention	Type of flexible activation	Comment	
15	Coal USC	0	0	0	0	100	Base		0	-	
16	Coal USC+CCS	0	0	0	0	100	Base		0	-	
17	Gas CCGT	0	0	0	0	0	Modulabile		3	PHDEF	
18	Gas CCGT+CCS	0	0	0	0	100	Modulabile		4	-	
19	Gas OCGT (back-up)	0	0	0	0	100	Modulabile		5	-	
20	Oil	0	0	0	0	0	Base		0	-	
21	Nuclear EPR	0	0	0	0	100	Base		0	-	
22	Nuclear SMR	0	0	0	0	100	Base		0	-	
23	Fusion	43.77961291	0	0	0	79.96575342	Intermittente		99	-	
24	Biogas (back-up)	0	0	0	0	100	Modulabile		6	-	
25	Biomass Waste	1.166666667	0	0	0	79.9086758	Base		0	-	
26	Bioenergy	3.154433794	0	0	0	62.78538813	Modulabile		2	PHDEF	
27	CSP with storage	0	0	0	0	45.66210046	Intermittente		61	-	
28	CSP without storage	0	0	0	0	100	Intermittente		20	-	
29	Wind onshore	7.283333333	0	0	0	21.68949772	Intermittente		81	-	
30	Wind offshore	0.666666667	0	0	0	22.83105023	Intermittente		82	-	
31	Floating Wind	0	0	0	0	100	Intermittente		83	-	
32	PV commercial roofs	17.93833333	0	0	0	13.69863014	Intermittente		71	-	
33	PV residential roofs	4.58	0	0	0	13.69863014	Intermittente		72	-	
34	PV utility scale (ground)	15.64833333	0	0	0	17.12328767	Intermittente		73	-	
35	Geothermal	1.314	0	0	0	90	Base		0	-	
36	Dam Hydro	5.226666667	0	0	0	27.96803653	Modulabile		1	TRP	
37	Hydro run of river	5.9	0	0	0	50.51369863	Intermittente		51	-	
38	Import	0	0	0	0	100	Base		0	-	
39	TOTAL	106.6580467	-	-	-	-	-		-	-	
40											

Figure 3-4: zones of the scenario input file

In the section A of the Figure 3-4, zoomed in Figure 3-5, they are specified:

- name of the scenario,
- author,
- date, when the scenario input file was created,
- the year to whom the scenario refers (i.e. 2080),
- the reference year used for generation and demand profiles
- the total energy demand of the scenario in [TWh] or alternatively the energy demand of the reference year in [TWh] with the annual grow rate in [%]

When it is specified the energy demand of the reference year and the annual grow rate, the demand of the horizon year is calculated with the equation:

$$(3.1) \quad En_{horizon} = En_{reference} \cdot (1 + grow\ rate)^n$$

$$(3.2) \quad n = horizon\ year - reference\ year$$

Otherwise it is used the value specified in the field “Energy demand on the time horizon”.

	A	B
1	Scenario Name	Scenario_test
2	Author	Daniele
3	Creation data	ago-18
4	Year time horizon	2080
5	Reference year	2015
6	Energy demand on the time horizon [TWh]	600
7	Energy demand for reference year	-
8	Annual growth rate [%]	-

Figure 3-5: Section A

In the section B, Figure 3-6, they are summarized the input information common to the scenario simulation and used both in the final calculation of the COE of each technology and in the evaluation of the Levelised Cost of Timely Electricity (LCOTE):

- the CO2 emission cost [€/t]
- the discount rate [%],
- the import energy cost [€/kWh]
- the electric grid cost [€/kWh]

The electric grid cost is added directly to the LCOTE of the system as an additional cost, because the COMESE code actually do not simulate the electric network (one node assumption of copper plate assumption).

9	Parameters common to technologies	Base value	Mode	Min	Max	Distribution
10	CO2 emissions cost [€/t]		0 -	-	-	-
11	Discount rate [%]		0.05 -	-	-	-
12	Import energy cost [€/kWh]		5 -	-	-	-
13	Electric grid cost [€/kWh]	-	-	-	-	-

Figure 3-6: Section B

14	Technologies used in the scenario	Share mix [%]	Energy [TWh]	Capacity installed [GW]	Equivalent hour of function [h]	Load factor [%]	Type of exerci	Order of intervention	Type of flexible activation
15	Coal USC	0	0	0	0	100	Base	0	-
16	Coal USC+CCS	0	0	0	0	100	Base	0	-
17	Gas CCGT	0	0	0	0	0	Modulabile	3	PHDEF
18	Gas CCGT+CCS	0	0	0	0	100	Modulabile	4	-
19	Gas OCGT (back-up)	0	0	0	0	100	Modulabile	5	-
20	Oil	0	0	0	0	0	Base	0	-
21	Nuclear EPR	0	0	0	0	100	Base	0	-
22	Nuclear SMR	0	0	0	0	100	Base	0	-
23	Fusion	43.77961291	0	0	0	79.96575342	Intermittente	99	-
24	Biogas (back-up)	0	0	0	0	100	Modulabile	6	-
25	Biomass Waste	1.166666667	0	0	0	79.9086758	Base	0	-
26	Bioenergy	3.154433794	0	0	0	62.78538813	Modulabile	2	PHDEF
27	CSP with storage	0	0	0	0	45.66210046	Intermittente	61	-
28	CSP without storage	0	0	0	0	100	Intermittente	20	-
29	Wind onshore	7.283333333	0	0	0	21.68949772	Intermittente	81	-
30	Wind offshore	0.666666667	0	0	0	22.83105023	Intermittente	82	-
31	Floating Wind	0	0	0	0	100	Intermittente	83	-
32	PV commercial roofs	17.93833333	0	0	0	13.69863014	Intermittente	71	-
33	PV residential roofs	4.58	0	0	0	13.69863014	Intermittente	72	-
34	PV utility scale (ground)	15.64833333	0	0	0	17.12328767	Intermittente	73	-
35	Geothermal	1.314	0	0	0	90	Base	0	-
36	Dam Hydro	5.226666667	0	0	0	27.96803653	Modulabile	1	TRP
37	Hydro run of river	5.9	0	0	0	50.51369863	Intermittente	51	-
38	Import	0	0	0	0	100	Base	0	-
39	TOTAL	106.6580467	-	-	-	-	-	-	-

Figure 3-7: Section C

The last section of the scenario input file is the section C, Figure 3-7, here they are specified for each technology the energy mix, the capacity installed, the load factor, the type of exercise, and the order and mode of intervention.

In the 1st column there are the names of the technologies currently planned in COMESE code, in the 2nd column the share mix of the technologies expressed in percentage value respectively to the total demand of electricity of the scenario (Figure 3-4 the field “Energy demand on the time horizon”) . The 3rd column can be used instead of the second one for defining the energy mix, using the energy instead the percentage value. All the values will be expressed in [TWh]. In Figure 3-7 the 3rd column is empty, because in the example it is use the 2nd one.

The 4th column contains the capacity installed for each technology and the 5th the equivalent hours of production. The 4th and 5th columns are used alternatively to the 6th one where it is specified the Load Factor or the Capacity Factor. The knowledge of the Load Factor and the share mix of a technology are the minimum information for calculating the value of the 4th and 5th columns.

In the 7th column it is specified the type of exercise of a technology, the possibilities are: “Base” corresponding a base power plant technology, “Modulabile” corresponding to a dispatchable generation technology, and “Intermittente” corresponding to a must-run technology. Depending on the type of exercise defined in the 7th column, to each technologies it is defined the order of intervention in the 8th column. Base power plant technologies have the higher priority here indicated with 0. The must run technologies have a unique number for the order of intervention, this value is important for the correct simulation of COMESE code. The number range for the must run technology is:

- 51-59 must-run hydroelectric technologies,
- 61-69 CSP technologies,
- 71-79 photovoltaic technologies
- 81-89 wind technologies
- 99 fusion technology.

If the dispatchable technologies are for example six, the order of intervention go from 1, the first that will be used, to 6, the last one used in for the peak generation. Only for the dispatchable technologies it is used the 9th column. In this column, for each dispatchable technology, it is written an acronym that specifies to the COMESE code which type of dispatchable routine must be used in the activation of that technology. The possibilities are three:

- “CMOD” – common mode. It is the default method, when COMESE finds a residual demand at the hour h, it activates the dispatchable technology up to its maximum level defined by the capacity installed, and until all the energy allocated for that technology has not been used.
- “PHDEF” – power hours deficit. It is an advance method of activation, this method is used for maximizing the hours of generation, varying the installed power.
- “TRP” – trapezoidal. It is an advanced method of activation, this method is used for maximizing the use of that technology, when there is the maximum value of residual demand of electricity, using as much as possible the maximum power installed.

The three methods of activation are deeply described in the paragraph 3.15.

3.3 Input file - the Load and Generation profile source for the data

In the input data of COMESE code, there are hourly profiles for Load (demand of electricity) and generation (hourly power generated by a type of power plant). The generation profiles loaded in the COMESE code are profiles for the must-run power plant technology, and the profile defined as special like the fusion technology generation profile. The electricity generation of these technologies is characterized by a seasonal trend like the hydroelectric run of a river technology, daily trend connected to the day-night cycle, for example the photovoltaic generation or a high variable trend i.e. the wind generation. All profiles are strongly influenced by the climate of a specific country, so in the COMESE code they are used like a reference for the future years, assuming that the trend doesn't change in the future.

Load profile represents the hourly demand of electricity of a country and for a year, this type of profile is used in the first section of COMESE code like an objective profile. The first section of the code tries to fill the Load profile, and it reaches the balance between generation and demand, with an appropriate mix of technologies chosen in the scenario input file (see paragraph 3.2 for an example of the input file for the scenario). The energy mix is composed of base power plant, must run power plant (i.e. photovoltaic - PV or WIND), storage system and dispatchable power plant. Dispatchable power plant is the only technology whose level of capacity installed can be changed inside of the simulation for reaching the balance between demand of electricity and generation.

Generation profile represents the hourly power generation of a specific type of power plant for one year. The profiles data are obtained from the national energy agencies, that registered the data year by year and made it available in the specific national web database. For the Italian system, Terna and GSE give these statistical data. At the European level, in the recent years it is active a huge database, recently updated with a new web page, the ENTSO-E transparency platform that collects all the data from the European country, including the Load and Generation data needed for the COMESE code simulation. Another useful database for collecting the profile, it is the Data Platform portal, where it is collected the European power system data, and some data taken also on the ENTSO-E database. Data Platform portal collects in a unique file all the data of each country and for more years, with a structure easier to use and standardized to the hour resolution. Some countries (i.e. Belgium, United Kingdom) provide Load and generation profiles with a resolution of half an hour or fifteen minutes.

In Table 3-1 it is presented an overview of the data collected and elaborated by the Data Platform portal based on ENTSO-E transparency platform and ENTSO-E power statistics for the 2015 with information about the completeness of the data. One main problem found during the collection of the data is that often the time series are incomplete. If the missing information is limited to few hours, the profiles can be completed manually with an interpolation; in case of missing information longer than a week, the profiles must be classified as unusable. In Table 3-1 for the 2015 they are indicated:

- in green with CD the countries with a complete information,
- in orange with ID the countries with a partial information for which is possible to recover the profile with an interpolation,
- in red with MD the countries with unusable profile where they are missing an high amount of data
- and with ND the data absent in that country.

Table 3-1: In this table, it is summarised the status of the data collected from the Data Platform portal database and base on the ENTSO-E data. In green “CD” indicates the complete hourly profile, in orange “ID” the profile with a low number of missing data, in red “MD” the profile with the higher number of missing information, and “ND” the data profile not present in that nation. In the table, they are shown in bold the nations with the dataset in the best condition.

Analysis of completeness of load and generation data for 2015 – data collected from OpenDataDatabase and based on Entsoe power statistics (EPS) and Entsoe transparency (ET)						
Complete Data - CD		Incomplete Data - ID		Missing Data - MD		No Data - ND
Acronym	Country	Load (EPS)	Load (ET)	PV	Wind onshore	Wind offshore
AT	Austria	CD	CD	CD	CD	ND
BE	Belgium	CD	ID	MD	MD	MD
BG	Bulgaria	CD	CD	CD	CD	ND
CH	Switzerland	CD	CD	MD	MD	ND
CY	Cyprus	CD	ND	ND	MD	ND
CZ	Czech Republic	CD	CD	CD	CD	ND
DE	Germany	CD	CD	CD	CD	ND
DK	Denmark	CD	CD	CD	CD	CD
EE	Estonia	ID	ID	MD	MD	ND
ES	Spain	CD	ID	ID	ID	ND
FI	Finland	CD	ID	ND	ID	ND
FR	France	CD	CD	CD	CD	ND
UK	United Kingdom	CD	CD	CD	CD	CD
GR	Greece	MD	CD	ID	ID	ND
HR	Croatia	CD	CD	ND	ND	ND
HU	Hungary	CD	CD	ND	CD	ND
IE	Ireland	CD	ID	ND	MD	ND
IT	Italy	CD	CD	CD	CD	ND
IS	Iceland	CD	ND	ND	ND	ND
LT	Lithuania	CD	MD	MD	MD	ND
LU	Luxembourg	CD	CD	ND	ND	ND
LV	Latvia	CD	CD	ND	CD	ND
ME	Montenegro	CD	CD	ND	ND	ND
MK	Republic of Macedonia	CD	MD	ND	ND	ND
NL	Netherlands	CD	CD	MD	MD	MD
NO	Norway	CD	MD	ND	CD	ND
PL	Poland	CD	CD	ND	CD	ND
PT	Portugal	CD	CD	CD	CD	ND
RO	Romania	CD	MD	MD	MD	ND
RS	Serbia	CD	MD	MD	ND	ND
SE	Sweden	CD	MD	CD	MD	CD
SL	Slovenia	CD	CD	CD	CD	ND
SK	Slovakia	CD	ID	MD	ND	ND

For 2015 the data of Load from ENTSO-E power statistic are complete for all the countries. A great number of incomplete and missing information is present for the PV and wind onshore profiles. Only few countries have a profile for wind offshore and generally those profiles are complete. In Table 3-1 are shown bold the countries with the most complete data, for these countries in Table 3-2 are presented the total of the energy demand and the total generation calculated from the respective

profile. One important thing to note is the profile for PV and wind onshore generation given by Germany are in the normalized format.

Table 3-2: Total energy demand and generation for some European countries

Total energy demand and total generation calculate from the data collected from the open database for the nation with the data in the best condition. All the value is express in [TWh]						
Acronym	Country	Load (EPS)	Load (ET)	PV	Wind onshore	Wind offshore
AT	Austria	69.62	59.16	0.82	4.91	-
BG	Bulgaria	38.62	37.73	1.35	1.41	-
CZ	Czech Republic	63.53	63.5	2.2	0.56	-
DE	Germany*	505.27	477.92	Norm*	Norm*	-
DK	Denmark	33.89	32.82	0.61	9.3	4.83
ES	Spain**	248.5	261.63**	12.75**	47.95**	-
FR	France	471.26	470.08	7.17	19.6	-
UK	United Kingdom	282.19	334.83	7.66	18.42	14.11
HU	Hungary	40.75	41.59	-	0.64	-
IT	Italy	314.35	314.35	1.09	14.65	-
LV	Latvia	7.07	7.07	-	0.1	-
PL	Poland	149.96	161.35	-	10.64	-
PT	Portugal	48.93	51.92	0.76	11.33	-
SE	Sweden***	135.93	133.22***	0.029	16.41***	16.8
SL	Slovenia	13.65	12.31	0.28	-	-
*Germany gives for PV and Wind onshore generation the normalized profile here indicated as Norm ** Spain, the data are obtained from incomplete profile recovered by interpolation *** Sweden, the data here indicated are the total value obtained from a missing profile; here Sweden is placed in the table because it is one of the countries that has a complete profile for wind offshore generation						

In Table 3-2 they are shown in bold six European countries chosen for having a complete profile and for the geographical position in the European Union. The countries chosen are the United Kingdom in the north, Italy in the south, Portugal in the west, Poland in the east, and Germany and France at the centre of Europe. For all these nations in the next paragraph they are given an overview of Load and generation profile. It is done a comparison between the regions of Europe, and for the Italian and the United Kingdom profiles a comparison for different years. In the same paragraph, it is presented the methodology used in COMESE code for creating the Load and generation profile for future scenarios, with major attention to the profiles that don't exist actually i.e. the generation profile for fusion technology or the wind offshore profile with 3800 equivalent hours of generation.

3.4 Load profile

Load profiles record the demand of electricity of a nation with an hourly resolution or higher (15 or 30 minutes). Figure 3-8, Figure 3-9, Figure 3-10 show examples of Load profile from 2015 to 2017 for the Italian national electric system, with the particular case of 2016. With the intention to compare simulation based on the 2016 profile respect to the other years, the Load profile of 2016 is modified for obtaining year profiles of 365 days. Two profiles were created:

- 2016_365_no29 profile obtained with the elimination of the 29 of February (Figure 3-11),
- 2016_365_noEND profile obtained with the elimination of the 31 of December (Figure 3-12).

The first solution (Figure 3-11) is obtained with the elimination of one day inside the year the 29th of February, the second one with the elimination of the last day of the year 31st of December (Figure 3-12). The two profiles do not have difference in the seasonal trend but for the order of the days in the weeks, the elimination of one day inside the year causes a shift of the days inside a week from the cancel day until the end of the year. The consequence is a modified sequence of working day and week-end days, working days and week-end days are characterized by a different demand of electricity, and this can cause a possible incorrect hourly evaluation between generation and demand. The second solution (Figure 3-12) doesn't have this problem and in the simulation it is preferable to the first one.

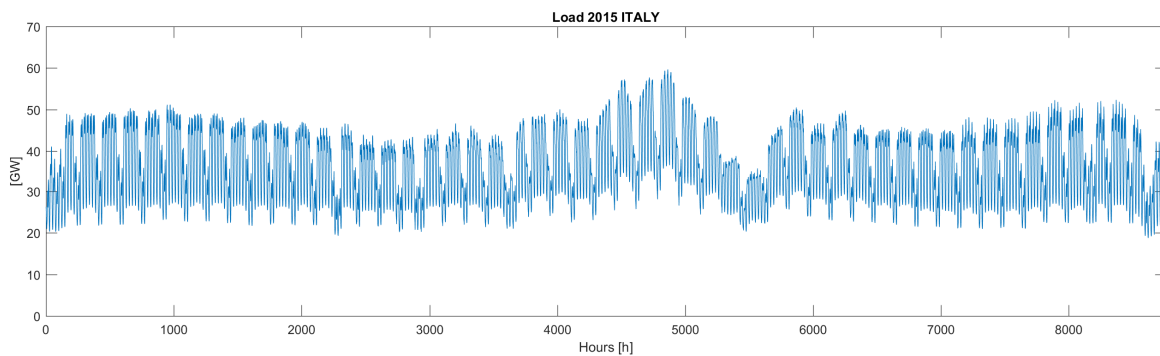


Figure 3-8: Load electricity profile for Italian Nation 2015

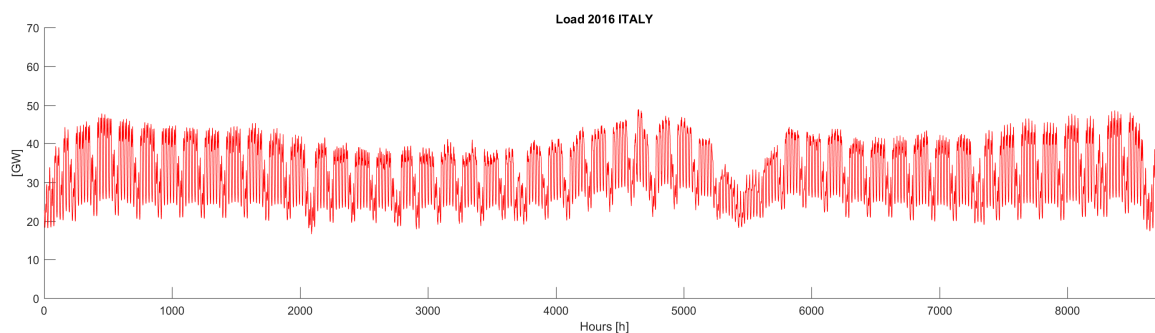


Figure 3-9: Load electricity profile for Italian Nation 2016 with 366 days

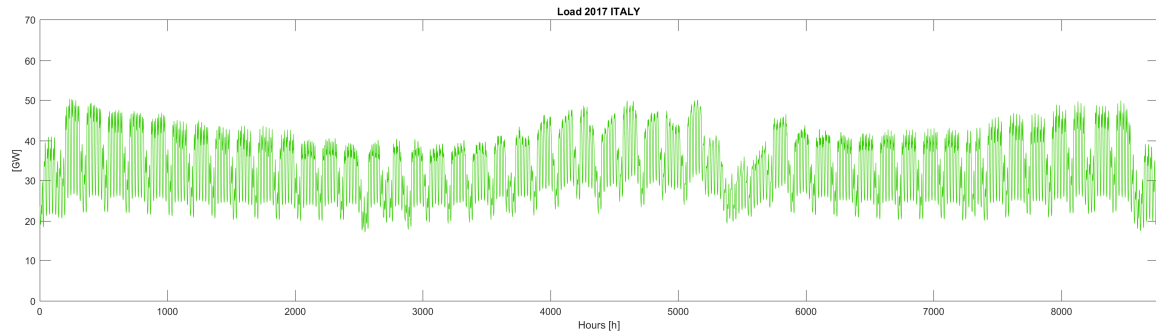


Figure 3-10: Load electricity profile for Italian Nation 2017

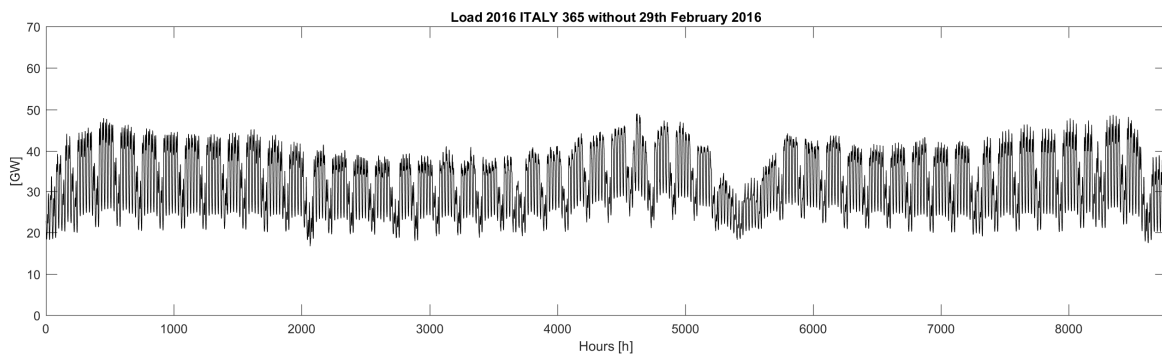


Figure 3-11: Load electricity profile for Italian Nation 2016 mod, profile modified for having an year of 365 days without the 29th of February

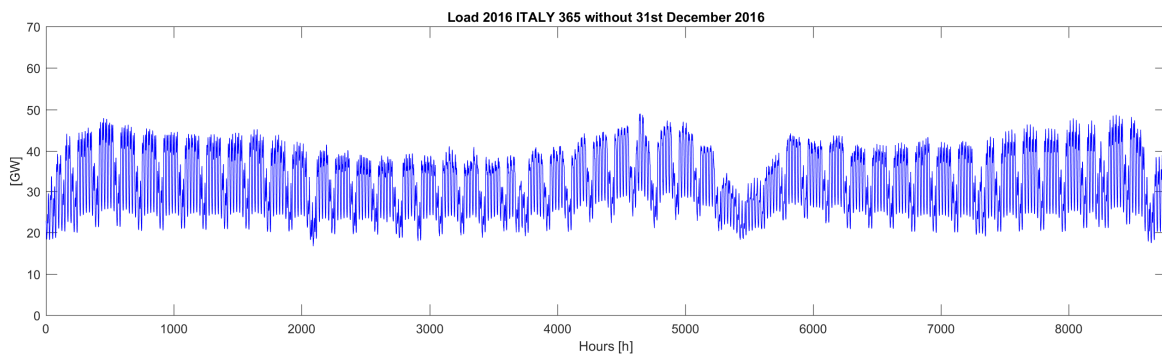


Figure 3-12: Load electricity profile for Italian Nation 2016 mod, profile modified for having an year of 365 days without the 31st of December. This profile maintains the correct order of the days in the week.

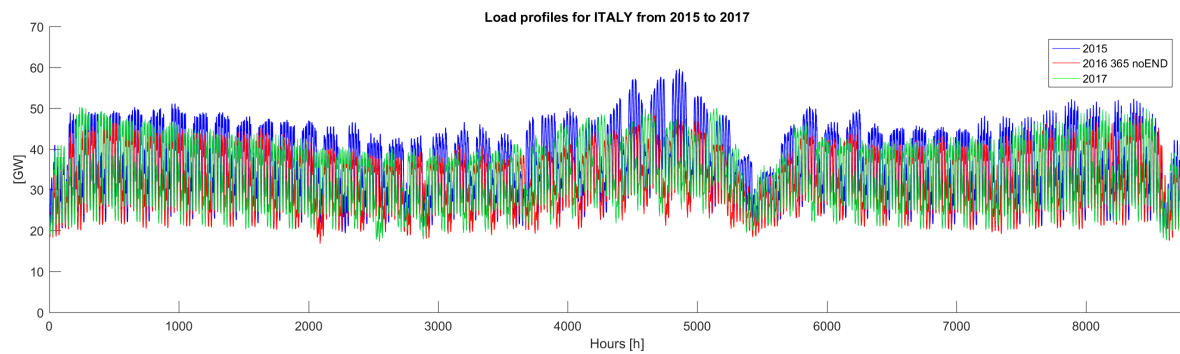


Figure 3-13: Comparison of the three Load profiles for Italian Nation for the year 2015, 2016 without the 31st of December, 2017. It is s clearly visible the similar trend for different years.

In Figure 3-13 three Load profiles for the Italian case are compared: all the present profiles have the same number of days, and have the same global trend along the year including, summer peak demand in June-July and subsequent decline in August. It is possible to observe the different level of demand in terms of electric power higher in 2015, it becomes lower in 2016 and grows in 2017. This signals a recovery in electricity consumption in the future years.

3.5 How COMESE uses load profile of a reference year

For a scenario simulation COMESE code uses the Load profile of a reference year (i.e. 2015) for determining the profile of a future scenario. Given that the global trend doesn't change from 2015 to 2017, Figure 3-13, in COMSE code it is assumed for simplification that the profile trend doesn't change in the future. For determining the new profile, COMESE code calculates the total energy of the reference profile (in this example the Load profile of 2015 for Italy) as integral over the entire year of the hourly power demand and it compares the result with the total demand of electricity defined in the scenario input file. Because the data provided is discrete in nature, hourly profiles, the integral is simply computed as a summation of terms with the equation 3.3.

$$(3.3) \quad E_{n \text{ ref}} = \sum_{h=1}^{8760} P_i \Delta t \text{ [MWh]}$$

Where with P_i [MW] it is indicated the power demand of electricity of the hour i of the year, and $\Delta t = 1$ hour. The new profile is obtained with a proportional scaling using the scaling factor calculated by the ratio of the desired value of the total demand for the new scenario, and the value of the reference profile. See equation 3.4.

$$(3.4) \quad f_{\text{scale}} = \frac{E_{n \text{ scenario}}}{E_{n \text{ ref}}}$$

Equation 3.5 describes how it is evaluated the proportional coefficient for scaling, $P_{i \text{ scenario}}$ is the new hourly power demand in the new profile.

$$(3.5) \quad E_{n \text{ scenario}} = f_{\text{scale}} E_{n \text{ ref}} = f_{\text{scale}} \sum_{h=1}^{8760} P_i \Delta t = \sum_{h=1}^{8760} f_{\text{scale}} P_i \Delta t = \sum_{h=1}^{8760} P_{i \text{ scenario}} \Delta t$$

$$(3.6) \quad P_{i \text{ scenario}} = f_{\text{scale}} P_i \text{ [MW]}$$

Figure 3-14 shows an example of the scaling process, in red the reference profile for the 2015 for Italy correspondent to a demand of electricity of 314 TWh and in blue the new profile with a demand of electricity of 600 TWh. The scaling factor used is $f_{\text{scale}} = 1.90871$.

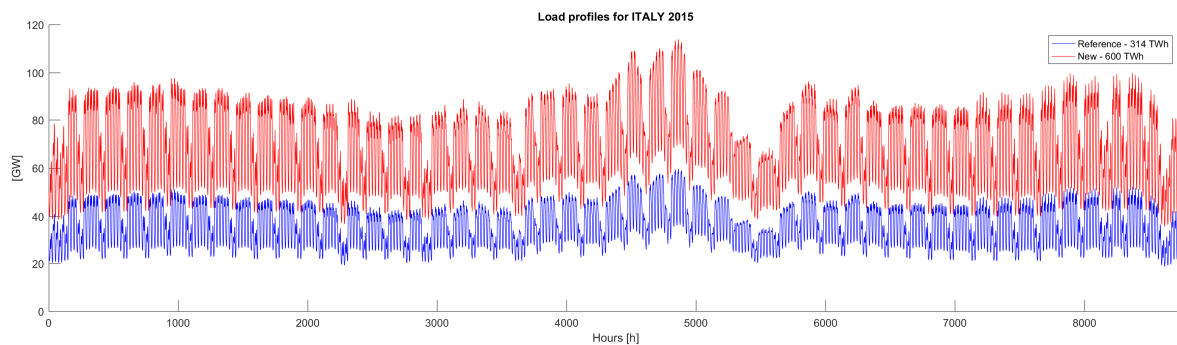


Figure 3-14: Reference Load profile Italy 2015 with demand of electricity of 314 TWh (blue), and new profile with a total demand of electricity of 600 TWh (red).

3.6 European Load profiles

One of the strengths of COMESE code is its flexibility; the program is completely transparent to the nation profiles used for the simulation. So it is possible to simulate scenarios of any nations, starting from the corresponding input data. Here the Load profiles of different European countries for 2015 are presented. In Figure 3-15 they are indicated the European countries selected among those for which complete data are available for Load and generation profile. See the Table 3-2 for a list of European countries with a complete set of data for the 2015. The regions here chosen are Germany Figure 3-17 and France Figure 3-18 for the central Europe, the United Kingdom Figure 3-20 for the north Europe, Portugal Figure 3-19 for the south west of Europe, Poland Figure 3-21 for the east Europe and Italy Figure 3-16 for the south of Europe. Italy is taken as an example of nation with an high level of photovoltaic generation and low wind generation, at the opposite side the United Kingdom with low photovoltaic generation and high generation of wind onshore and offshore power plant. Portugal is taken as an example of European country of the south of Europe, but near the ocean so with generation both from photovoltaic a wind, Poland as an example of nation without photovoltaic generation. And finally, Germany and France more central in the UE and characterized by the highest level of electrical demand.

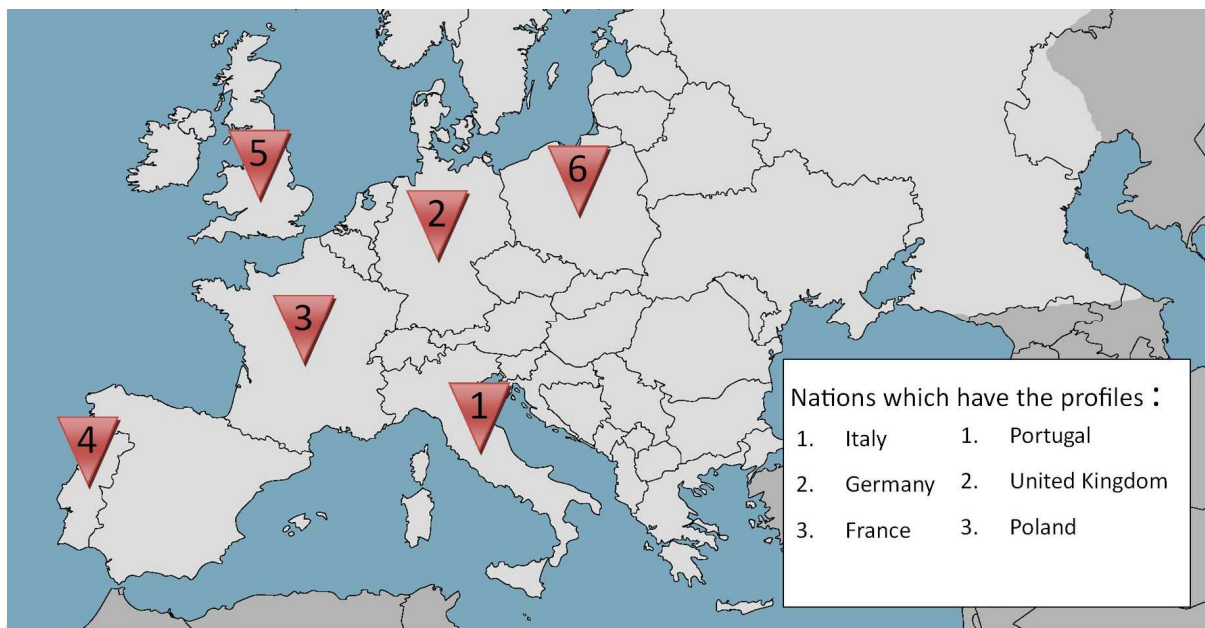


Figure 3-15: position of the European country considered for the profiles presented

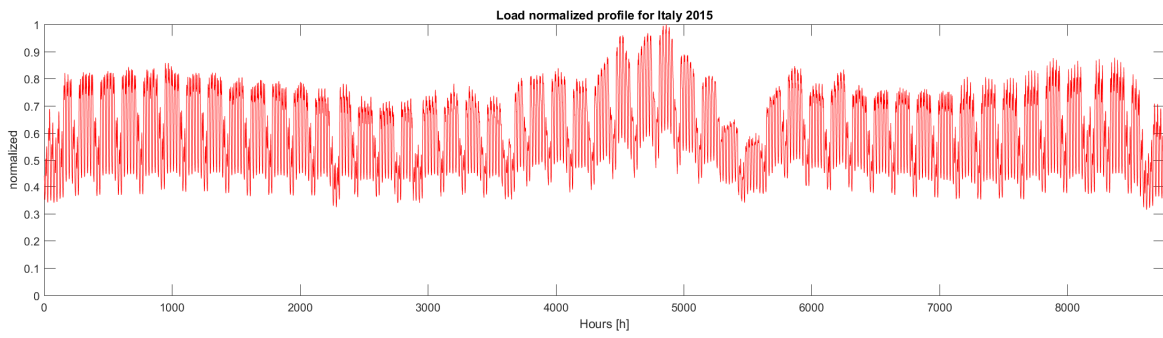


Figure 3-16: Normalized Load profile for Italy, $E_n=314$ TWh, $P_{max}=59.6$ GW

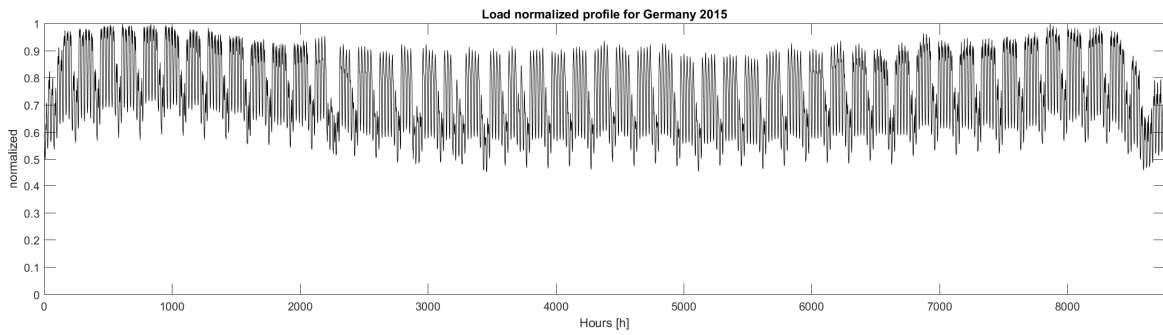


Figure 3-17: Normalized Load profile for Germany, $E_n=505$ TWh, $P_{max}=77.3$ GW

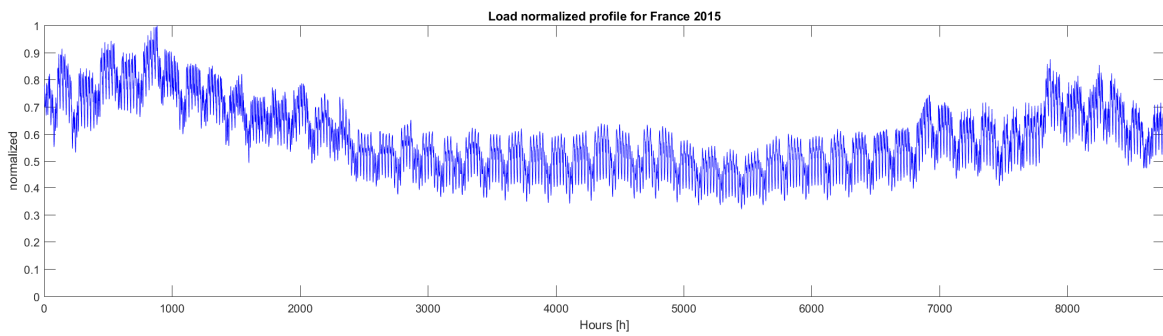


Figure 3-18: Normalized Load profile for France, $E_n=471$ TWh, $P_{max}=91.6$ GW

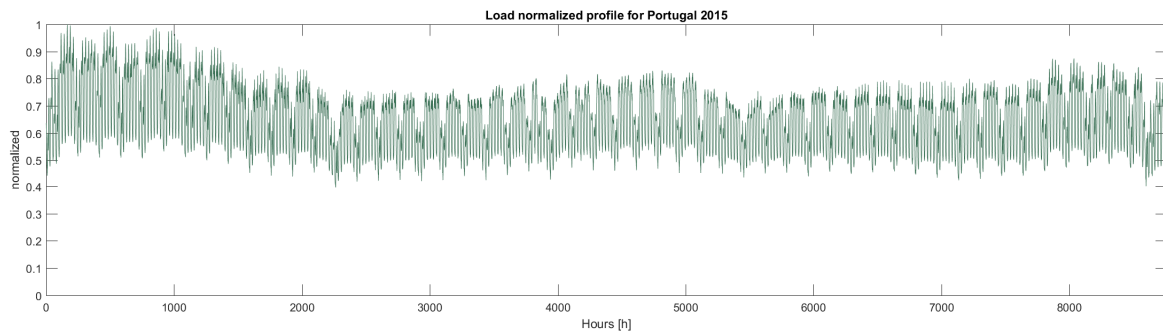


Figure 3-19: Normalized Load profile for Portugal, $E_n=48.9$ TWh, $P_{max}=8.62$ GW

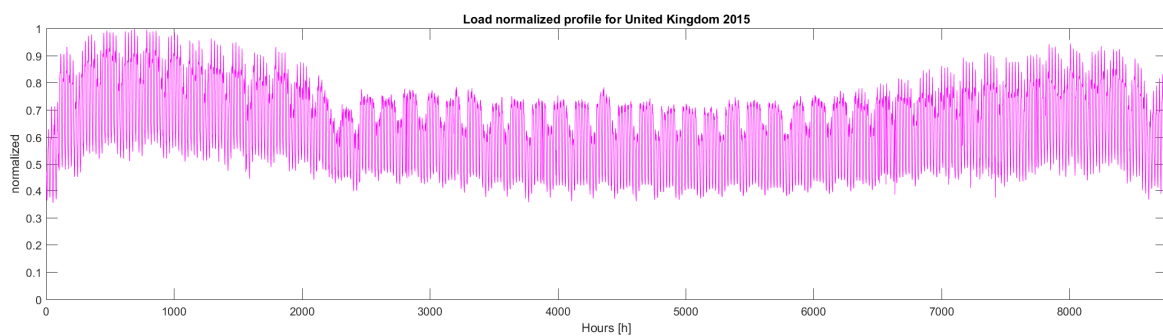


Figure 3-20: Normalized Load profile for United Kingdom, $E_n=335$ TWh, $P_{max}=59$ GW

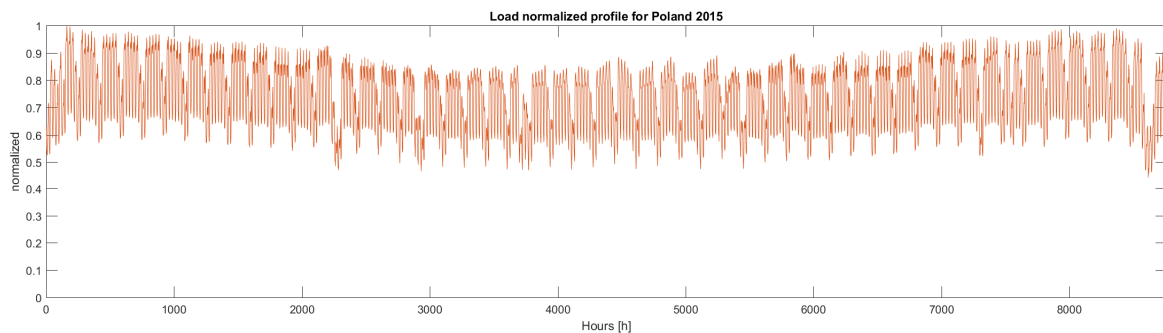


Figure 3-21: Normalized Load profile for Poland, $E_n=150$ TWh, $P_{max}=23.1$ GW

The Italian profile, as described before, Figure 3-16 is characterized by a peak of electric power demand in June-July with a strong reduction of the demand in August. The trend in the rest of the year is approximately constant, the demand of electricity is greater in the winter period, it decreases slowly in the spring month. The German load profile, Figure 3-17, in comparison to the others here presented have the more constant trend. The Load profile of France, Figure 3-18, has a peak of electricity demand in the winter period (January, February) corresponding the use of the electric heating in the home, after that the profile decreases to a lower and regular level and then it grows again in the autumn-winter periods. The nation with the higher electricity power demand in 2015 is France with 91.6 GW peak reach in February. The second one is the Germany, Italy and the United Kingdom have a similar peak of demand, Poland and finally Portugal minor peaks. The load profiles of Portugal (Figure 3-19), the United Kingdom (Figure 3-20) and Poland (Figure 3-21) have a regular trend

similar to the German one but with an electricity power demand greater in the winter period, and lower in the spring-summer month. Comparing north Europe profiles with the south Europe ones, it is possible to see that northern European countries have more regular profiles, and the higher demand of electricity in the winter period, different for the south European countries where the peak of electricity power demand is in the summer period. All the profiles have the same decrease in the trend at the end of December.

3.7 Generation profile from real data

The second type of profiles used in COMESE code simulation is the generation profiles of technologies. The generation profile for a specific technology plots the power generated by all the power plants of that type installed in a nation, with an hourly resolution and for a specific year. The generation profiles used in COMESE code are:

- PV generation profiles,
- WIND onshore and offshore generation profiles,
- Hydroelectric run of a river generation profiles,
- Concentrating solar power (CSP) with molten salt storage profiles,
- Fusion power plant generation profiles.

All these profiles are currently used in COMESE code, the code with the addition of a specific module can be easily extended to the use of other profiles if needed. Here the profiles are presented for different technologies and for different years, from 2015 to 2017, for the Italian case. In Table 3-3 it is listed the value of peak power and total electric energy demand and total electric energy generated corresponding to load and generation profiles of the Italian country. The profiles refer to 2016, the leap year, are reduced to 365 days with the elimination of the last day of the year (same logic used for the load profiles for maintaining the correct order of working and not working days).

Table 3-3: Total energy generated of demand and peak power for the Italian profile

Profile	LOAD		PV		WIND		Hydro run of river	
	P peak [GW]	En tot [TWh]	P peak [GW]	En tot [TWh]	P peak [GW]	En tot [TWh]	P peak [GW]	En tot [TWh]
2015	59,65	314,35	0,60	1,09	6,29	14,64	4,89	23,42
2016_366days	48,99	283,26	15,81	17,91	6,38	16,35	7,69	31,06
2016_365days	48,99	282,63	15,81	17,88	6,38	16,28	7,69	31,02
2017	50,33	291,45	10,36	19,60	6,70	17,58	6,57	26,65

3.7.1 Generation CSP with storage normalized profile for Italy

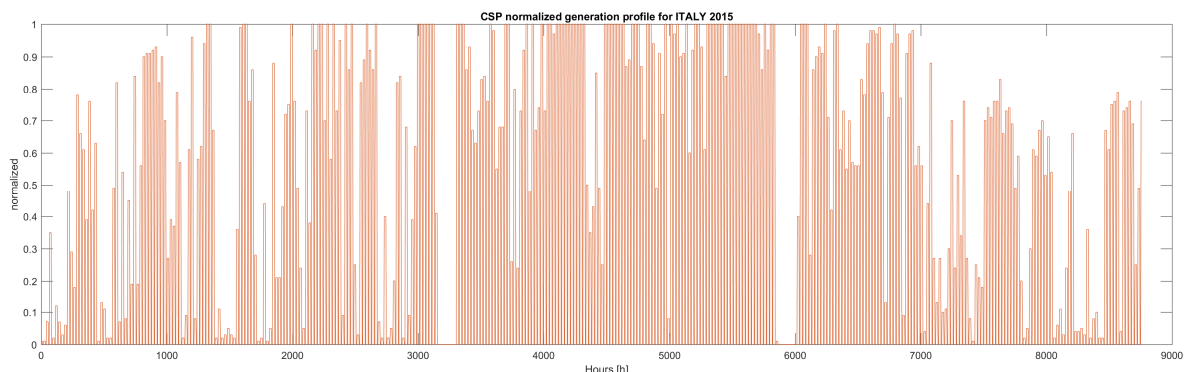


Figure 3-22: Concentrating solar power normalized profile for Italy-2015 data collect from Enea

In Figure 3-22 it is presented the generation profile normalized for concentrating solar power technology, profile characterized by the maximum production in the central month (spring-summer) of

the year and a less production in the winter period. The generation profile of CSP plants comes from a combination of the data of the direct normal irradiation (DNI), recorded in Casaccia, Rome, Italy in 2015 and the configuration of the CSP plant (IEA, 2010).

In Figure 3-23, Figure 3-24, Figure 3-25 there are generation profiles of photovoltaic technology for Italy respectively for 2015, 2016 without the 31st of December and 2017. The three profiles are compared in Figure 3-26, and in Figure 3-35 where the three profiles are normalized to the peak power production. The seasonal trend of photovoltaic generation presents a generation high in the spring-summer period and low in the winter-autumn period for all the years considered. The spike of generation for the 2016 probably is related to an error on the data but this does not change the global trend of the profile for 2016.

In Figure 3-27, Figure 3-28, Figure 3-29 there are the generation profiles for the wind onshore technology for Italy for the year 2015, 2016 without the 31st of December and 2017. First thing that appear is the high variation of the generation of wind power plant along weeks of the year, respect to the more uniform generation of PV power plant. A variation that doesn't change from one year to another. In Figure 3-30 the three profiles are compared in the same graphic, in Figure 3-36 the same profiles are compared normalized respect to the peak power production of each year. Figure 3-36 displays a similar global trend quite constant for different years. Respectively to the photovoltaic one, wind onshore technology can produce and high level of power in autumn-winter months respect to the summer-spring months. Even if this difference is less pronounced than in that of photovoltaic generation. The high production in the autumn-winter period can be exploited in a scenario using the wind generation as a possible complementary technology of the photovoltaic one.

In Figure 3-31, Figure 3-32, Figure 3-33, there is the generation profile for the hydro run of river technology for Italy for the year 2015, 2016 without the 31st of December and 2017. While in Figure 3-34 and Figure 3-37 there is a comparison of the three profile respectively real and normalized to the peak power production for each years. The hydro run of a river technology production is linked with the water regime of the river and present a greater production in the spring and summer period compared to the winter one. The three years present a similar trend from 2015 to 2017 and it is also possible to see a progressive increase of the production linked with the installation of new power plants.

As seen for the Load profiles from 2015 to 2017, also for the generation of Photovoltaic, Wind onshore and hydro run of river technologies, it is possible to see a similar seasonal trend that repeats itself from one year to a next one. This supports the assumption that it is possible to obtain the new generation profile for the future year, with a proportional scaling from a base year with logic that is the same used for the load profile. So for each technology, they are compared the energy production set in the scenario input file and the total energy production of the reference profile, as integral of the power generate hourly over the entire years, than it is evaluated the scaling factor as the ratio between the desired value and the reference. Finally the new profiles are obtained by multiplying the dataset of the reference profile for the scaling factor. This approach is used until the technology of the scenario has the same hour of production of the reference profiles. An example of scaled profile is presented in Figure 3-38, Figure 3-39, Figure 3-40 respectively for photovoltaic, wind onshore and hydro run of river. If the simulation of a scenario required a particular technology with a generation profile with different hour of production, more carefully studies of the profile used as input are required.

3.7.2 Generation PV profile for Italy

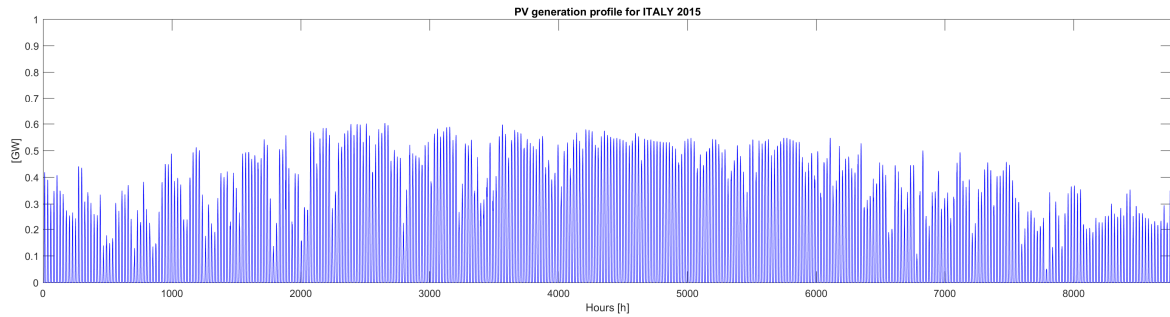


Figure 3-23: Photovoltaic generation profile for 2015 Italy

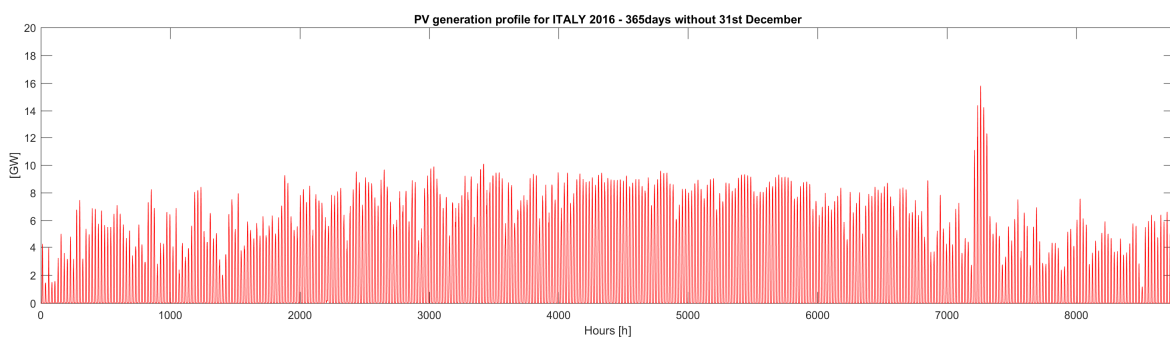


Figure 3-24: Photovoltaic generation profile for 2016 Italy, profile reduced to 365 days with the elimination of 31st of December

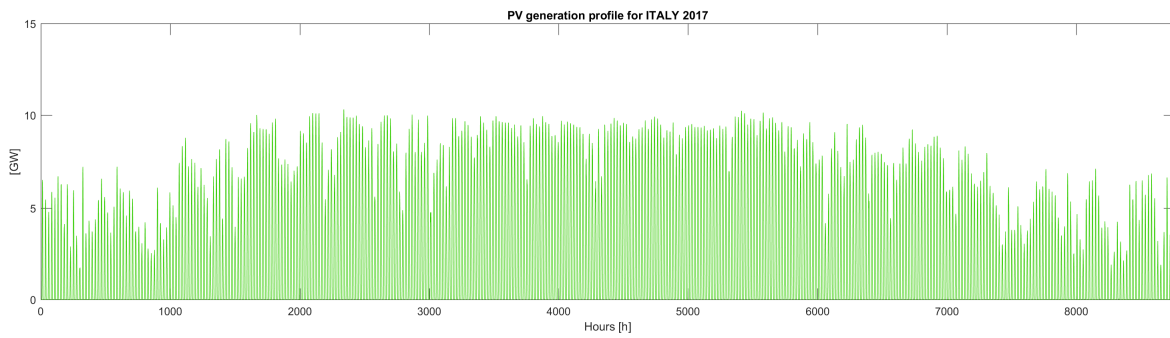


Figure 3-25: Photovoltaic generation profile for 2017 Italy

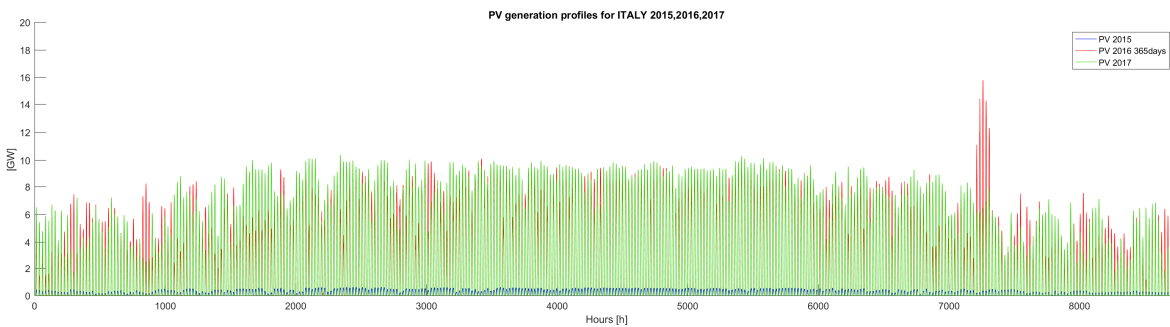


Figure 3-26: Comparison of Photovoltaic generation profiles for 2015,2016,2017 Italy

3.7.3 Generation Wind onshore profile for Italy

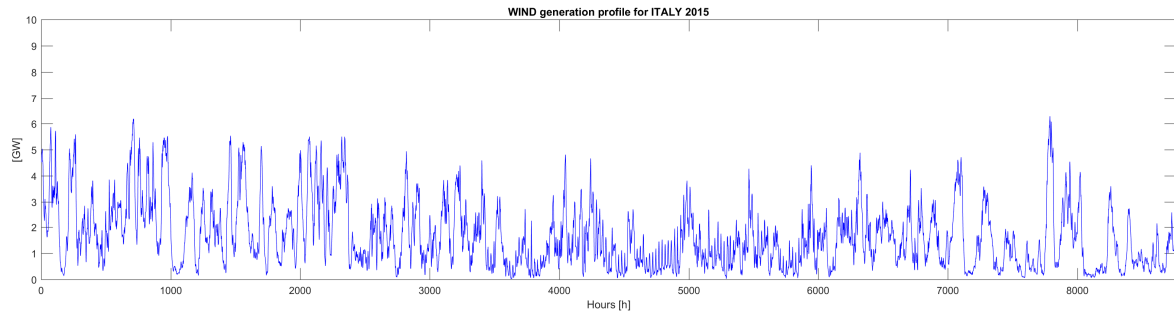


Figure 3-27: Wind onshore generation profile for 2015 Italy

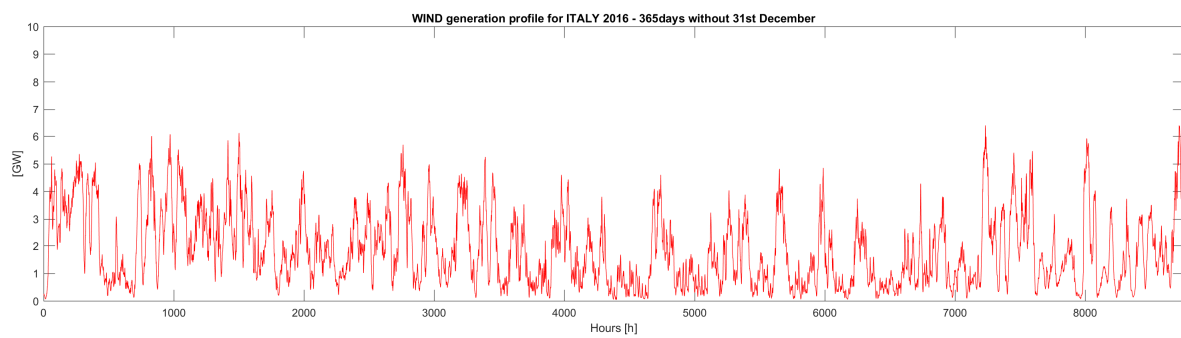


Figure 3-28: Wind onshore generation profile for 2016 Italy, profile reduced to 365 days with the elimination of 31st of December

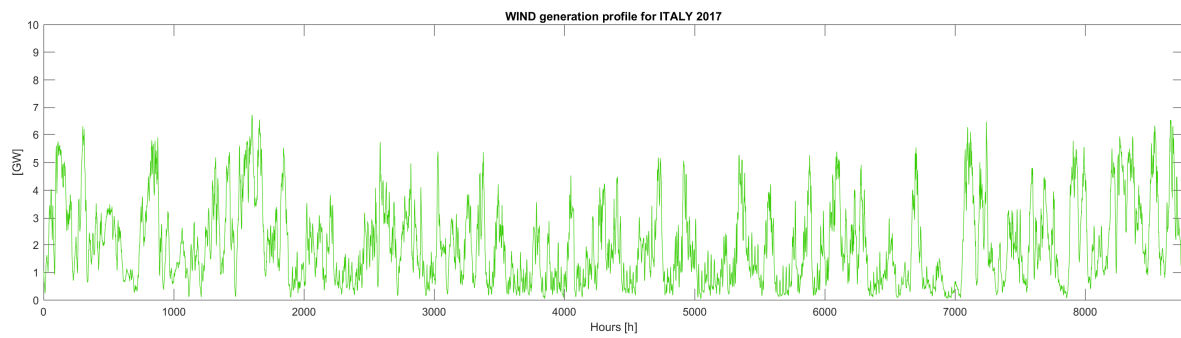


Figure 3-29: Wind onshore generation profile for 2017 Italy

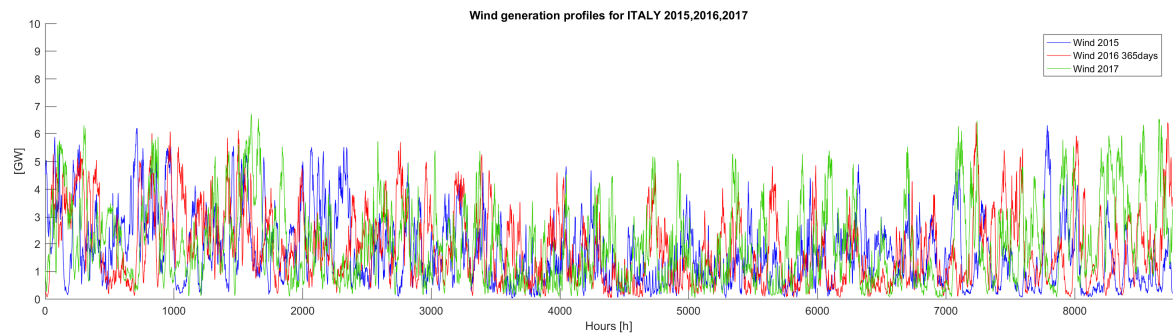


Figure 3-30: Comparison of Wind onshore generation profiles for 2015,2016,2017 Italy

3.7.4 Generation Hydro run of river profile for Italy

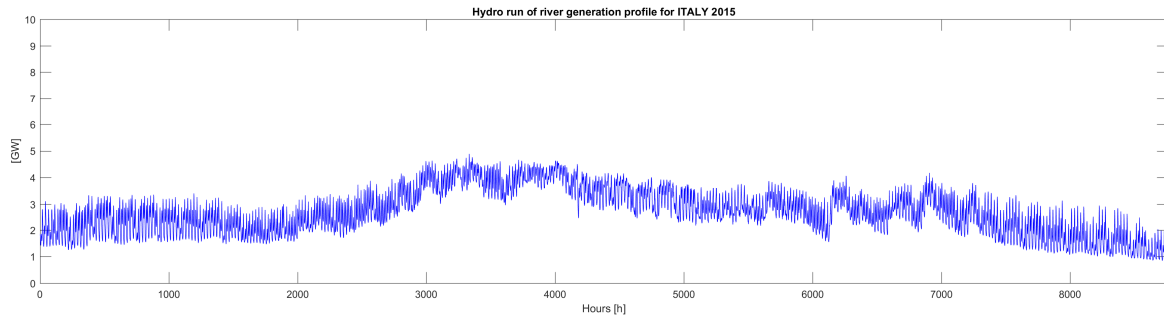


Figure 3-31: Hydro run of river generation profile for 2015 Italy

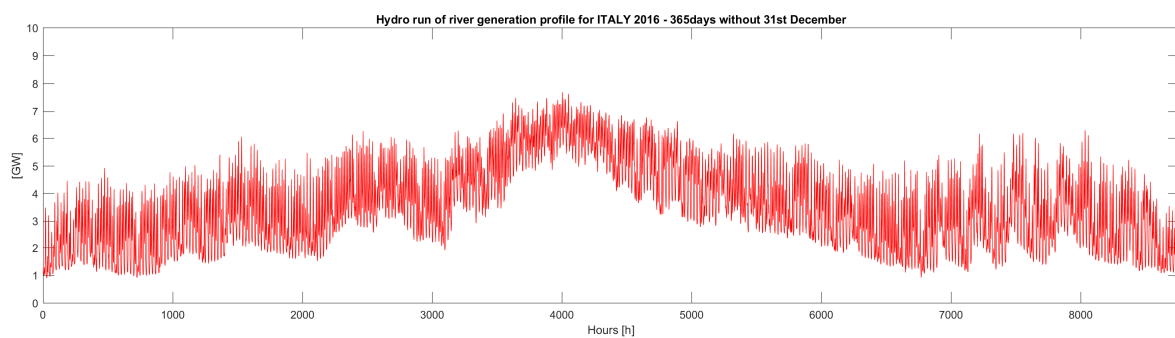


Figure 3-32: Hydro run of river generation profile for 2016 Italy, profile reduced to 365 days with the elimination of 31st of December

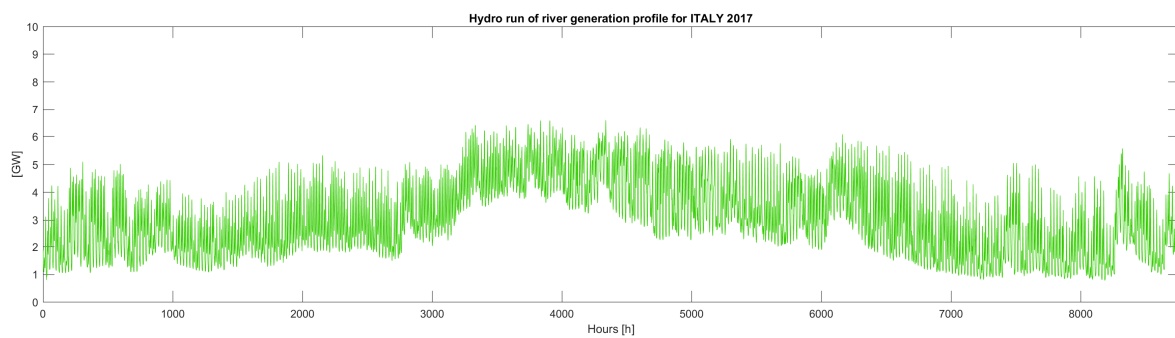


Figure 3-33: Hydro run of river generation profile for 2017 Italy

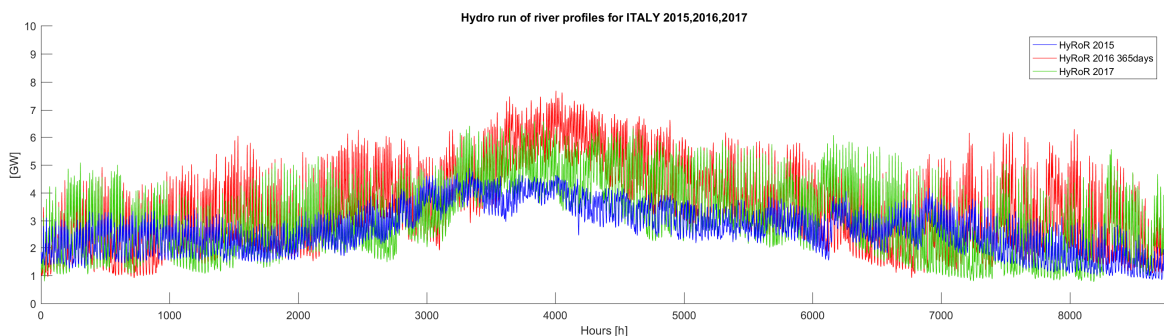


Figure 3-34: Comparison of Hydro run of river generation profiles for 2015,2016,2017 Italy

3.7.5 Comparison of Generation normalized profile for Italy

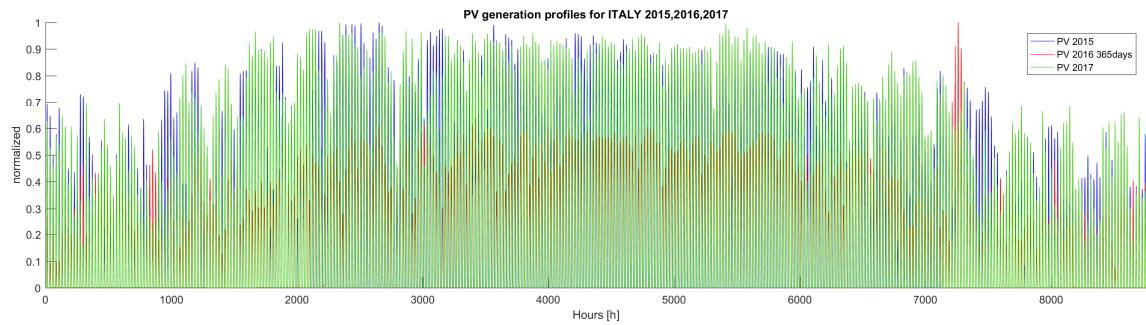


Figure 3-35: Comparison of PV generation normalized profiles for 2015,2016,2017 Italy

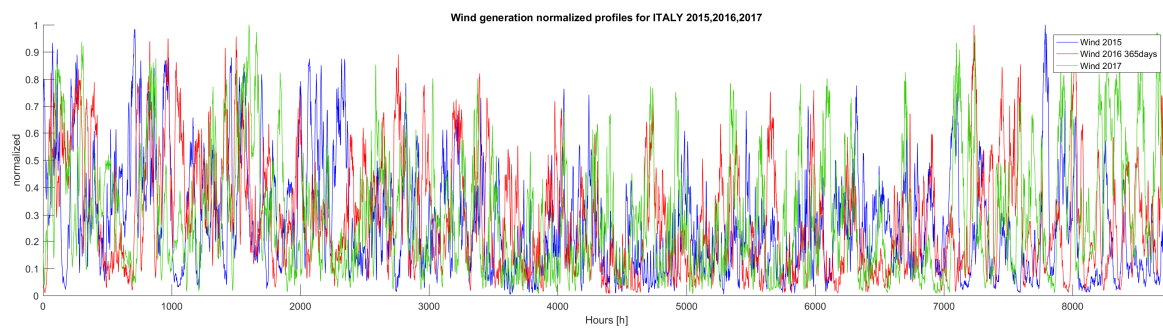


Figure 3-36: Comparison of Wind onshore generation normalized profiles for 2015,2016,2017 Italy

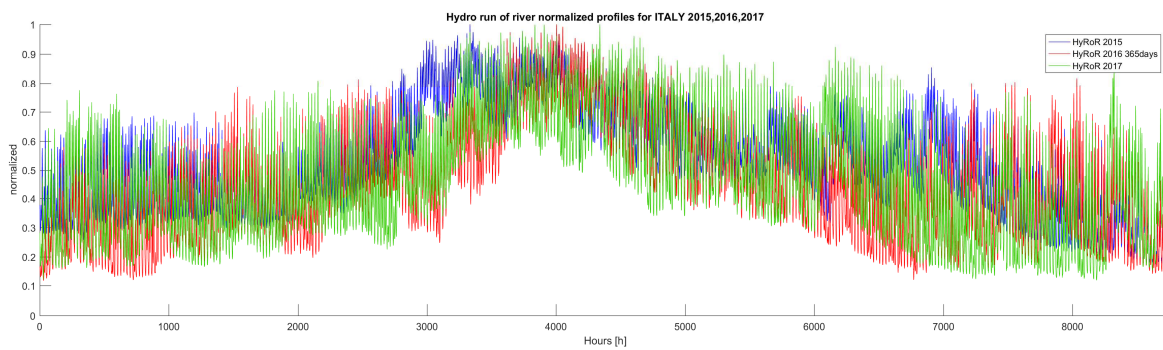


Figure 3-37: Comparison of Hydro run of river generation normalized profiles for 2015,2016,2017 Italy

3.7.6 Example of scaled Generation profile

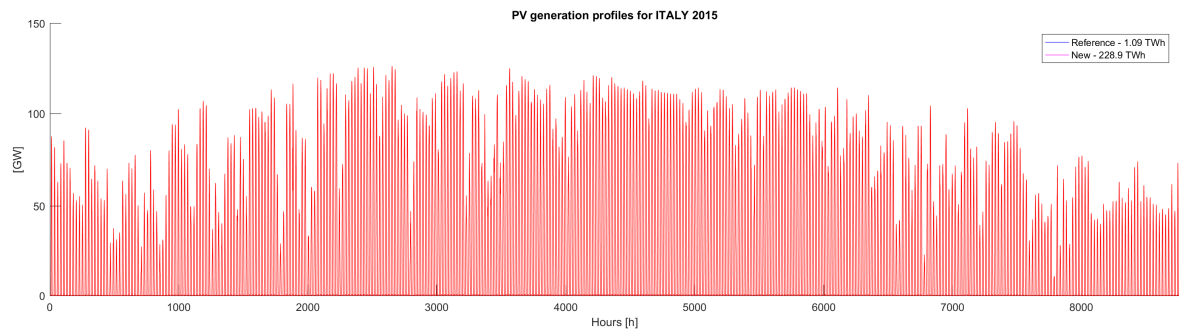


Figure 3-38: Reference Generation PV profile Italy 2015 with a generation of electricity of 1.09 TWh (blue), and new profile with a generation of electricity of 228.9 TWh (red).

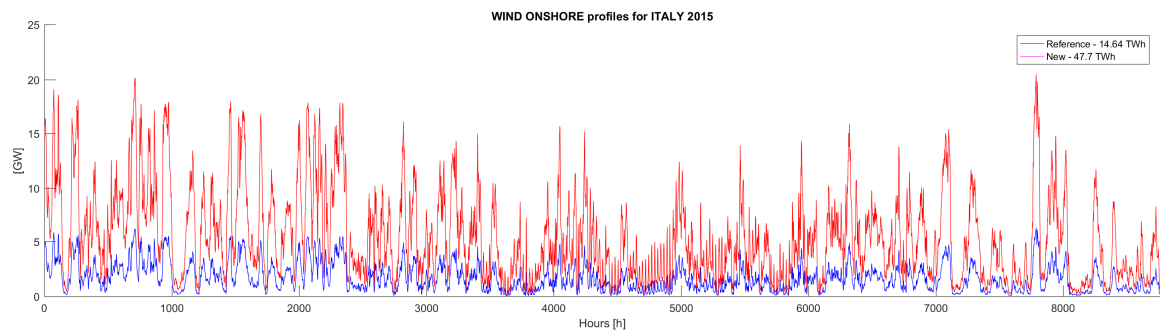


Figure 3-39: Reference generation Wind profile Italy 2015 with a generation of electricity of 14.64 TWh (blue), and new profile with a generation of electricity of 47.7 TWh (red).

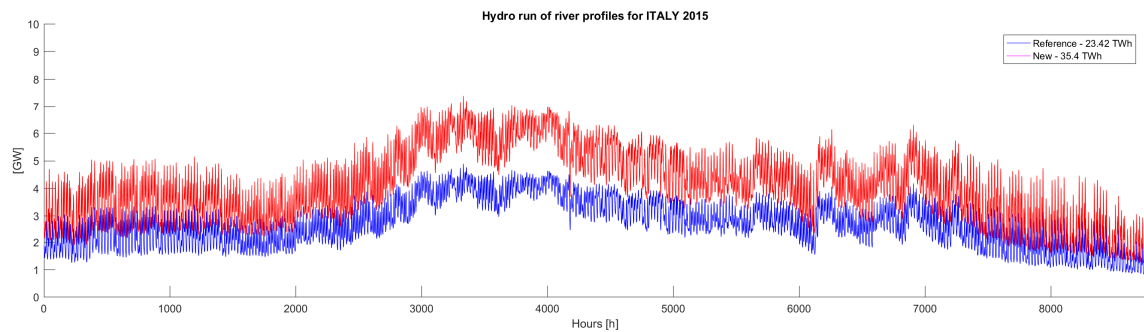


Figure 3-40: Reference Generation hydro run of river profile Italy 2015 with a generation of electricity of 23.42 TWh (blue), and new profile with a generation of electricity of 35.4 TWh (red).

3.8 Generation profiles for technology with different capacity factor

The new scaled profiles presented in Figure 3-38 for the photovoltaic technology, in Figure 3-39 for wind onshore technology and in Figure 3-40 for hydro run of river technology are profile obtained with the assumption of using a technology with the same equivalent hours of production of the reference case. Respectively 1200h for PV, 1600 h for wind, 4425 h for hydroelectric run of river. So the installed power is greater or equal to the maximum peak power of the profile, and the contemporaneity factor for the three technologies is less than one.

The **Contemporaneity factor (fc)** is a parameter that gives an indication of how much the power plants can generate power at the same time, if for an hour of the year its value is one, this corresponds to a situation of power generated equal to the installed power. For renewables technologies, like photovoltaic, or wind where the solar panel or the turbine are placed in different areas of the country, it is clear that it is impossible to have a contemporaneity factor equal to one. Unless you have very few power plants in a restricted area

$$(3.7) \quad f_c = \frac{P_{peak}}{P_I}$$

The **Capacity factor (CF)** is defined as the ratio between the amount of energy generated by a power plant and the energy that the same power plant can generate at maximum power over a period of time. Thanks to the capacity factor, it is possible to define the equivalent hours of production h_{eq} as the ratio between the energy generated by a power plant and the power installed for that type of power plants over a period of time, i.e. one year. The **equivalent hours** are the number of hours that a power plant operating at maximum power must be in function for generating the same amount of energy generate over the considered period of time.

$$(3.8) \quad CF = \frac{E_n \text{ generate}}{E_n \text{ th generable}} = \frac{E_n \text{ generate}}{P_I \cdot \Delta t}$$

$$(3.9) \quad CF = \frac{E_n \text{ generate}}{P_I \cdot 8760} = \frac{E_n \text{ generate}}{P_I} \frac{1}{8760}$$

$$(3.10) \quad CF_{\%} = \frac{E_n \text{ generate}}{P_I} \frac{1}{8760} * 100$$

$$(3.11) \quad h_{eq} = \frac{E_n \text{ generate}}{P_I}$$

The Capacity factor is always lesser than the Availability factor (AF). The **Availability factor (AF)** of a power plant is defined as the amount of time that the power plant is able to produce energy over a certain period of time, divided by the length of the time interval.

$$(3.12) \quad AF = \frac{\text{mean time between failure}}{\text{mean time between failure} + \text{mean downtime}}$$

When in a simulation of a scenario a technology is set up for operating with a number of equivalent hour greater than the reference, COMESE code use the same approach of scaled profiles. The reference profile is scaled with a multiplying factor in function of the energy used. But since the

equivalent hours are greater for the same power installed, the energy generated is greater, the result is that the new profile obtained has a peak power closer to the installed one. The contemporaneity factor tends to be near 1. Until the equivalent hour is close to the value of the specific profile, this is not an issue; but if the set hours are greater than the reference case, the peak power of the scaled profile may be greater than the installed one. In this situation COMESE code gives a warning, a power plant can't generate more power than to the installed one (contemporaneity factor greater than one). For that simulation, the input profile must be replaced with a modified one.

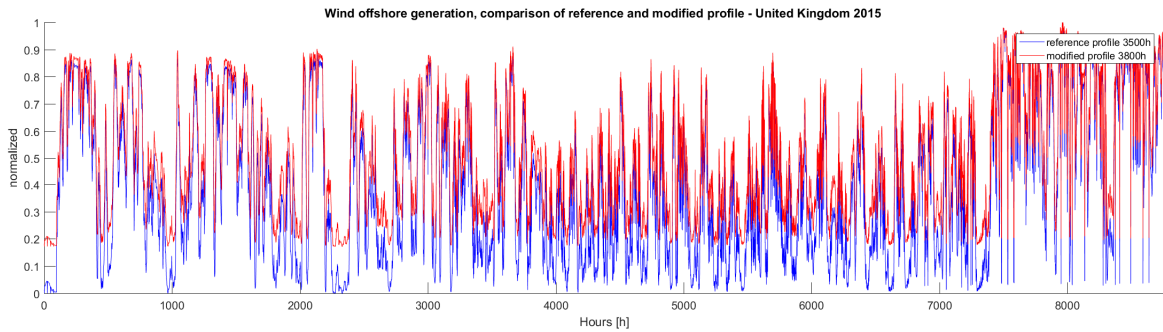


Figure 3-41: Comparison between the reference profile of generation for wind offshore in the United Kingdom for the 2015 corresponding to 3500h equivalent and the new generation profile of 3800h equivalent obtain shifting the first one up.

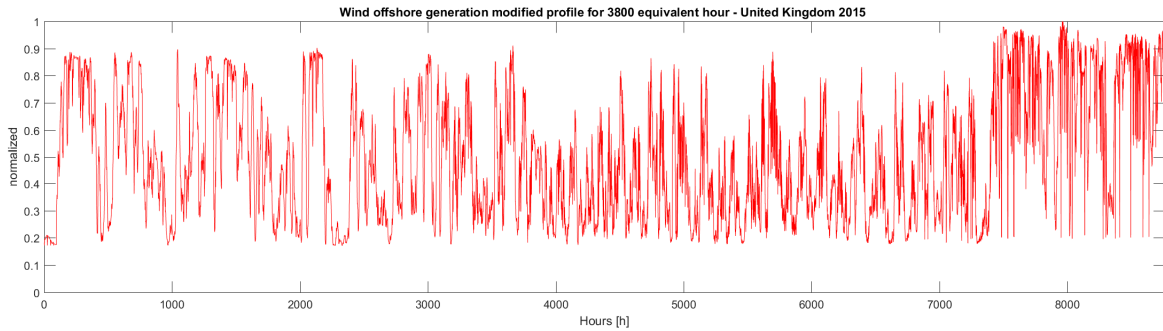


Figure 3-42: new generation profile for wind offshore technology at 3800h equivalent

From the equation of the equivalent hours, for increasing the value of the equivalent hours, the energy generated by that technology must increase with the same power installed, and for increasing the energy there are two possibilities: one is to increase the contemporaneity factor, a solution used if the equivalent hours are near to the original value of the profile; second one is to increase the total energy of the reference profile. This involves changing the original profile. In this case the generation profile is modified adding at the bottom of the profile curve a fixed generation of 8760h shifting up the profile and increasing the amount of energy, maintaining at the same time the variation of the profile along the year. This choice is based on the assumption that installing more power plant in different region permits to have a low, but a constant level of generation in each hour of the year. The contemporaneity factor of the new profile is considered constant and equal to the original one. In Figure 3-41, it is presented the reference profile and the new profile of wind offshore generation for the United Kingdom, in blue the reference profile of a wind offshore generation with 3500h, in red the modified profile for a generation of 3800h. In Figure 3-42 it is presented only the new modified profile of wind offshore used in the simulation of the European scenario with fusion technologies.

3.9 Generation profiles for European Country

As explained for the Load profile in paragraph 3.6 COMESE code is completely transparent to the nations profiles used for the simulation, so it is possible to simulate the scenario of any nation. Here they are presented the generation profiles for photovoltaic, wind onshore, wind offshore of the countries indicated in Figure 3-15. The intention is to highlight the variation on seasonality of photovoltaic and wind onshore generation in different areas of Europe, from south to north, and from regions near to the ocean to regions without access to the sea. The regions selected are Germany, France, the United Kingdom, Portugal, Poland and Italy. All the profiles are collected for the same type of production and all the profiles are normalized to the maximum peak of hourly generation in order to highlight the different trend along the year, and enable their comparison. For Germany, it is available directly the normalized profile for photovoltaic and wind generation. All the nations have the data both for photovoltaic generation and for wind onshore generation, except Poland that has only the data of wind onshore. The United Kingdom has both the data from Wind onshore and offshore.

3.9.1 European photovoltaic generation normalized profiles

From Figure 3-43 to Figure 3-47 they are presented the photovoltaic generation profiles. Moving from the north of Europe, United Kingdom Figure 3-43 to the south of Europe it is possible to see how the photovoltaic generation increase and the trend becomes more regular, see for example the Portugal Figure 3-47 or the Italian case Figure 3-46. In all the profiles, it is possible to see that the peak of generation of photovoltaic power plants is in the spring summer period, while the less production is concentrated in the autumn winter period.

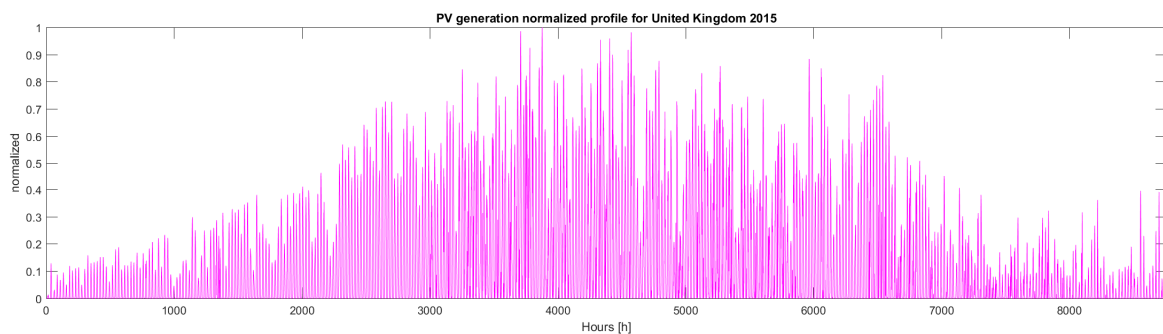


Figure 3-43: Photovoltaic generation profile normalized to the peak of power production for the United Kingdom 2015

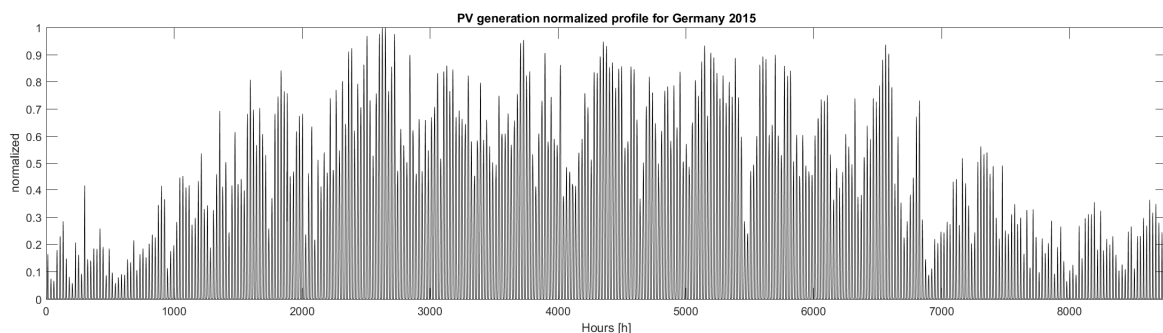


Figure 3-44: Photovoltaic generation profile normalized to the peak of power production for Germany 2015

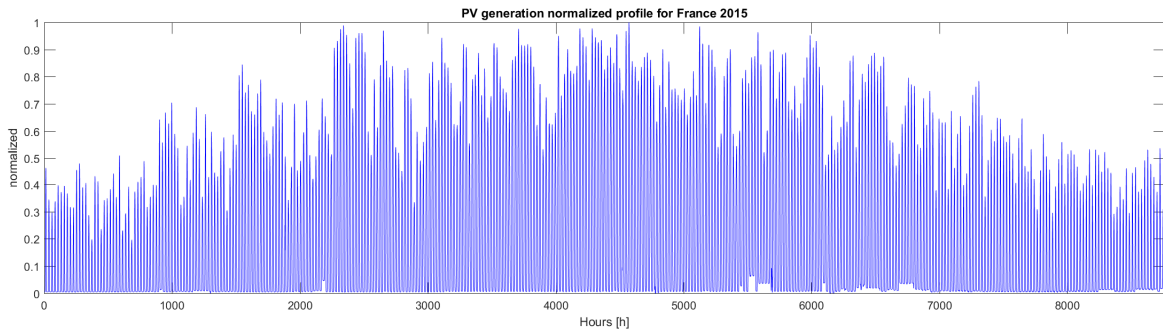


Figure 3-45: Photovoltaic generation profile normalized to the peak of power production for France 2015

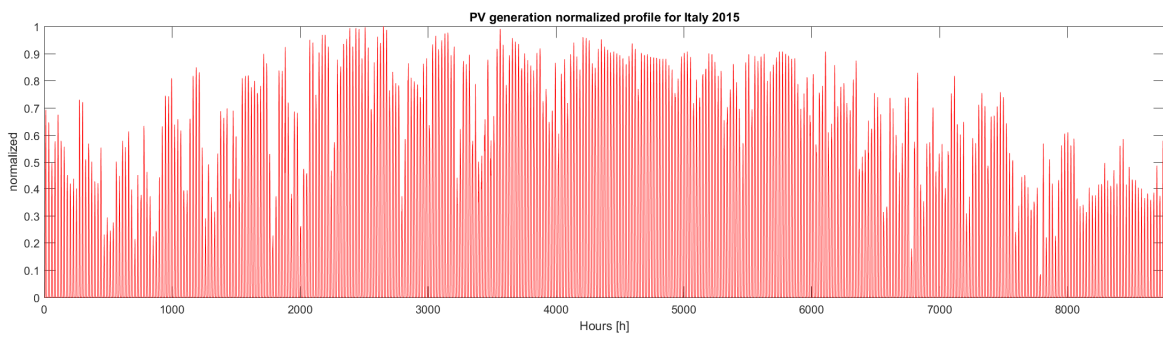


Figure 3-46: Photovoltaic generation profile normalized to the peak of power production for Italy 2015

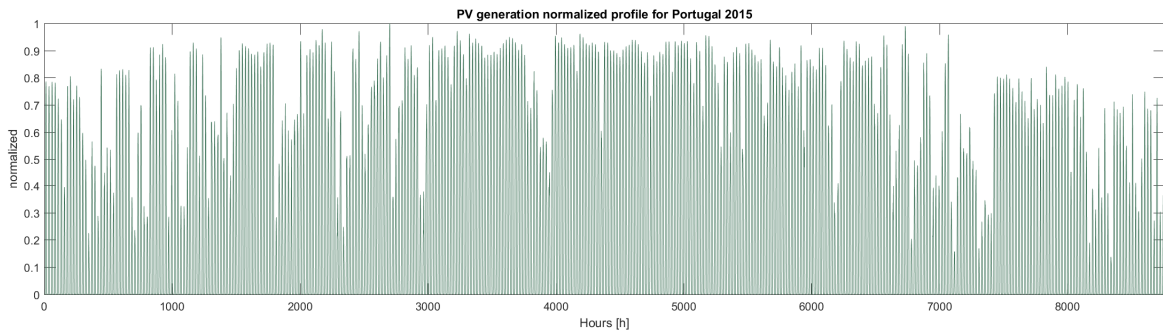


Figure 3-47: Photovoltaic generation profile normalized to the peak of power production for Portugal 2015

3.9.2 European Wind onshore generation - normalized profiles

From Figure 3-48 to Figure 3-53 it is presented the wind onshore generation profile. Moving from the north of Europe, the United Kingdom Figure 3-48 to the south of Europe, it is possible to see a weekly trend more variable along the year. The seasonality of the electricity generation changes respectively to the photovoltaic one, the peak of wind onshore energy production is located in the winter period at the end of the year and it is quite constant in the north of Europe, becoming less constant and lower moving to the south. Compare for example the case of Italy in Figure 3-52 and the United Kingdom in Figure 3-48. At the same time, going from south to north, the generation grows even in the central months of the year.

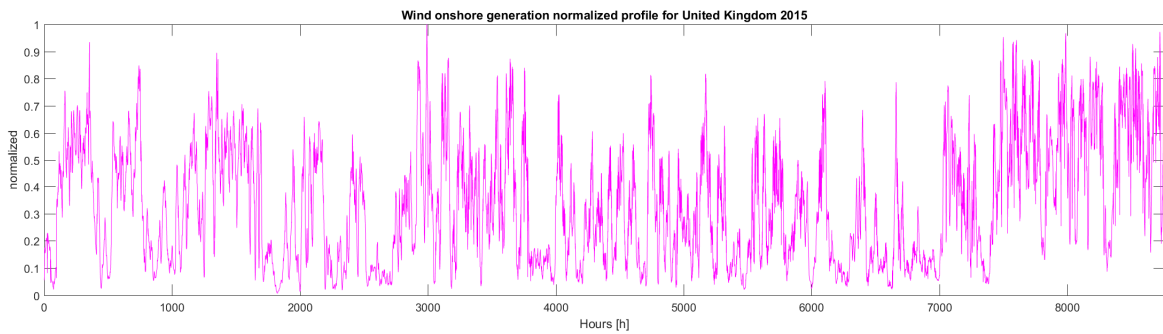


Figure 3-48: Wind onshore generation profile normalized to the peak of power production for United Kingdom 2015

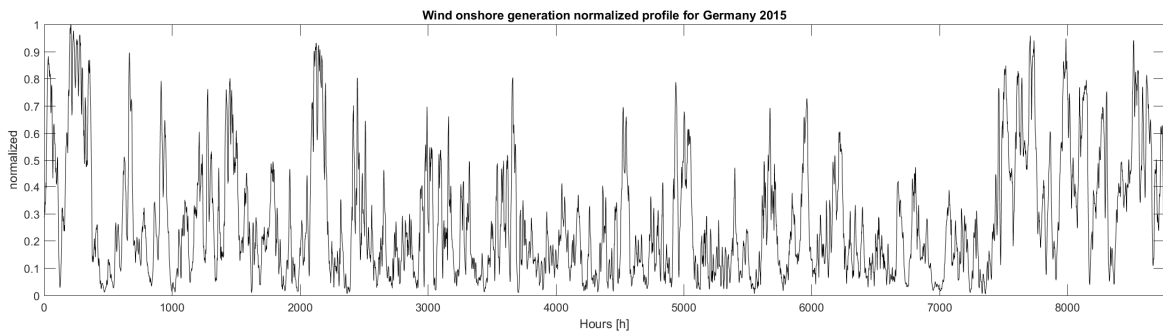


Figure 3-49: Wind onshore generation profile normalized to the peak of power production for Germany 2015

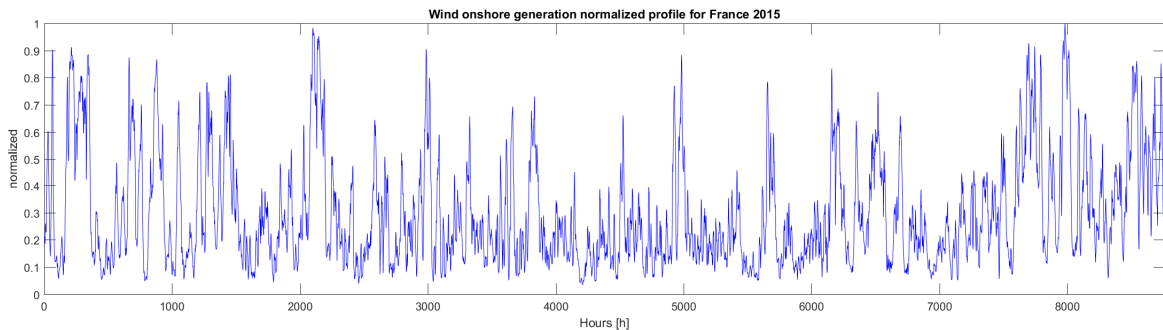


Figure 3-50: Wind onshore generation profile normalized to the peak of power production for France 2015

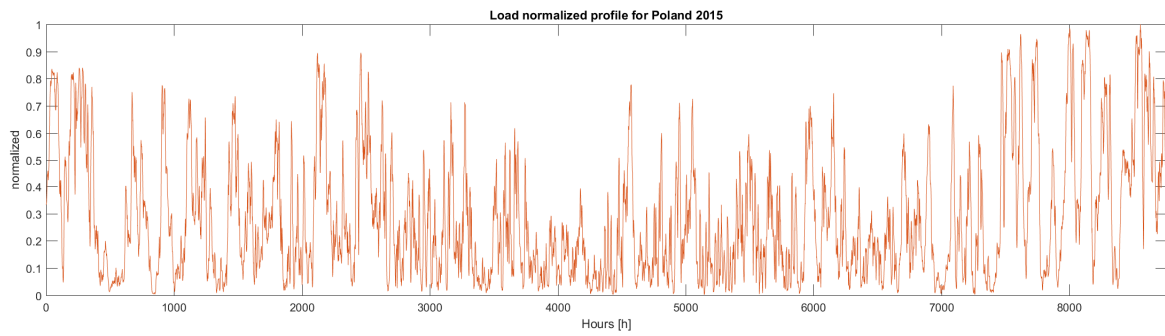


Figure 3-51: Wind onshore generation profile normalized to the peak of power production for Poland 2015

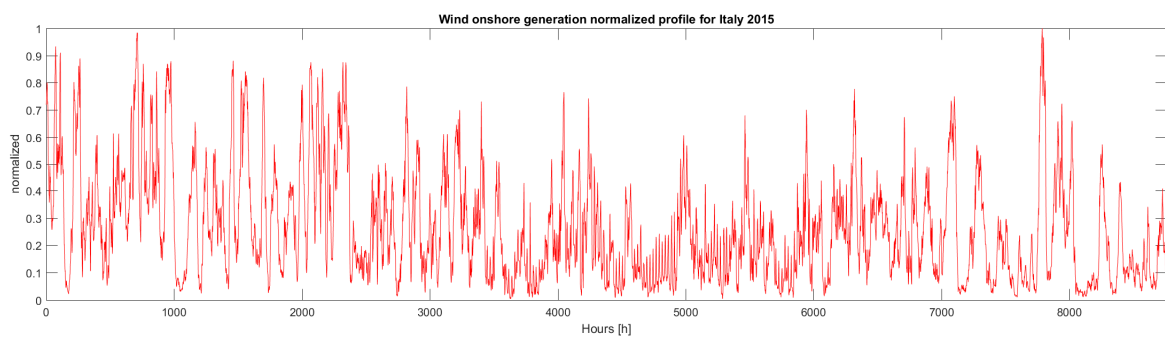


Figure 3-52: Wind onshore generation profile normalized to the peak of power production for Italy 2015

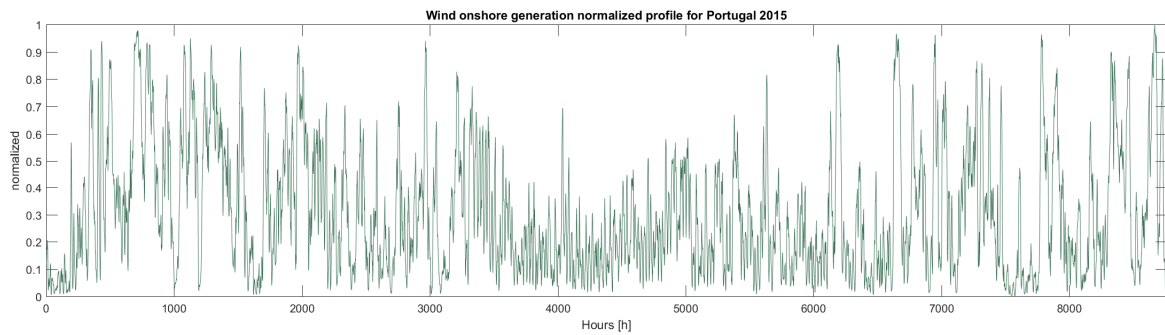


Figure 3-53: Wind onshore generation profile normalized to the peak of power production for Portugal 2015

3.9.3 European Wind offshore generation - normalized profiles

From the selected countries, the only region with the offshore profile is the United Kingdom, in Figure 3-54 is presented that profile. The profile is quite regular for the global trend with a less production and high variability in the summer period, and a very uniform and high production in the winter months. The weekly trend is variable. In Figure 3-55 the two profiles of onshore and offshore wind generation are compared. The two generation profiles have the same global trend, related to the same wind regime of the area, but the offshore wind has an higher level of generation. In Figure 3-56 the generation of wind offshore is compared to the photovoltaic one for the United Kingdom highlighting the complementary of the two technologies, aspect that can be used in the project of new possible scenarios.

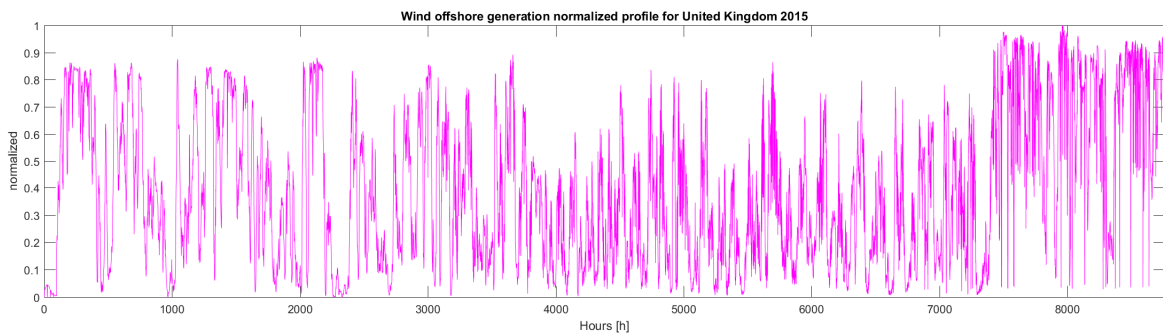


Figure 3-54: Wind offshore generation profile normalized to the peak power production for the United Kingdom 2015

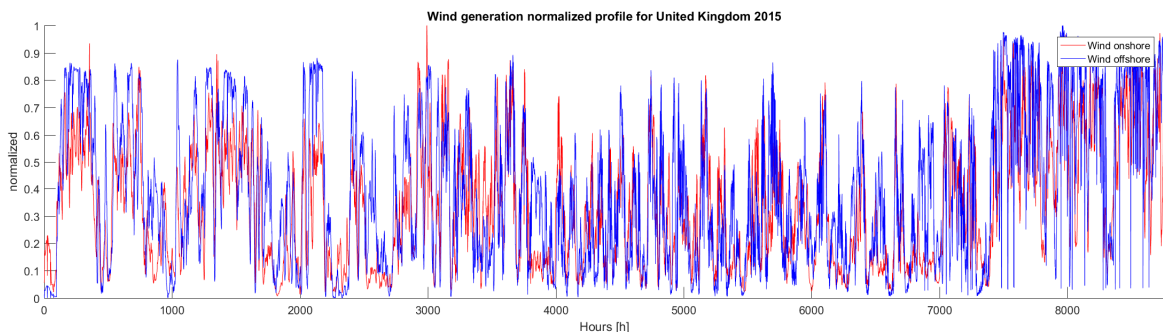


Figure 3-55: Wind onshore and offshore generation profile normalized to the peak power production for the United Kingdom 2015, comparison of the two trend.

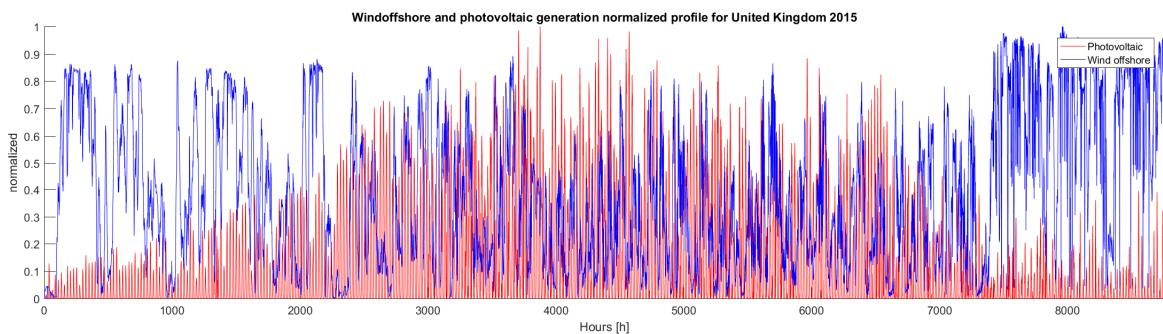


Figure 3-56: Wind offshore and photovoltaic generation profile normalized to the peak power production for the United Kingdom 2015, comparison of the two trend.

3.10 Load and generation profile comparison for United Kingdom in different years

Likely for Italy, here they are presented the comparison of Generation and Load profiles for the United Kingdom. The choice of the United Kingdom is in function of the study carried to the SOFT 2018, where it was the study future scenarios with the fusion technology in two regions, the South of Europe with an high generation of photovoltaic, and the North Europe characterized by an high wind generation. For the north Europe the region profiles chosen are the United Kingdom profiles. Because United Kingdom has a similar value for the total demand of electricity of Italy and a peak of power demand similar to the Italian Load profile. See Table 3-3 for Italian profile and Table 3-4 for the United Kingdom data.

Table 3-4: Total energy generated od demand and peak power for the United Kingdom profile, data from own calculation base on opendatabase. *The data for the 2016 and 2017 are not complete but are useful for describe the seasonality.

United Kingdom Year	LOAD		PV		WIND onshore		WIND offshore	
	P peak [GW]	En tot [TWh]	P peak [GW]	En tot [TWh]	P peak [GW]	En tot [TWh]	P peak [GW]	En tot [TWh]
2015	59.03	334.83	6.84	7.66	6.21	18.42	4.04	14.11
2016_366days*	57.90	334.64	7.36	8.41	6.74	18.52	3.89	11.73
2016_365days*	57.90	333.75	7.36	8.40	6.74	18.42	3.89	11.68
2017*	54.89	305.47	8.68	10.13	7.04	25.91	4.33	14.95

The data here presented cover the years 2015, 2016 and 2017. With the same approach used for Italy the profile of 2016 are modified to have 365 days with the elimination of the last day of the year. Unfortunately the data for the profile of the years 2016 and 2017 are not complete; this does not preclude the possibility to compare the different profile observing the seasonality but the total value presented in Table 3-4 is affected to this missing of information. In Figure 3-57 it is possible to see that in the last three years the trend of demand of electricity in United Kingdom remain similar; the same observation can be done for the photovoltaic generation presented in Figure 3-58. Wind generation is more variable for the three years, 2015, 2016 with 365 days, 2017, Figure 3-59 presents the profile for the onshore and Figure 3-60 for the offshore, except the high variation, is clear that the wind technologies can generate the same power independent to the season, and more in winter months rather than the spring-summer period.

3.10.1 Comparison of Load normalized profile for United Kingdom

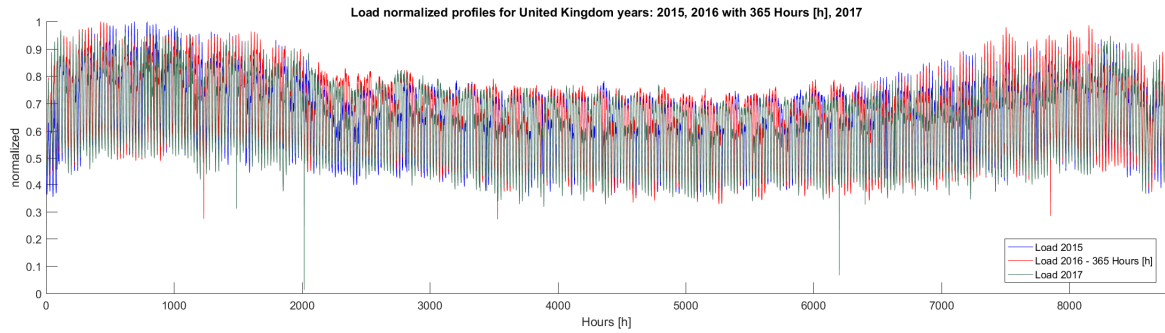


Figure 3-57: comparison of normalized Load profile for years 2015, 2016 with 365 days and 2017 for the United Kingdom

3.10.2 Comparison of Photovoltaic generation normalized profile for United Kingdom

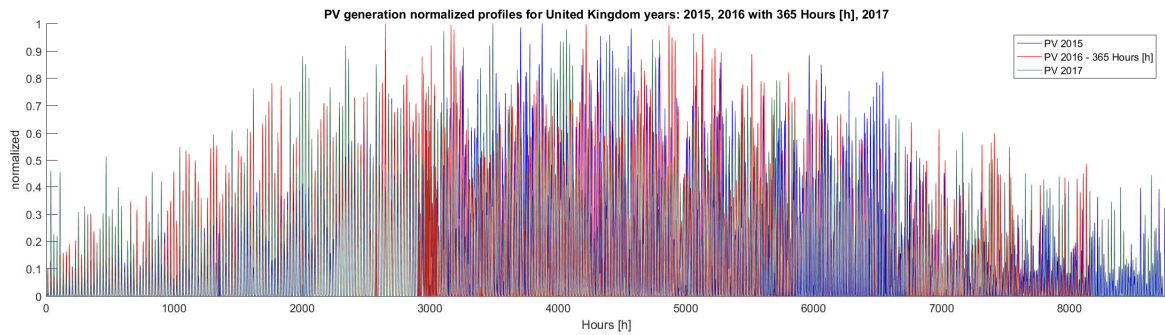


Figure 3-58: comparison of normalized photovoltaic generation profile for years 2015, 2016 with 365 days and 2017 for the United Kingdom

3.10.3 Comparison of Wind onshore generation normalized profile for United Kingdom

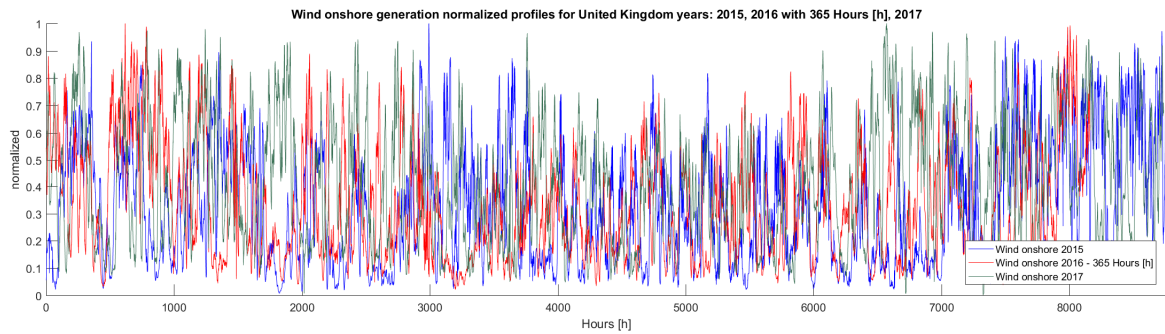


Figure 3-59: comparison of normalized wind onshore generation profile for years 2015, 2016 with 365 days and 2017 for the United Kingdom

3.10.4 Comparison of Wind offshore generation normalized profile for United Kingdom

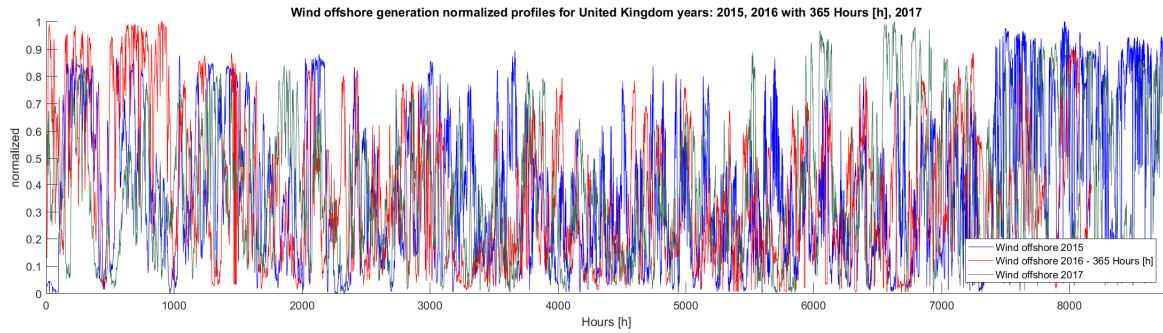


Figure 3-60: comparison of normalized wind offshore generation profile for years 2015, 2016 with 365 days and 2017 for the United Kingdom.

3.11 Generation profile from assumption – Fusion power plant profile

Since there are actually no fusion power plant facilities based, two arbitrary profiles for the fusion power generation are used in the COMESE code simulations. The first one is constant profile and the second one is called 2-season profile.

The creation of the first profile starts from the assumption that a fusion power plant operates as a base power plant, so for the entire year with a constant level of power. This is the same approach used for all the base technologies like geothermal technology or a fossil fuel technology.

Read from the scenario input file the energy that the fusion power plant must generate En , and the capacity factor $FC_{\%}$, COMESE code calculates first the power installed P_I with the equation 3.13 and then with the equation 3.14 the equivalent power that this power plant must generate for the entire year for generating the same amount of energy. For a future power plant, it is assumed a value for the capacity factor equal to a fission one, around 80%. The value of P_{eq} define the fixed power level of the constant profile. In Figure 3-61 it is presented an example of constant generation profile for fusion technology.

$$(3.13) \quad P_I = \frac{En}{\left(8760 \cdot \frac{FC_{\%}}{100}\right)}$$

$$(3.14) \quad P_{eq} = \frac{En}{8760}$$

The second solution for the fusion generation profile is based on the assumption to concentrate all the maintenance of the power plant in the central months of the year, where the great production of the photovoltaic power plants can provide more energy and balance the less production of fusion. The idea is exactly to decrease the fusion power when we can use other renewable technologies like the photovoltaic one, and create a complementary profile to these. With this idea, it was created a generation profile with two power levels: one that approximately covers the winter and autumn period,

one the spring and summer period. Approximately because in function of the scenario it is possible to reduce or increase the two periods. In Figure 3-62 is plot an example of 2 season profile.

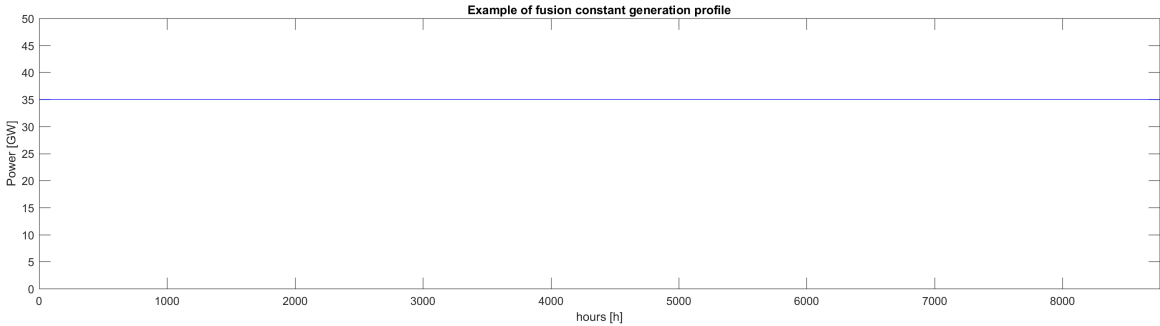


Figure 3-61: example of constant fusion generation profile. Capacity installed 44 GW with a capacity factor of 80%

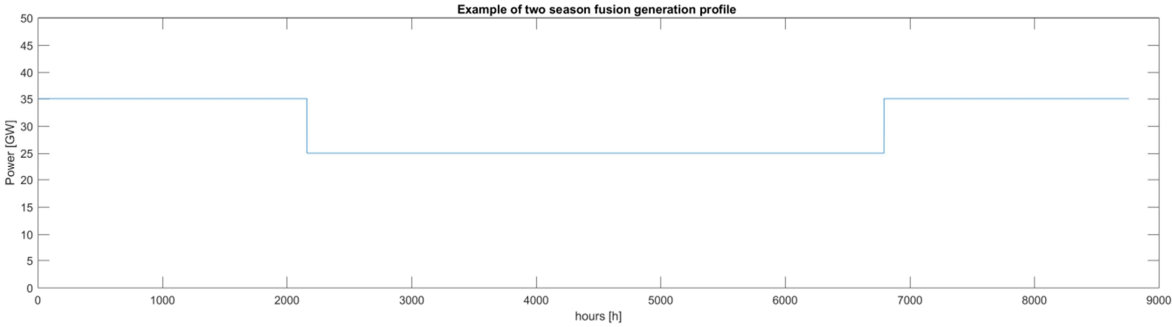


Figure 3-62: example of 2-season fusion generation profile.

3.12 Input file - the power plant technology data

The input files for the technologies are “csv” files that collect all the economic information needed for the calculation of the COE of a power plant. The input file is common for all the technologies, but it is populated with different data depending on the type of technology. I.e. while a fossil fuel technologies will be characterized by the cost of the fuel, the calorific value of the fuel, the photovoltaic technology does not. The input data for the technologies are obtained principally from the “Energy Technology Reference Indicator projections for 2010-2050” [79]. ETRI 2014 is a document from the European Commission that collect for many technology the economic data for all the European country and it give a projection of the economic data to the 2050. In addition to the ETRI 2014 other useful documents for the data are: the report from the Polytechnic of Milan “Costi di produzione di energia elettrica da fonti rinnovabili” [80] for the bioenergy technologies, the portal of the International Renewable Energy Agency (IRENA) for the photovoltaic technologies, and “Energia elettrica, anatomia dei costi. 2014” for the Italian power plant [81]. In Figure 3-63, Figure 3-64, Figure 3-65 there are three example of input file respectively for a fossil fuel tech, for a renewable tech and for a nuclear tech. In Figure 3-66 it is presented the file that contains the list of the technologies taken as input by COMESE code. In this summary file, at the beginning it is specified the number of technologies used, and then they are collected the names of all the technologies with the input file for each one.

	A	B	C	D	E	F
1	Technology name	CoalUSC				
2	Author	Daniele				
3	Creation date	23-feb-18				
4	Information	Base	Mode	min %	max %	distribution
5	Overnight cost [€/kW]	1600	1600	-3	6	tri
6	Own capital cost	0.05	-	-	-	-
7	Debt cost	0.05	-	-	-	-
8	Debt fraction [%]	50	-	-	-	-
9	Years of construction [years]	4	4	-25	25	tri
10	Efficiency	48	48	-10	10	tri
11	Life [year]	40	40	-10	10	tri
12	O&M fix cost [€/kW.a]	40	40	-3	6	tri
13	O&M variable cost [€/MWh]	3.6	-	-	-	-
14	skewness	1.357	-	-	-	-
15	Calorific value of the fuel [MJ/kg] o [MJ/m3]	25	25	-17	17	lin
16	Fuel price [€/kg] o [€/m3] o [€/bbl]	0.15	0.15	-30	30	lin
17	Burn-up [MWd/kgUarr]	-	-	-	-	-
18	consumption Unat for kg Uarr [kgUnat/kgUarr]	-	-	-	-	-
19	conversion cost of enrichment [€/kg Uarr]	-	-	-	-	-
20	Combustion cycle closing cost [€/kg Uarr]	-	-	-	-	-
21	Natural uranium price [€/kgUnat]	-	-	-	-	-
22	Kg of CO2 released for kg of fuel [-]	2.5	-	-	-	-
23	CO2 capture efficiency [%]	-	-	-	-	-
24	CO2 emission price [€/t]	20	20	-25	25	lin
25	CO2 transport price [€/t]	-	-	-	-	-
26	CO2 storage price [€/t]	-	-	-	-	-
27	GCs (green certificates)	-	-	-	-	-
28	Additional cost for storage [€/kWh]	-	-	-	-	-
29	Decommissioning cost [%]	-	-	-	-	-
30	Years before decommissioning [years]	-	-	-	-	-
31	Provision for decommissioning	-	-	-	-	-

Figure 3-63: example of input file for a fossil fuel technology, (coal USC)

At the beginning of the input file for the technologies, it is specified the technology name, the author, and the creation date. Useful information for remembering when and who created that input file. Then it is specified the economic information, each line corresponds to a parameter, and for each parameter it is possible to define a base value, the mode, the min and max variation respectively to the mode and the type of distribution. The reason of this is that COMESE code is prepared for statistical analysis using a Monte Carlo simulation, so each parameter can be defined as an interval with the correspond uncertainties and a determinate distribution of probability. In the table presented in Figure 3-63 for example it is possible to see two types of distribution: with “tri” is indicated a probability distribution triangular centred to the mode value, with “lin” a uniform distribution, each value of the interval has the same probability.

	A	B	C	D	E	F
1	Technology name	PV residential 1200				
2	Author	Daniele				
3	Creation date	08-feb-18				
4	Information	Base	Mode	min %	max %	distribution
5	Overnight cost [€/kW]	1000	1000	-15	15	tri
6	Own capital cost	0.05	-	-	-	-
7	Debt cost	0.05	-	-	-	-
8	Debt fraction [%]	50	-	-	-	-
9	Years of construction [years]	1	-	-	-	-
10	Efficiency	30	30	-10	10	tri
11	Life [year]	25	25	-17	17	tri
12	O&M fix cost [€/kW.a]	20	20	-15	15	tri
13	O&M variable cost [€/MWh]	0	-	-	-	-
14	skewness	1.357	-	-	-	-
15	Calorific value of the fuel [MJ/kg] o [MJ/m3]	-	-	-	-	-
16	Fuel price [€/kg] o [€/m3] o [€/bbl]	-	-	-	-	-
17	Burn-up [MWd/kgUarr]	-	-	-	-	-
18	consumption Unat for kg Uarr [kgUnat/kgUarr]	-	-	-	-	-
19	conversion cost of enrichment [€/kg Uarr]	-	-	-	-	-
20	Combustion cycle closing cost [€/kg Uarr]	-	-	-	-	-
21	Natural uranium price [€/kgUnat]	-	-	-	-	-
22	Kg of CO2 released for kg of fuel [-]	-	-	-	-	-
23	CO2 capture efficiency [%]	-	-	-	-	-
24	CO2 emission price [€/t]	-	-	-	-	-
25	CO2 transport price [€/t]	-	-	-	-	-
26	CO2 storage price [€/t]	-	-	-	-	-
27	GCS (green certificates)	-	-	-	-	-
28	Additional cost for storage [€/kWh]	-	-	-	-	-
29	Decommissioning cost [%]	-	-	-	-	-
30	Years before decommissioning [years]	-	-	-	-	-
31	Provision for decommissioning	-	-	-	-	-

Figure 3-64: example of input file for a renewable technology, (residential photovoltaic)

	A	B	C	D	E	F
1	Technology name	Nuclear_EPR				
2	Author	Daniele				
3	Creation date	mar-17				
4	Information	Base	Mode	min %	max %	distribution
5	Overnight cost [€/kW]	3700	3700	-25	25	tri
6	Own capital cost	0.05	-	-	-	-
7	Debt cost	0.05	-	-	-	-
8	Debt fraction [%]	50	-	-	-	-
9	Years of construction [years]	7	7	-20	30	tri
10	Efficiency	37	37	-10	10	tri
11	Life [year]	60	60	-20	20	tri
12	O&M fix cost [€/kW.a]	80	80	-50	50	tri
13	O&M variable cost [€/MWh]	1.8	-	-	-	-
14	skewness	1.357	-	-	-	-
15	Calorific value of the fuel [MJ/kg] o [MJ/m3]	-	-	-	-	-
16	Fuel price [€/kg] o [€/m3] o [€/bbl]	-	-	-	-	-
17	Burn-up [MWd/kgUarr]	60	-	-	-	-
18	consumption Unat for kg Uarr [kgUnat/kgUarr]	8.41	-	-	-	-
19	conversion cost of enrichment [€/kg Uarr]	1500	1500	-30	30	tri
20	Combustion cycle closing cost [€/kg Uarr]	630	630	-25	25	lin
21	Natural uranium price [€/kgUnat]	90	90	-60	60	lin
22	Kg of CO2 released for kg of fuel [-]	-	-	-	-	-
23	CO2 capture efficiency [%]	-	-	-	-	-
24	CO2 emission price [€/t]	-	-	-	-	-
25	CO2 transport price [€/t]	-	-	-	-	-
26	CO2 storage price [€/t]	-	-	-	-	-
27	GCs (green certificates)	-	-	-	-	-
28	Additional cost for storage [€/kWh]	-	-	-	-	-
29	Decommissioning cost [%]	16	16	-25	25	lin
30	Years before decommissioning [years]	30	-	-	-	-
31	Provision for decommissioning	0.025	0.025	-25	25	lin
32						

Figure 3-65: example of input file for a nuclear technology, (EPR)

```
ElencoTecnologie2050 - Blocco note
File Modifica Formato Visualizza ?
Numero di tecnologie      23
Carbone USC      Input_Fossil_Carbone_USC_2050.csv
Carbone USC+CCS  Input_Fossil_Carbone_USC+CCS.csv
Gas CCGT         Input_Fossil_Gas_CCGT_2050.csv
Gas CCGT+CSS    Input_Fossil_Gas_CCGT+CCS.csv
Gas OCGT        Input_Fossil_Gas_OCGT_2050.csv
Fossil Oil      Input_Fossil_Oil_2050.csv
Nuclear EPR     Input_Nuclear_EPR.csv
Nuclear SMR     Input_Nuclear_SMR.csv
Fusione Input_Nuclear_Fusion.csv
RenewBiogas     Input_Renewable_Biogas_2050.csv
Biomasse RSU   Input_Renewable_Biomasse_RSU_2050.csv
Biomasse Modulabili  Input_Renewable_Biomasse_Modulabili_2050.csv
CSPconAccumulo Input_Renewable_CSP_con_Accumulo_2050.csv
CSPnoAccumulo  Input_Renewable_CSP_senza_Accumulo.csv
EolicoOnshore  Input_Renewable_Eolico_onshore_2050.csv
EolicoOffshore Input_Renewable_Eolico_offshore_2050.csv
EolicoOffshoreGalleg  Input_Renewable_Eolico_offshore_galleg_2050.csv
FotovoltaicoInd  Input_Renewable_Fotovoltaico_ind_2050_1200.csv
FotovoltaicoRes Input_Renewable_Fotovoltaico_res_2050_1200.csv
FotovoltaicoTerra  Input_Renewable_Fotovoltaico_terra_2050_1500.csv
Geotermico     Input_Renewable_Geotermico_2050.csv
IdroGrande     Input_Renewable_Idro_Grande_2050.csv
IdroFluente    Input_Renewable_Idro_Fluente_2050.csv
Linea 24, colonna 50
```

Figure 3-66: example of summary input file for the technologies

3.13 Input file - the storage technology data

Also for the energy storage systems there is an input file that collects all the economics and operational parameters. For the Hydroelectric storage data referred to the European documents, ETRI 2014 [80]. For the data of the lithium batteries referred to the Lazard's Levelized Cost of Storage Analysis [101], where it is collected the information for different type of electric storage systems. In Figure 3-67 it is given an example of input file for an Hydroelectric storage system, in Figure 3-68 an example for a batteries storage system.

	A	B	C	D	E	F
1	Technology name	StorageHydro2050				
2	Author	Daniele				
3	Creation date	lug-17				
4	Information	Base	Mode	min %	max %	distribution
5	Overnight cost [€/kW]	1500	1500	-53.33	33.33	tri
6	Overnight cost [€/kWh]	-	-	-	-	-
7	Own capital cost	0.05	-	-	-	-
8	Debt cost	0.05	-	-	-	-
9	Debt fraction [%]	50	-	-	-	-
10	Years of construction [years]	4	4	-25	25	tri
11	Efficiency INPUT [%]	90	-	-	-	-
12	Efficiency OUTPUT [%]	90	-	-	-	-
13	Depth of discharge (DOD) [%]	100	-	-	-	-
14	Life [anni]	60	60	-10	10	tri
15	O&M fix cost [€/kW.a]	22.5	22.5	-53.33	33.33	tri
16	O&M variable cost [€/MWh]	-	-	-	-	-
17	skewness	1.357	-	-	-	-
18	Nominal power [GW]	9	-	-	-	-
19	Maximum capacity [GWh]	100	-	-	-	-
20	Available capacity at t=0 (optional) [GWh]	0	-	-	-	-
21	Power of one module [MW]	-	-	-	-	-
22	Duration of storage for module [h]	-	-	-	-	-

Figure 3-67: example of input file for hydroelectric storage

From a comparison between the input file for the technologies and for the energy storage systems, it is possible to see that some parameter are the same like the overnight cost in [€/kWh] or the life of the system. In addition there is the new parameter specific for the energy storage systems.

Overnight cost for a storage system can be defined also in [€/kWh]. For the batteries storage system there is a strong connection between the energy capacity of the modules and the nominal power, so it is possible to make an easy conversion from overnight cost in [€/kWh] and overnight cost in [€/kW]. In the input file it was maintaining the possibility to define both of them.

For storage systems two efficiencies are defined: an input and an output one, as described in the paragraph about the operation of the storage system. In addition, it is possible to set the depth of discharge parameters, that defines the minimum level of the energy that must remain inside of the storage.

Nominal power here is defined as the maximum power accepted as input or the maximum power released as output at net of the efficiency.

Maximum capacity: defined as the maximum amount of energy that can be stored in the system, if this level is set to a very high level (i.e. 1000TWh) is equal to have an unlimited storage system, for the batteries the Maximum capacity it is related to the nominal power via the number of hours for which the system can store the energy.

Example:

If it is defined a battery storage system of 800 TWh of maximum energy, and this system is built with batteries modules that have a duration of the storage of 8 hours, the corresponding nominal power of the system is the ratio of the energy capacity and the hours of storage:

$$(3.15) P_n = \frac{\text{Energy capacity [GWh]}}{\text{Storage time [h]}} = \frac{800}{8} = 100 \text{ GW}$$

Normally it is used the assumption that a storage system at the beginning of the year is empty, but if the simulation required a different solution, it is possible to set the initial level of storage in the field “Available capacity at t=0” where with t=0 is the first hours of the years. Last two parameters are the power of one module of the storage, parameter defined only for the batteries systems, and the “Duration of the storage”, in other words the time for which the module can store the energy.

	A	B	C	D	E	F
1	Technology name	Lithium Batteries 2050				
2	Author	Daniele				
3	Creation date	lug-17				
4	Information	Base	Moda	min %	max %	distribuzione
5	Overnight cost [€/kW]	768	768	-20	20 tri	
6	Overnight cost [€/kWh]	-	-	-	-	-
7	Own capital cost	0.05	-	-	-	-
8	Debt cost	0.05	-	-	-	-
9	Debt fraction [%]	50	-	-	-	-
10	Years of construction [years]	1	-	-	-	-
11	Efficiency INPUT [%]	92	-	-	-	-
12	Efficiency OUTPUT [%]	92	-	-	-	-
13	Depth of discharge (DOD) [%]	100	-	-	-	-
14	Life [anni]	10	10	-25	25 tri	
15	O&M fix cost [€/kW.a]	13.44	13.44	-20	20 tri	
16	O&M variable cost [€/MWh]	0.0208	-	-	-	-
17	skewness	1.357	-	-	-	-
18	Nominal power [GW]	100000	-	-	-	-
19	Maximum capacity [GWh]	800000	-	-	-	-
20	Available capacity at t=0 (optional) [GWh]	0	-	-	-	-
21	Power of one module [MW]	100	-	-	-	-
22	Duration of storage for module [h]	8	-	-	-	-

Figure 3-68: example of input file for lithium batteries storage

3.14 Storage system model

One of the major improvements of COMESE code with respect to the previous version is the introduction of a computing module for the simulation of one or more electric storage systems.

Using an hydraulic analogy, the storage system can be modelled like a graduated cylinder, where the cylinder represents the tank where to store electric energy. The dimensions of the tank define the capacity, the fluid the energy loaded and discharged and the flow rate of the connections with which the fluid is carried to the cylinder representing the electric power in input and in output of the system. The losses in the connections can be seen as the losses in the charge and discharge processes of the system for which an entry efficiency and an outgoing efficiency are defined.

So the storage system is like this tank defined with a maximum capacity C_{stor} [GWh], the maximum energy that can be stored in that system, a nominal power $P_{n\ stor}$ [GW] defined as the internal power that the system can managed, two efficiencies, one for the charging process η_{in} and one for the discharging η_{out} process. The round trip efficiency η_{tot} is defined as the product of the input and output efficiency:

$$(3.16) \quad \eta_{tot} = \eta_{in} \times \eta_{out}$$

Because the storage is modeled like a tank with input and output connections, more than one electric storage systems can be easily modeled by connecting more system in series. From a programming point of view in COMESE code the programming instructions represented by all the variables that define a storage system and the functions, methods proper of a storage system (like the charge or the discharge) are contained in a single file the “storage.h” class. So for the COMESE program, simulating two or more storage systems means simply defining two or more objects of the storage class that will then be used in the simulation. (define an object of a class are like define a variable, but formed by a larger and more organized structure).

So for example in a simulation they can defined two storage systems: an hydroelectric storage system who usually in the simulation is defined for working first, and a batteries’ storage system who works for second. In the paragraph 3.13, they are summarized the main parameters defined for a storage system used in COMESE code. The storage energy capacity is usually limited by technical constraints (e.g. the available volume of basins for pumped hydro power stations that varies according to the ground morphology and hydrology). However, in case of batteries, the storage system is modular, that is n modules of nominal power ($P_{n\ stor\ unitary}$ [GW]) and energy capacity ($C_{stor\ unitary}$ [GWh]) are connected in series and parallel, so for the overall system nominal power $P_{n\ stor}$ [GW] and energy capacity C_{stor} [GWh] no evident limits exists.

In principle the maximum capacity defined for a storage systems in COMESE code can be set to a very high value (1000TWh); the consequence of this solution is that the code sees the storage as a theoretical unlimited storage systems. In this condition COMESE code do all the same operation of a limited one, but at the end gives as a result the capacity of the storage system that allows the electric system to store all the excess energy without curtailment.

3.14.1 Charging and discharging process

Each storage system is modeled as a tank, the charge and discharge routine progressively fills or empties the storage system based on generation and load dynamics. Scrolling through the hours of the year, evaluate for each hour if there is a generation surplus or a residual demand.

In the first case it evaluates the surplus in terms of power and compares it with the maximum power surplus storable in hour i :

$$(3.17) \quad P_{in} = P_n / \eta_{in}$$

If the surplus power exceeds this value, the system loads at maximum the maximum input power. The remaining surplus power should be stored in one of subsequent storage systems. Before loading the storage using the input power, the routine performs a check on the energy already stored, checking if the system can store the energy of that time. Eventually reducing the power used in charge for that time. When the charge and discharge routine detect a residual demand for one hour, the routine makes two checks first controls if the stored energy is adequate to meet this residual demand then if the residual demand is consistent with the maximum output power. The maximum power the storage system can deliver to fill deficits is:

$$(3.18) \quad P_{out} = P_n \times \eta_{out}$$

After these checks fill the residual demand with the appropriate level of power in output. During the charging process and discharging, the level of energy stored in the storage system varies. In case the system has been set with a capacity [GWh] so high as to be approximate to an unlimited system, the maximum level of energy stored during the year defines what is the capacity of the system to store all the annual surplus.

3.14.2 Optimization method for the discharge process

The method for charging and discharging just described is the simplest solution but it is not the best, in fact the routine thus set unloads the stored energy as soon as required, without any control over the remaining residual demand level after the storage activation. This electrical residual demand is the one that must be covered by the modular technologies, whose generation cost depends on the installed power and grows with it for the same level of energy generated. The discharge of storage system without a control can leave in the residual demand a peak of required power higher than the installed power of dispatchable technologies. In the optimization method that is presented here, a solution was studied in order to model a controlled discharge of storage energy.

The routine starts with an evaluation for the year of all the events of deficit in terms of time duration, energy required to cover the events of deficit and peak power of the event. All these data are collected and saved in appropriate vectors. For doing this, the storage activation routine calculate a vector with the hourly difference between the Load and the generation from base, must-run power plant.

$$(3.19) \quad \Delta P_{y,i} = E_{y,i} - D_{y,i}$$

Where $\Delta P_{y,i}$ is the power difference between the generation and the load, $E_{y,i}$ the power generate and $D_{y,i}$ the demand of electricity all for year y and the hour i . $\Delta P_{y,i} > 0$ denotes an overproductions for the hour i , $\Delta P_{y,i} < 0$ a deficit while $\Delta P_{y,i} = 0$ when the generation meet the load.

Whenever overproductions occur, the energy surplus can be stored only if $\Delta P_{y,i} \leq P_{in}$ and $E_{st,y,i-1} < C_{st}$ where P_{in} the maximum power accepted as input, $E_{st,y,i}$ is the energy level of the storage for the hour $i-1$ and C_{st} the maximum capacity for the storage. A generation curtailment occurs otherwise.

On the other hand, the first time that the routine finds $\Delta P_{y,i} < 0$ following a surplus event, it starts the optimization process for the discharge. The first hour of deficit following a surplus event is the beginning of a deficit event. The amount of energy needed for covering the deficit $En_{def}(j)$ is read from the vector just evaluated, and it is compared to the total energy stored previously in the storage system $En_{stor}(j)$. With j are indicate the index of the vector for the deficit events. Now the routine calculates the energy availability coefficient kD as:

$$(3.20) \quad Kd = (En_{stor} * \eta_{out}) / En_{def}$$

The energy availability coefficient allows to know if the stored energy can cover the whole event of deficit or not. If $Kd \geq 1$ the storage system has all the energy necessary to cover the deficit later and optimizing system does not turn on and the storage system fills the deficit event without any control. Otherwise if $Kd < 1$ the storage system hasn't all the energy needed and the power demand for each hour of the deficit event that the storage system has to fill are reduced by the Kd coefficient. With these methods the energy stored is spread in all the deficit in a more uniform way, even if the storage doesn't have all the energy for cover it. And the peak of the residual demand is reduced.

3.14.3 Storage optimization method with activation of dispatchable technologies

Always with the final goal of reducing the generation cost for the modular technologies, the possibility of preloading the storage with modular technologies was introduced with the aim of further reducing the power peak of the residual demand (relatively recent development in the COMESE code). In few words, in addition to the coefficient kD , a second coefficient kD_{mod} is calculated for each deficit events in function of the energy that the storage must have for cover the deficit event, so that the maximum remaining residual power is lower than a fixed power level.

If $Kd_{mod} \geq 1$ the storage system has all the energy necessary to cover the deficit so that the residual demand has a power level lesser or equal to the dispatchable technology installed. Otherwise if $Kd_{mod} < 1$ the storage system hasn't the energy needed and the routine starts to evaluate the individual deficits that make up the deficit event. For each hour of deficit, the routine uses at first the energy stored, and if the level of the residual power demand is higher than the reference value, the routine scroll the vectors and it goes back of a fixed number of hours, and it activates in those hours a modifiable power to preload the storage in order to have for the hour in question an additional stored energy to be used.

The advantage of this method lies in the fact that the storage system can be charged for many hours with a low power and can provide a high power in a few hours. This type of use does not affect the cost of the storage system that is related to capacity, but it allows to greatly reducing the installed power from the modular that, instead, impacts a lot on the cost of the system.

3.15 Optimized flexible technology activation.

In COMESE code, for meeting the residual demand after the activation of base power plants, must-run power plants and the storage systems the dispatchable technologies are activated. In this chapter it is described the routine for the activation of the dispatchable technologies and the three solution adopted for covered the residual demand and at the same time try to reduce the cost of the electric system.

Dispatchable technologies are activated with a priority order and with three methods specified in the input file of the scenario. The possible activation methods are:

- “common activation” named in the input file as CMOD, developed for fill residual deficits as much as possible, in function of the energy set for that technology and the capacity installed.
- “power – hours deficit” named as PHDEF, developed for maximize the energy use for a dispatchable technologies, but with the lowest level of capacity installed. This method has been designed to reduce the cost of those dispatchable power plants that have high installation costs (fixed costs) compared to fuel costs.
- “trapezoidal activation” named as TRP developed for use maximum power in case of greater residual demand.

In general, the “common activation” method is used for the latest dispatchable technology like gas technologies (OCGT – open gas cycle turbines), while the “trapezoidal activation” is used for hydroelectric technologies to make the most of the installed power. “PHDEF” is used for bioenergy technology, where making the most of an installed plant allows to reduce the fixed realization costs.

As described in the flowchart of Figure 3-69, the main routine for the dispatchable technologies takes as first input the array of the residual demand wrote at the end of storage module, then it reads the first dispatchable technology data and in function of the operational-code (CMOD, PHDEF, TRP) it activates one of the three subroutine. Each one fills properly the residual demand and at the end returns an array of residual demand update, where the hourly value is reduced in function of the dispatchable power activated hourly. This array becomes the new residual demand array for the next dispatchable technology. The routine continues iteratively until they are used all the dispatchable technologies or the residual demand is completely covered. Naturally, if the dispatchable technologies are not sufficient to cover the residual demand, this will be reported at the end of the calculation routine.

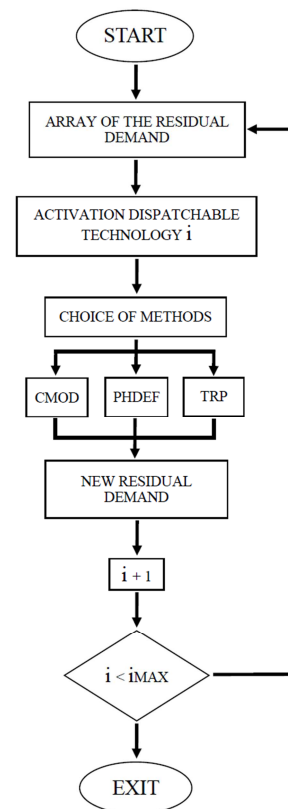


Figure 3-69: dispatchable routine flowchart

Key point of the COMESE code is to maintain the possibility to be able to say whether a scenario is feasible or not. For this reason, no automatic routine has been introduced that modifies the values set in the initial scenario in order to cover the demand. COMESE code gives a result if a scenario is feasible or not, and provides to the user the information to correct it. But it is always up to the user to choose how to do it.

All the three methods start the routine from the array of the residual demand $\Delta P_{y,i}$, difference between Load and Generation from base, must-run and storage systems. The residual demand array in the routines are sorted in ascending or descending order with respect to the value of the residual demand, keeping the hourly information of the year. A duration curve of the residual demand is obtained from this process. The hourly information of the year is kept, since it allows to return to the ordered vector $\Delta P_{y,i}$ according to the hours of the year at the end of the routine. Crucial passage to know for every hour of the year, those plants are called to cover the electricity demand. The three routines operate on the duration curve of the residual demand according to a logic similar to that of the storage, they fill the residual demand respecting power and energy constraints of the dispatchable technologies and one of the three different objectives set in the scenario input file.

3.15.1 Common activation routine - CMOD

In the common activation routine, energy allocated for that technology is spread proportional in the duration curve with a profile of activation scaled form the duration curve itself.

The residual demand vector, containing the hourly data of the residual demand, is loaded and sorted in a decreasing order. Then for the first hour $i = 0$ of the duration curve, the routine evaluates the activation coefficient $kD_{mod}(i)$ as the ratio between the total energy that the dispatchable technology should generate $En_{mod_{th}}(i)$ and the total energy for cover the residual demand $En_{res_{dem}}(i)$. With i is indicated the iteration.

$$(3.21) \quad kD_{mod}(i) = \frac{En_{mod_{th}}(i)}{En_{res_{dem}}(i)}$$

The activation coefficient is used for calculating the required power P_{req} to the dispatchable technology for the i iteration, as the product of the residual demand of the i hour of the array of the residual demand and the activation coefficient.

$$(3.22) \quad P_{req}(i) = P_{dem}(i) * kD_{mod}(i)$$

Now P_{req} are compared to the installed power for the technology and if it is greater, they are limited to the installed one. The request for residual power for the hour is covered for a quota equal to P_{req} .

$En_{mod_{th}}(i)$ and $En_{res_{dem}}(i)$ values are update in function of the power activate, becoming $En_{mod_{th}}(i + 1)$ and $En_{res_{dem}}(i + 1)$. In the new iteration a new activation coefficient is calculated for the new hour and so on. The routine ends if the total residual energy demand becomes zero, if the energy set for that technology becomes zero (all the energy was used for that technology) or if the routine reaches the end of the array. At the end all the arrays are reordered according to the hours of the year. In Figure 3-70 it is presented an example of CMOD activation, in blue the duration curve for the residual demand and in red the portion of the residual demand covered by the CMOD activation method.

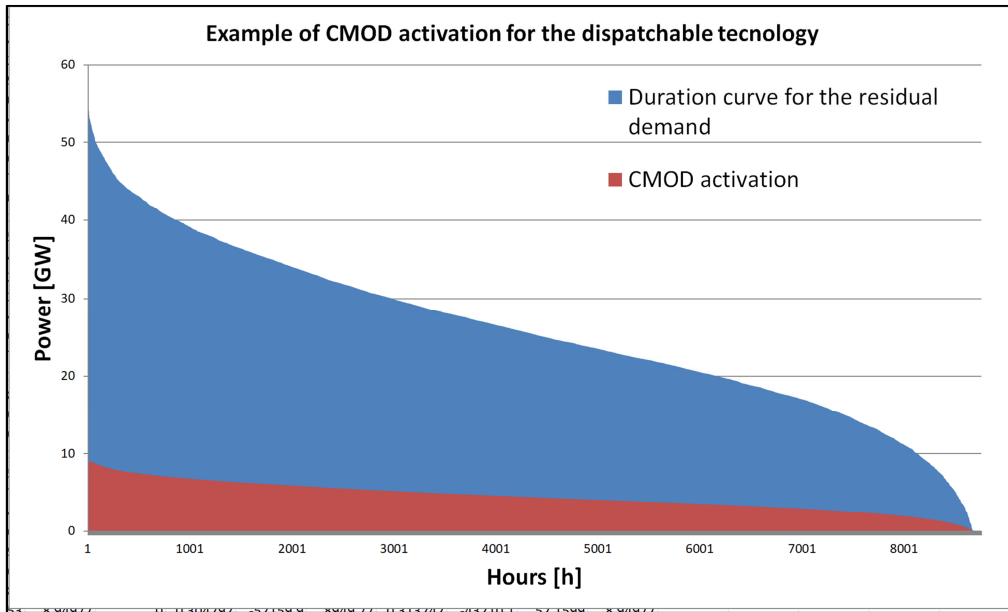


Figure 3-70: Example of common activation methods for a dispatchable technology

3.15.2 Power – hour deficit routine - PHDEF

The “PHDEF” method (developed for biomass technology) is designed to distribute the available energy covering the maximum possible hours by appropriately adjusting the installed electrical power (not known a priori). Only for this method, the hourly deficit is sorted in increasing order. At the beginning it is calculated the first attempt power P_{mod_th} :

$$(3.23) \quad P_{mod_th} = E_{nmod}/h_{defMax}$$

where E_{nmod} is the energy associate with that technology and h_{defMax} the total hours of deficit whenever $\Delta P_{y,i} < 0$. For the first hour the deficit is filled completely if

$$(3.24) \quad \Delta P_{y,i} \leq P_{mod_th}$$

or only partially if

$$(3.25) \quad \Delta P_{y,i} > P_{mod_th}$$

than the value of the remain energy of that technology is updated, the deficit hours will decrease, and it will be calculated the new iteration power. The installed power level is adjusted iteration after iteration until the optimal level and the final hours are reached.

Figure 3-71 presents an example of PHDEF activation, in blue the duration curve for the residual demand and in red the portion of the residual demand covered by the PHDEF activation method.

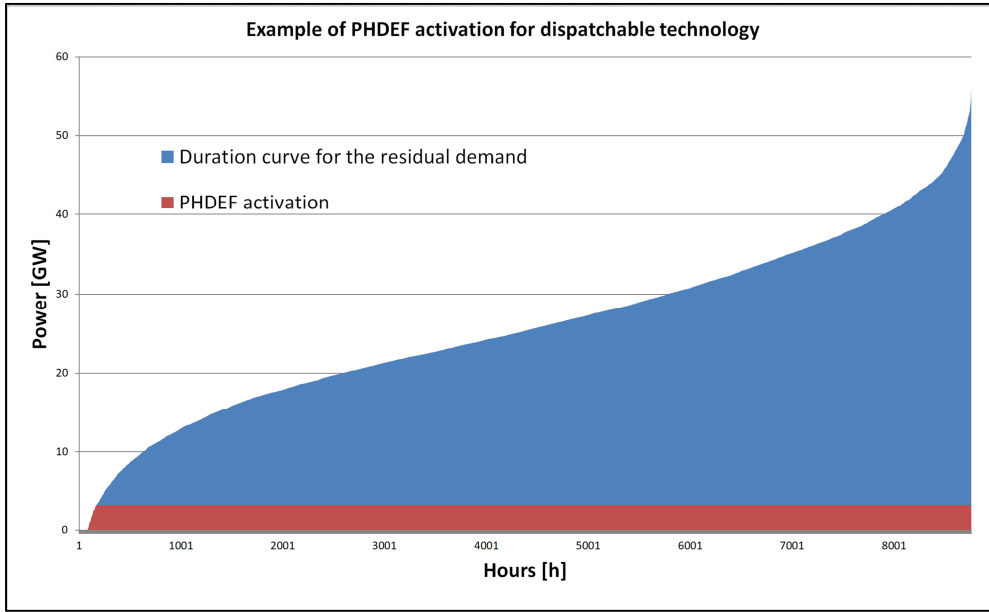


Figure 3-71: Example of PHDEF activation for dispatchable technology

3.15.3 Trapezoidal activation - TRP

“**Trapezoidal activation**” is used when an electrical power and an energy associated with that technology are known, and with the aim to activate the maximum installed power and generate the greater part of the energy in the hours of greater residual demand, consequently reducing its use in the hours where the demand is lower. The method bases its function in the idea of covering the base of the duration curve with a trapezoidal activation profile.

From the scenario input, it is known the power installed P_I and the energy that the technology has to generate En_{mod} . From the array of the residual demand, it is obtained the duration curve with a decreasing order. And from this curve, it is calculated the total number of hours of the residual demand h_{max} . With these data are prepared the trapezoidal profile of activation, where the major base of the trapeze is h_{max} , the height are P_I and the minor base is h_{peak} . The value of h_{peak} are computed with the equation 3.26.

$$(3.26) \quad h_{peak} = \frac{[(2 \cdot En_{mod}) - (P_I \cdot h_{max})]}{P_I}$$

If the value of $h_{peak} < 0$ is set to $h_{peak} = 0$ and the trapezoidal profile degenerate in a triangular one. Where the base of the triangle are the h_{max} and the height are P_I .

The h_{peak} value indicates the transition index for the activation. For the hours index lesser than h_{peak} the dispatchable technology can be activated with a power level equal to the installed power. For the hours index greater than h_{peak} the dispatchable technology is activated with a power reduce and equal to $P_{activate}$ equation 3.27.

$$(3.27) \quad P_{activate} = P_I \cdot \frac{h_{defres}}{h_{defres} - h_{peak}}$$

Where with h_{defres} is indicated the remaining hours of the residual to be covered.

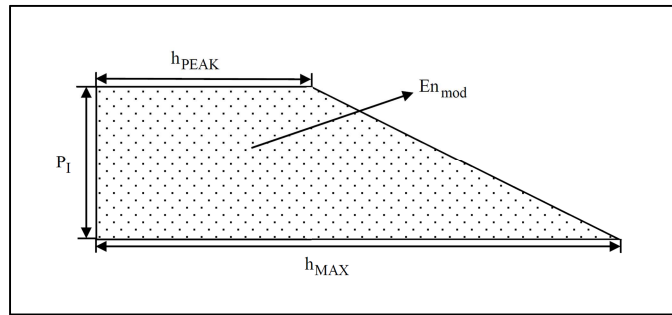


Figure 3-72: trapeze with the parameters used in the TRP activation method

In Figure 3-72 it is described the parameter use for the evaluation of the trapezoidal profile and in Figure 3-73 it is presented an example of the TRP activation, in blue the duration curve for the residual demand and in red the portion of the residual demand covered by the TRP activation method. Figure 3-74 gives another example TRP activation, where the trapezoidal profile degenerates into a triangular shape.

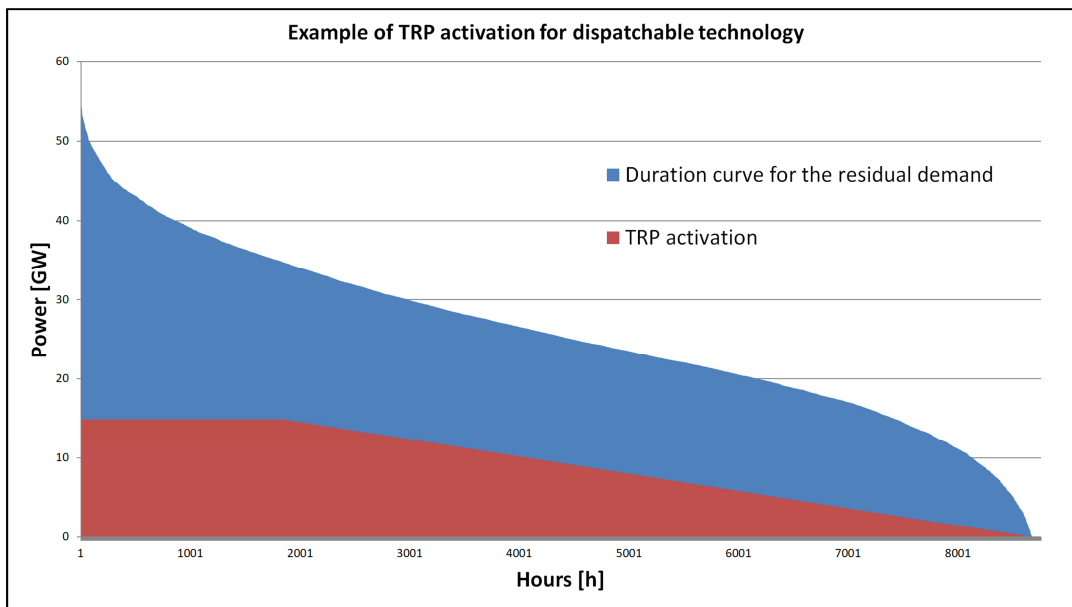


Figure 3-73: Example of TRP for dispatchable technology

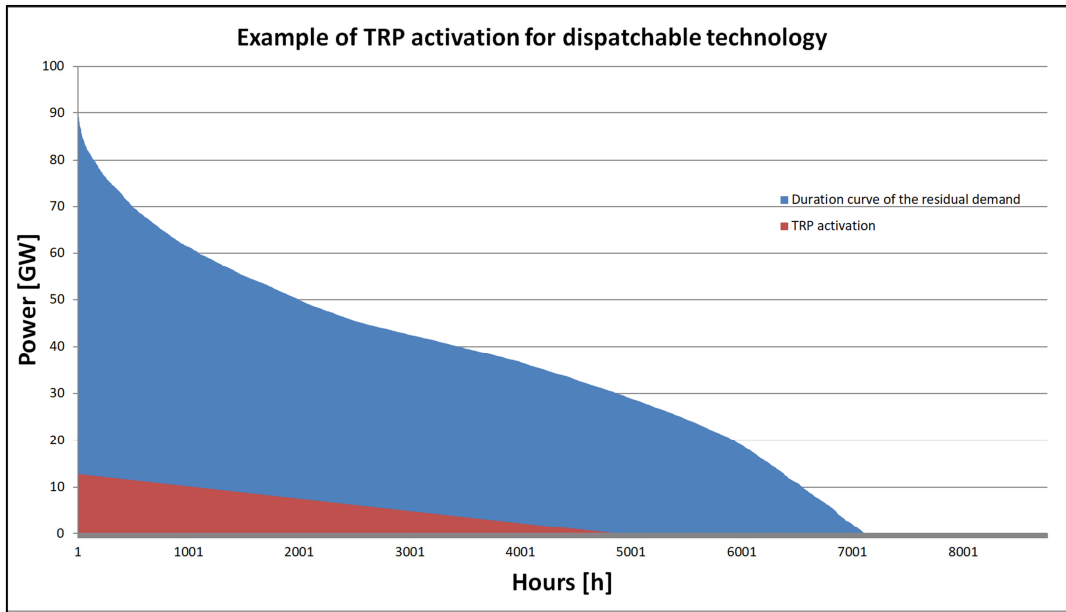


Figure 3-74: Example of TRP for dispatchable technology, case of a triangular shape.

3.16 Curtailment

The COMESE code reduction routine is only activated if, after the activation of the storage systems, there is still a surplus of energy generated. The routine loads the surplus array and scrolls the hours of the year curtailed the hourly surplus from the must-run technologies generation. The curtailment operates first on the photovoltaic generation and then on the wind generation dividing the curtailment proportionally between the various types of photovoltaic or wind power plants. The consequence of the curtailment is that the power plant generate less energy respectively to the installed power, so the capacity factor decreases and consequently the COE of the correspond technology increases. The increase in the generation cost can be explained by the fact that at the level of the electricity system the energy we throw is also paid.

3.17 Demand and generation

In this chapter before the description of the economic calculation of the COE and the LCOTE, some figures show how COMESE code gradually meets the load profile with the activation of the different power plant technologies and storage systems. All the figures here are limited to some days of the year for a better representation.

In Figure 3-75, it is presented the starting point the demand of electricity and the generation from Base and must run technologies; as can be seen, the generation exceed the demand in some hours, surplus events, and in other remain under the demand, deficit events. Figure 3-76 plots the trend of the storage system in the charge and discharge process.

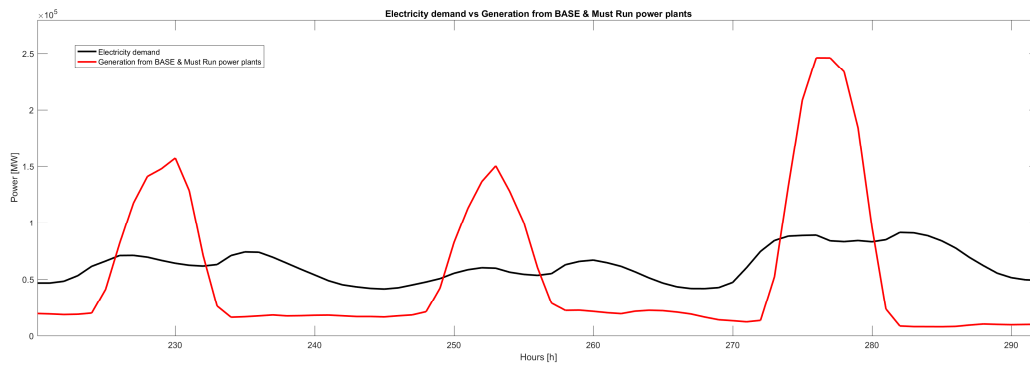


Figure 3-75: Load profile of the electricity demand and generation from base and must run power plants.

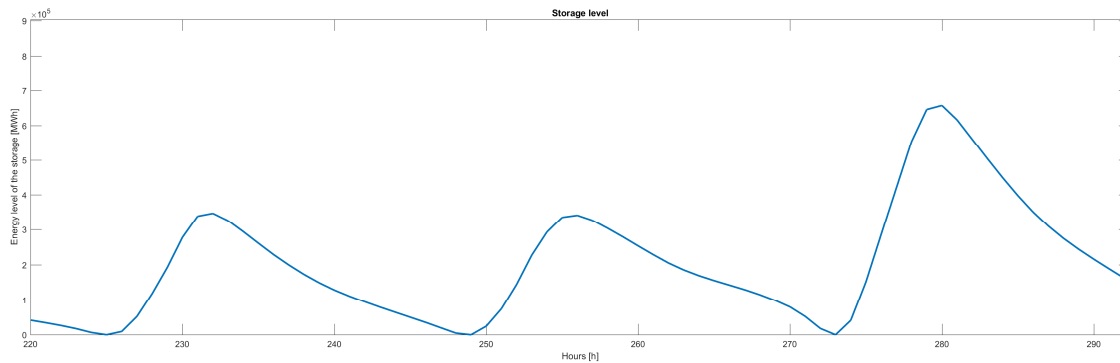


Figure 3-76: Storage level trend for stored the energy surplus of the Figure 3-75: Load profile of the electricity demand and generation from base and must run power plants.

Figure 3-77 presents the electricity demand and the residual demand that must be covered by the storage systems and the dispatchable technologies. Finally in Figure 3-78 the result of the simulation when the generation meets the demand is presented.

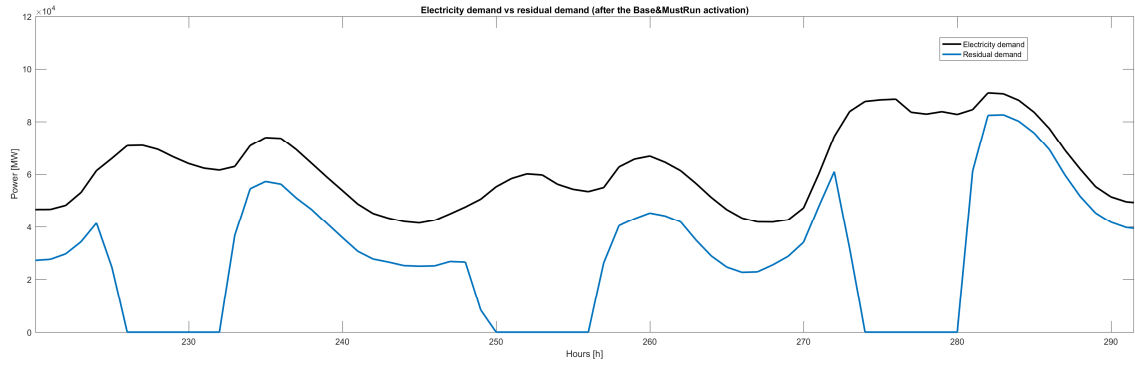


Figure 3-77: Load profile of the electricity demand and residual energy demand after the activation of the base and must run power plants.

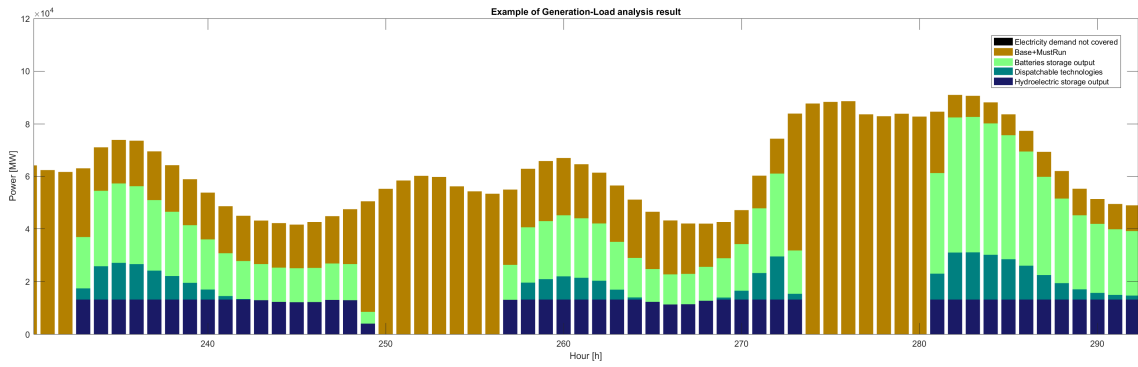


Figure 3-78: example of how COMESE meets the electricity demand using the Base, Must-Run technology, storage and dispatchable technologies.

3.18 LCOTE and SLCOTE

Once the power mix technical feasibility is checked and the hourly balance between demand and generation plus stored power verified, COMESE performs an economic assessment. The SLCOTE, system levelized cost of timely electricity is used as a benchmark between alternative energy scenarios. Thus, assuming that in year y the electricity is generated by a brand new power plants' fleet, i.e. neglecting any existing capacity and the related amortized investment. Provided that N generating plants are serving the system in year y , the SLCOTE of a system is calculated as follows:

$$(3.28) \quad SLCOTE_y = \frac{\sum_{i=1}^N (LCOTE_{i,y} \times E_{i,y}) + C_{add}}{E_{tot,y}}$$

where $LCOTE_{i,y}$ is the levelized cost of timely electricity generated by the i -th technology, $E_{i,y}$ and $E_{tot,y}$ are the electricity generated by the i -th technology and the energy system respectively. C_{add} [€] are additional costs due to energy storage systems and/or expenditures related to transmission grid upgrades. The formula of the SLCOTE can be rewritten using also the energy values related to the energy demand:

$$(3.29) \quad SLCOTE_y = \sum_{i=1}^N \left(LCOTE_{i,y} \times \frac{E_{i,y}[\%]}{100} \right) + C_{add}$$

In these equation $C_{add} \left[\frac{\text{€}}{\text{kWh}} \right]$

The $LCOTE_{i,y}$ for each technology is computed as follows (IEA/NEA, 2010):

$$(3.30) \quad LCOE_i = \frac{\sum_{t=0}^{PP_{elife}} (I_{t,i} + O\&M_{t,i} + F_{t,i} + D_{t,i} + C_{t,i})(1+r)^{-t}}{\sum_t E_t(1+r)^{-t}}$$

where t is the year in which the sale of production takes place, PP_{elife} is the power plant economical life, $I_{t,i}$ is the power plant investment cost, $O\&M_{t,i}$ the operation and maintenance costs, $F_{t,i}$ the fuel cost, $D_{t,i}$ the cost of decommissioning, $C_{t,i}$ the carbon cost, E_t is the amount of electricity produced, all evaluated in year t . Finally $(1+r)^{-t}$ is the discount factor and r the real discount rate for year t (inflation is neglected). The levelized cost method also neglects the presence of specific market or technology risks, so that the cost of electricity corresponds to the cost of an investor assuming the certainty of production and the stability of electricity price.

In order to allow comparisons between different electricity generation options unbiased by uncertainties on the future technology and national economy developments, COMESE can also provide the probability density function of the SLCOTE. In this case, $SLCOTE_y$ is computed as a function of a user-defined number of stochastic variables. Although in principle all the code variables can be consider random with a known probability distribution (uniform or triangular), the default stochastic parameters are those listed in the input file for the technologies, see the paragraph 3.12. The value of the $SLCOTE_y$ is then computed n times ($n = 10^4$ is default value of the random samplings) to get the corresponding probability distribution.

3.19 LCOTE calculation: extra cost due to the battery storage system

As presented in the storage batteries system description chapters 3.14 and 3.14 , the batteries storage system is based on batteries modules, the same logic is found for evaluation of extra cost due to the batteries storage system. Single module of batteries is characterized by operational and economic parameters, here it is summary the parameter used for the evaluation of the cost:

- The maximum power of the module $P_{\max module}$ [MW]
- The time for complete charge and discharge at maximum power $\Delta t_{storage}$ [h]
- The overnight cost of one module [€/kWh]
- The operative and maintenance cost of one module [€/kWh]

In COMESE code, it is used the overnight cost and the operative and maintenance cost express in [€/kW] obtain from the value in [€/kWh] simply multiplying the value for the $\Delta t_{storage}$

From the first generation for covering the demand analysis in COMESE code is determined the maximum level of energy stored in the batteries storage system along the year $E_{n \max stored}$ and the maximum power exchanged in the same year $P_{\max exchange}$. This information is used for the evaluation of the maximum number of module that composes the storage system. With equation 3.31 is evaluated the number of module needed for storing the maximum peak of energy and with the equation 3.32 the number of module needed for the required power level. The number of module installed for the system is the maximum value of the two rounded to the greater integer, equation 3.33.

$$(3.31) \quad nr_{moduleEn} = E_{n \max stored} / (P_{\max module} \cdot \Delta t_{storage})$$

$$(3.32) \quad nr_{moduleP} = P_{\max exchange} / P_{\max module}$$

$$(3.33) \quad nr_{moduleInstalled} = \max(nr_{moduleEn}, nr_{moduleP})$$

From the number of battery modules installed, it is calculate the capacity of the storage system as the product between the energy that can be stored in one module with the total number of module, equation 3.34.

$$(3.34) \quad Storage \ Capacity = nr_{moduleInstalled} \cdot (P_{\max module} \cdot \Delta t_{storage})$$

If in the COMESE code simulation, it is fixed a limit on the batteries storage system capacity, the result is that the number of module is fixed and the maximum power exchange by the system is determined by the time for complete charge and discharge specific by the type of module used.

The capital cost of one module is calculated with equation 3.35 where the interest on capital and the actualization factor is calculated as a common technology.

$$(3.35) \quad Capital \ Cost_u = (OvernightCost_u \cdot (1 + interest)) \cdot \frac{1}{f_{att}} \left[\frac{\text{€}}{kW} \right]$$

The cost of one module is now evaluated with the sum of capital cost and operative and maintenance cost, equation 3.36.

$$(3.36) \quad Cost \ of \ one \ module \left[\frac{\text{€}}{kW} \right] = Capital \ Cost_u \left[\frac{\text{€}}{kW} \right] + O\&M_u \left[\frac{\text{€}}{kW} \right]$$

$$(3.37) \text{ Cost of one module } [\text{€}] = \text{Cost of one module } \left[\frac{\text{€}}{\text{kW}} \right] \cdot P_u[\text{MW}] \cdot 1000$$

$$(3.38) \text{ Cost of storage battery system } [\text{€}] = \text{Cost of one module } [\text{€}] \cdot nr_{\text{moduleInstalled}}$$

From the cost of one module in $\left[\frac{\text{€}}{\text{kW}} \right]$ it is calculated first the cost in [€] of one module multiplying for the power of the module, equation 3.37 and then the cost of the complete system multiplying for the number of modules equation 3.38 . The extra cost due to battery storage system is finally calculated with the ratio between the cost of the system and total electricity demand of the scenario. See equation 3.39 . Where $C_{\text{addBattery}}$ is the extra cost due to batteries storage system in $\left[\frac{\text{€}}{\text{kWh}} \right]$

$$(3.39) C_{\text{addBattery}} \left[\frac{\text{€}}{\text{kWh}} \right] = \frac{\text{Cost of storage battery system } [\text{€}]}{\text{Total electricity demand } [\text{TWh}] \cdot 10^9}$$

Extra cost due to batteries storage system is simply added to the system levelized cost of timely electricity (SLCOTE), because it is just expressed in function of the total electricity demand. In particular, it is possible to observed that the contribute to the SLCOE of the batteries storage system for a fixed electricity demand is directly proportional to the capacity installed. Greater is the system greater is the impact of in the SLCOE.

3.20 Future improvement for COMESE code C++

As presented from the beginning COMESE code C++ were developed with the precise intention to have a computer tool flexible, made of different module, a code open to new improvements. Here they are listed some of the new improvements that could be added in the future.

A first improvement is that of providing COMESE with a graphical interface that allows an untrained user of advanced programming languages to be able to use it, without having to modify the source code. A second improvement can be added to the COMESE code the graphic libraries and the possibility to create the result graphs without the use of an external post-processing program.

Alternatively, two parallel programs could be created with a preprocessing program for the creation of input files and a post processing program for data processing, which could also be done in a different programming language such as Matlab. In this regard, a first version of post processing is already being realized in Matlab language.

A great improvement that could be added, starting from the results obtained with FRESCO, would be that of couple the COMESE code with a genetic algorithm that allows to perform optimization operations. This would allow us to perform a study to see which hypotheses are the best to create a scenario with a low SLCOTE.

From the point of view of possible simulations, the COMESE code has opened a door to numerous studies, which may derive from the simulation of scenarios with different technologies from those set, to the study of new storage systems, up to the verification of scenarios already studied with curves of generation and load updated.

Here a further development could be to add a module to be able to carry out a variation of the generation profile or of the load profile in order to study different configurations of the annual electricity demand. For example the study of scenarios in which the electric demand is modified by the introduction of electric mobility.

4 Simulation of European scenarios with COMESE

As a final result at the end of the design of the COMESE code C++, in this chapter the results obtained from the simulation of energy scenarios including the fusion technology at European level are collected. The question that leads to this first study on energy scenarios was to understand how fusion technology could enter an energy scenario and in particular at what cost level it could enter.

From current developments on renewable technologies, photovoltaic and wind technologies are experiencing a strong development in recent years also linked to incentives. Numerous studies are conducted on energy storage systems in support of these technologies. In the last year, the interest in the storage of electricity and renewable technologies is growing, and numerous solutions are proposed in this area, the last news a series of batteries the zinc-air batteries that promise to store the energy to competitive costs. If the fusion technology will be ready after 2050 and ready at a commercial level around 2080 under what conditions it can be competitive when compared with technologies such as photovoltaics and wind power that from now to 2050 will surely know a further development. It is a hard question to be answered.

Without the pretense of obtaining a definitive answer, with the COMESE code start from some first assumptions for the future were studied a lot of possible European scenarios and among these neither have been identified some 100% renewable scenarios in which to try to see the effects of the introduction of the fusion technology.

According to the current forecasts and international pledges on climate change, decarbonization of Energy is a must, almost worldwide; the European Union has adopted an Energy Road-map to 2050, setting 80% cut of Energy CO₂ emissions and fixing the ambitious target of fully decarbonizing EU electricity generation by 2050. The carbon free power generation technologies likely available by 2050 are: 1) fossil fueled power plants with Carbon Capture and Storage (CCS), 2) nuclear power plants (III+ and IV generation fission) 3) power plants using renewable energy sources.

The following assumptions hold:

- Fusion will be commercially available in the second half of this century (say 2080),
- The development of the fusion technology leads to a complete phase out from the fission power plants in Europe, with a gradual but decisive and planned way such that the nuclear energy if present is produced only by fusion plants.
- The CCS technologies will not be available so not included in the mix, since technology development and learning factor rate is nowadays lagging behind expectations.
- The renewable technologies experience a great development, considering a strong deployment of solar photovoltaic (PV) and wind plants, as indicated by national potential and the outstanding tariff reduction recently registered in national audition.
- The energy storage systems are available to manage the high variations of renewable sources, in order to store the excess energy and use it in the hours of maximum residual demand.

- Finally, dispatchable technologies cover the residual demand not satisfied by the other technologies like hydroelectric Dam and Bioenergy.

From this assumption with COMESE code, five possible European energy scenarios with and without fusion technology have been identified and simulated. Three energy scenarios for southern Europe based on the Italian load and generation profiles, which have photovoltaic as the most renewable technology. And two energy scenarios for northern Europe based on the UK load and power profiles, in which the wind energy technology plays a key role. For all the scenarios, an energy demand of 600 TWh was hypothesized.

Table 4-1: Scenarios for southern Europe

	South Europe					
	100% RES		Fusion - BaseLoad		Fusion - 2 seasons	
	[GW]	[TWh]	[GW]	[TWh]	[GW]	[TWh]
PV - commercial	230.4	277	63.4988	76	78.3333	94
PV - residential	58.83	70	16.2125	18.6	20	24
PV - utility scale	160.8	241	44.3141	67	54.6667	82
Wind onshore	23	43.68	23	43.68	23	43.68
Wind offshore	2	4.02	2	4.02	2	4.02
Dam hydro	12.8	28.899	12.8	31.38	12.8	31.38
Run of river hydro	8	35.4	8	35.4	8	35.4
Bioenergy	28.34	49.38	21.62	61.8	15	30.6
Municipal Waste Incinerator	1	7.02	1	7.02	1	7.02
Geothermal	1	7.86	1	7.86	1	7.86
Fusion			37.5	262.8	37.5	262.68
Total generation		764.259		615.56		622.64
Curtailed Energy		131.16		7.38		10.74
Charging/discharging losses		33.099		8.18		11.9
Pumped Hydro Storage	9	100	9	100	9	100
Battery Storage		1.2		0.4		0.5

In Table 4-1, they are presented the three energy scenarios studied for the south of Europe, a scenario 100% RES (renewable energy source) based on photovoltaic generation, and two energy scenarios which include fusion as a technology able to generate at least 44% of the total electricity demand. In the “Fusion – BaseLoad” scenario the fusion technology operate as a base power plant without any modulation in the year, in the “Fusion – 2 season” scenario is assumed that the fusion power plant operate with a two level profile like the one presented in Figure 3-62. Where it is assumed that all the maintenance for the power plants can be concentrated in the spring summer period, so that the reduced fusion generation can be balanced by increased photovoltaic generation.

In Table 4-2, they are presented the corresponding energy scenarios for the northern Europe, as for the south Europe, for the north Europe is created a 100% RES scenario based on wind onshore and offshore generation, and only one scenario with fusion technology able to generate at least 44% of the total electricity demand and operating as a based power plant. Given the high variability of wind generation, and the absence of a clear generation variation between winter and summer months, no

two-season scenario was simulated for the north Europe. In the last five lines of the Table 4-1 and Table 4-2 are summarized some of the result of the Generation-Demand analysis made in the first section of COMESE code, in particular it is worth noting the cut energy and the level of storage that are much higher for the south than northern Europe.

Table 4-2: Scenarios for northern Europe

North Europe				
	100% RES		Fusion - Baseload	
	[GW]	[TWh]	[GW]	[TWh]
PV - commercial				
PV - residential	10.0376	7.98	10.0376	7.98
PV - utility scale				
Wind onshore	12	30	12	30
Wind offshore	165	637	72.8947	287.02
Dam hydro				
Run of river hydro	1.85128	6	1.85128	6
Bioenergy	40.8975	40.92	39.63	40.38
Municipal Waste Incinerator	1	7.98	1	7.98
Geothermal				
Fusion			37.5	262.8
Total generation		729.88		642.16
Curtailed Energy		121.44		37.8
Charging/discharging losses		8.44		4.36
Pumped Hydro Storage	3	50	3	50
Battery Storage		1		0.4

4.1 The economic analysis with COMESE code

After the evaluation that the generation meet the demand for all the five scenarios with COMESE code are performed the economic analysis for the evaluation of the SLCOTE for all the five scenarios using the economic parameter for the scenarios presented in Table 4-3. In that table are collected Capital and O&M costs, lifetime, load factor, for all the technologies with the variation range for stochastic analysis. Equivalent generation hours are also provided for each technology, along with a trial calculation of the LCOTE in the best condition for all the technologies.

The stochastic analysis for the evaluation of the SLCOTE for the five electric systems was performed with a Monte Carlo Simulation of 500000 of sample and the probability distribution function obtain from the analysis are presented in Figure 4-1. It is possible to observe that the introduction of fusion power technologies with the economic parameter of table Table 4-3 allows to decrease the SLCOTE both of the north and the south European scenarios and the two European scenario with fusion as a baseload technologies have an SLCOTE values next to each other. The SLCOTE for all the scenarios with fusion varies between 8 and 11-12 c€/kWh.

Figure 4-3 presents how the LCOTE of the technologies contributes to the SLCOTE of the systems to note the noteworthy contribution to the cost given by bioenergy, the constant in the three scenarios given by the fusion technologies, and that of the storage systems comparable to that of other technologies.

Table 4-3: Capital and O&M costs, lifetime, load factor, levelized cost of electricity for the generation technologies considered

		Overnight cost [€/kW]	O&M costs		Lifetime [years]	Nominal Load hours		LCOE [c€/kWh]	
			FIX [€/kW y]	VAR [€/MWh]		NORD	SUD	NORD	SUD
Photovoltaic	Residential roof	1000 ±15%	20 ±15%		25 ±15%	800	1200	11.5	7.7
	Commercial roof	800 ±15%	20 ±12%		25 ±15%	800	1200	9.7	6.5
	Utility-tracking	800 ±15%	20 ±15%		25 ±15%	1100	1500	7.1	5.2
Wind	on shore	1100 ±20%	20 ±30%		25 ±15%	2500	1900	4	5.3
	near shore	2100 ±20%	30 ±30%		25 ±15%		2200		8.3
	off shore	1800 ±20%	50 ±30%		25 ±15%	3800		4.7	
Hydro	Run of River	3000 ±40%	80 ±30%	5	60 ±10%	3200	4500	8	6
Geothermal		3500 ±15%	80 ±25%		30 ±15%	7800	7800	4.3	4.3
Municipal Waste * ($\eta=30\%$)		4500 ±20%	130 ±25%	30	25 ±15%	7800	7800	0	0
Fusion		6000 ±30%	110		60	7000	7000	6.3	6.3
Dispatchable Energy	Dam Hydro	2500 ±40%	50 ±30%	5	60 ±10%		2500		8
	Bioenergy** ($\eta=33\%$)	3000 ±20%	100 ±25%	8	15 +35%	1000 - 3000			50-24
Storage	Pumped Hydro ($\eta=80\%$)	1500 ±40%	20 ±25%		60 ±10%				
	Batteries ($\eta=85\%$) (8 h storage)	750 ±20%	8 ±20%		10 ±25%				

* fuel cost is assumed as negative at -80 €/ton

** fuel cost 100 €/ton

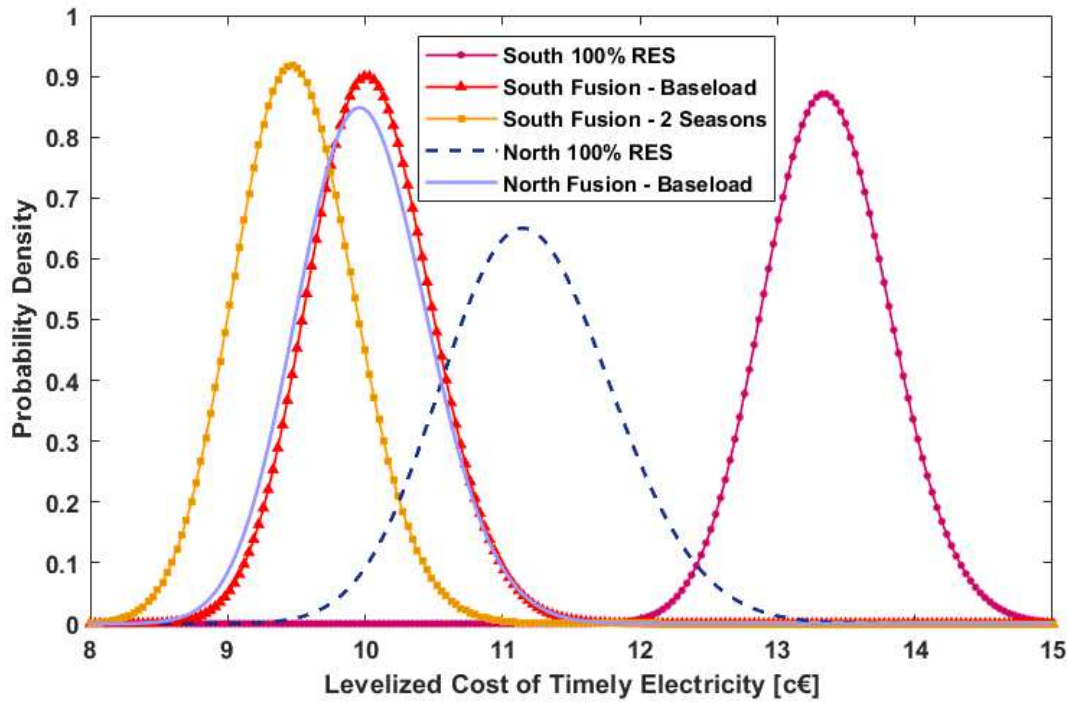


Figure 4-1: Probability distribution function for the stochastic analysis for the five European scenarios with and without fusion.

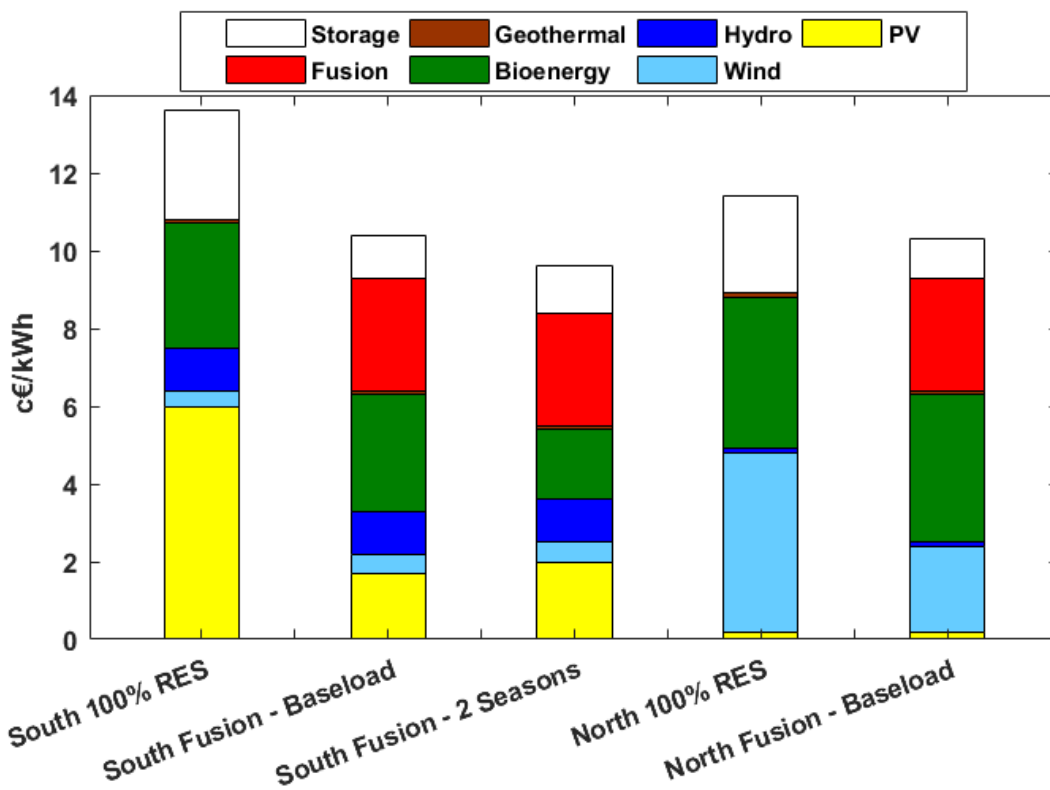


Figure 4-2: Cost items that compose LCOTE for the five simulated scenarios

4.2 Assessment of the economics of fusion technology

An independent chapter deserves the last analysis performed with the COMESE code, identified two 100% RES reference scenarios for southern Europe with lots of sun, and for northern Europe with wind, and calculated the SLCOTE for the two scenarios. It was decided, for the two fusion technology scenarios as a base technology, to change the overnight cost of the fusion technology and see to what extent it was possible to increase the overnight cost for the system's LCOTE to remain below the value of the scenarios 100% RES. The results of these simulation was presented in Figure 4-3, here it is possible to see that 100% RES scenarios for the north Europe are cheaper than the south one. The overnight cost limit for which the fusion technology can enter and play a positive effect on the SLCOTE of the scenario are around 8000 €/kW for the north Europe and 13000 €/kW for the south of Europe. High values when compared with that of Table 4-3 but accessible at the electrical system level.

Subject to the starting hypothesis, on which discussions and changes are possible, this result obtained thanks to the COMESE code is an example of how it is possible to study the economic conditions that allow the fusion technology to become part of a typical energy scene. This is the first example and in the future many other scenarios can be used. This first example opens the way to a many other scenarios and a more new simulations possible with the COMESE code.

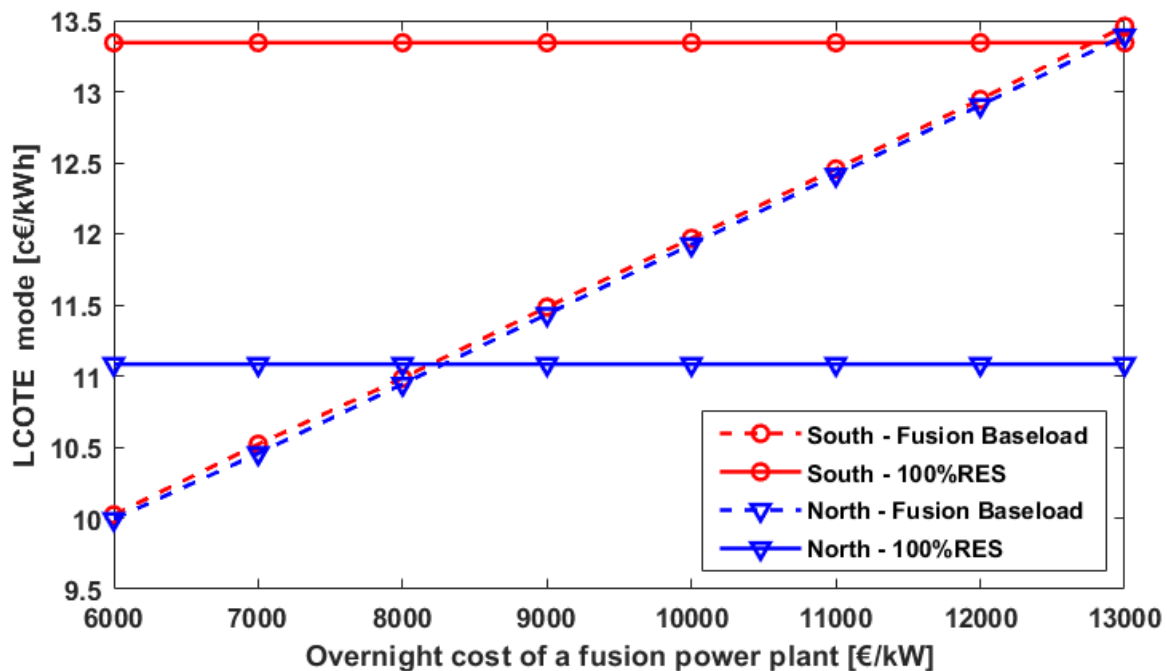


Figure 4-3: Assessment of the economics of fusion technology inside two possible European scenarios

5 Conclusion

In order to be able to evaluate how fusion technology can be part of a future electricity generation system, computer tools that can perform physical, engineering and economic analysis are indispensable. Codes that can be adapted to a constantly evolving field of study such as that of renewable energy and research on controlled thermonuclear fusion.

The doctoral activities started with the study and enhancement of the FRESCO code (Fusion REactor Simplified COst), a code written in C++ language with the aim to model in a simplified way a D-T fusion power plant based on the tokamak model. A computer tool where a power plant can be studied from technical and an economical point of view computing the reactor parameters i.e. geometrical and physical dimension of the power plant, electromagnetic parameters of the machine, net electricity production, auxiliary energy needed, the operative cycle phases especially for the pulse configuration, and not the last the related capital cost and the cost of electricity. FRESCO has been revised, rearranged and updated with new approaches that allow a better study of the economy of a fusion reactor. Completely new sections have been introduced, such as those for the evaluation of the pumping time to empty the vacuum vessel between one pulse and the next. The coupling to a genetic optimization algorithm has been a further improvement.

With the FRESCO code, as described in the paper “Economic assessment of different operational reactor cycle structures in a pulsed DEMO-like power plant”[125], an optimization analysis of the operative phases of a pulsed fusion power plant was performed. The different operating phases that compose the operative cycle have been optimized to get the minimum COE. The study made it possible to understand that by acting on the operating cycle phases for a pulsed fusion generator, it is possible to optimize the system cost and an absolute optimal solution does exist. The uncertainties on the costs and reliability of the components together with the uncertainty on financial aspects enlarge the estimate of the COE. The FRESCO code coupled to the genetic algorithm can now be used for optimization studies involving many other reactor parameters.

Next step in the thesis work was the creation of COMESE code C++, (COSto MEDio del Sistema Elettrico, Average Cost of the Electric System), a code developed with the aim to have a computer tool able to develop, study and test the sustainability of new future energy scenarios possibly including nuclear fusion power plants. The new version of COMESE looks as a flexible computer tool useful to better shape and study energy scenarios.

In the COMESE code C++ new modules have been included: a module to simulate the operation of an energy storage system, a module for the optimal use of dispatching systems, and a module that make storage systems and dispatching technologies working jointly. A routine for stochastic simulation based on the Monte Carlo method, which is able to vary any parameter of any technology has been also added.

With the COMESE code it was therefore possible to simulate European energy scenarios, for both southern Europe (largely based on photovoltaic technology) and for northern Europe (based on wind energy). The 100% renewable European reference scenarios highlight how a northern European scenario based on wind technology has lower costs than a south European based on photovoltaics and storage. Alternative scenarios have been produced by introducing the fusion technology. The results of

the analysis demonstrate that an overnight cost limit for a fusion power plant exists such that, under this value, the power plant has a positive effect on the cost of generating the system (cost reduction), above it the situation would be worse.

Concluding the improvement of the FRESCO code and the development of COMESE code C++ has opened a door to numerous studies and numerous possibilities and future research activities. Coupling COMESE to a genetic algorithm for optimization, studying scenarios of different world countries, using the cost of generation obtained in COMESE code like the objective cost for the FRESCO code optimization analysis are examples of new future studies.

6 Reference

- [1.] IEA, "World Energy Outlook 2017 - Executive Summary" available at:
<https://www.iea.org/Textbase/npsum/weo2017SUM.pdf>, 2018
- [2.] FATIH, Birol. World energy outlook 2015. *Organisation for Economic Co-Operation and Development (OECD): Paris, France, 2015.*
- [3.] IEA, «World Energy Outlook 2014 - Executive Summary - Italian version,» 2014,
http://www.iea.org/bookshop/477-World_Energy_Outlook_2014.
- [4.] C. Lombardi, Impianti nucleari, Milano: Polipress, 2009, pp. Capitolo 1-2-7.
- [5.] ONGENA, Jef; OGAWA, Yuichi. Nuclear fusion: Status report and future prospects. *Energy Policy*, 2016, 96: 770-778.
- [6.] <https://www.yes-energy-europe.com/>, 2018
- [7.] "Future of Energy by Young leaders for Energy and Sustainability 2018", available at:
<https://zenodo.org/record/1215680#.WtqYVVMvz4M>, 2018
- [8.] COMMISSIONE EUROPEA. *Energy roadmap 2050*. Publications Office of the European Union, 2012.
- [9.] Wendelstein 7-X, <https://www.ipp.mpg.de/16900/w7x>,
- [10.] Introduction – the Wendelstein 7-X stellarator,
<https://www.ipp.mpg.de/16931/einfuehrung>,
- [11.] Kyle Maxey, Stellarators Back Online After Decades in the Dark, 30 maggio 2014,
<http://www.engineering.com/DesignerEdge/DesignerEdgeArticles/ArticleID/7657/Stellarators-Back-Online-After-Decades-in-the-Dark.aspx>,
- [12.] World's Largest Fusion Experiment Of The Stellarator Type -- Wendelstein 7-X -- Taking Shape, <http://www.sciencedaily.com/releases/2008/03/080313124448.htm>,
- [13.] New Energy and Fuel, What is a Stellarator?, 18 marzo 2008,
<http://newenergyandfuel.com/http://newenergyandfuel.com/2008/03/18/what-is-a-stellarator/>,

- [14.] Stellarator Cutaway View,
<http://newenergyandfuel.com/http://newenergyandfuel/com/2008/03/18/what-is-a-stellarator/stellarator-cutaway-view/>
- [15.] ITER Organization ,Milestones in the History of the ITER Project,
<http://www.iter.org/proj/itermilestones>, 2018
- [16.] E.S.A., http://www.esa.int/images/soho_1,2.jpg.
- [17.] OECD/IEA, «Signs of stress must not be ignored, IEA warns in its new World Energy Outlook,», <http://www.iea.org/newsroomandevents/pressreleases/2014/november/signs-of-stress-must-not-be-ignored-iea-warns-in-its-new-world-energy-outlook.html>.
- [18.] A. E.-E. s. F. Consorzio RFX, Fisica e ingegneria della fusione: la ricerca verso una nuova fonte di energia.
- [19.] <https://www.igi.cnr.it/>, 2018
- [20.] https://it.wikipedia.org/wiki/Metodo_Monte_Carlo, 2018
- [21.] <https://www.iter.org/>, 2018
- [22.] <http://www.ccfе.ac.uk/glossary.aspx#F>, 2018
- [23.] <http://fusionforenergy.europa.eu/understandingfusion/broaderapproach.aspx>, 2018
- [24.] <https://scripps.ucsd.edu/programs/keelingcurve/2018/05/02/carbon-dioxide-in-the-atmosphere-hits-record-high-monthly-average/> ,2018
- [25.] WESSON, John; CAMPBELL, David J. *Tokamaks*. Oxford University Press, 2011.
- [26.] Bustreo, C. et al., The Monte Carlo approach to the economics of a DEMO-like power plant, *Fusion Engineering and Design* 98–99 (2015) 2108–2111
- [27.] BUSTREO, C., et al. FRESCO, a simplified code for cost analysis of fusion power plants. *Fusion Engineering and Design*, 2013, 88.12: 3141-3151.
- [28.] TROYON, F., et al. Beta limit in tokamaks. Experimental and computational status. *Plasma Physics and Controlled Fusion*, 1988, 30.11: 1597.
- [29.] BOSCH, H.-S.; HALE, G. M. Improved formulas for fusion cross-sections and thermal reactivities. *Nuclear fusion*, 1992, 32.4: 611.

- [30.] ITER Physics Expert Group on Disruptions, Plasma Control, MHD, Energetic Particles, Heating and Current drive, Diagnostic, et al., Nuclear Fusion 39 (1999) 2577
- [31.] WYKES, M., et al. Assessment of the ITER dwell pump-down. In: Fusion Engineering 2005, Twenty-First IEEE/NPS Symposium on. IEEE, 2005. p. 1-4.
- [32.] BATTES, Katharina; DAY, Christian; ROHDE, Volker. Basic considerations on the pump-down time in the dwell phase of a pulsed fusion DEMO. Fusion Engineering and Design, 2015, 100: 431-435.
- [33.] KOVARI, M.; CLARKE, R.; SHEPHARD, T. Compound cryopump for fusion reactors. Fusion Engineering and Design, 2013, 88.12: 3293-3298.
- [34.] EHST, David A. Tokamak power plant burn cycle options. Fusion technology, 1994, 26.3P2: 1133-1140.
- [35.] TODD, T. N. Pulsed DEMO design assessment studies. Fusion Science and Technology, 2013, 64.2: 76-85.
- [36.] DUCHATEAU, J. L.; HERTOUT, P.; JOHNER, J. Discussion about the size of a future fusion demonstration reactor: the impact of the toroidal magnetic field. IEEE Transactions on Applied Superconductivity, 2007, 17.2: 1342-1347.
- [37.] ZOHM, Hartmut. Assessment of DEMO challenges in technology and physics. Fusion Engineering and Design, 2013, 88.6-8: 428-433.
- [38.] FEDERICI, G., et al. Overview of EU DEMO design and R&D activities. Fusion Engineering and Design, 2014, 89.7-8: 882-889.
- [39.] TODD, T. N., et al. The Key Impacts of Pulsed Operation on the Engineering of DEMO. 2010.
- [40.] BARANA, Oliviero, et al. Conceptual design of a generic pulse schedule and event handling editor for improved fusion device operation. Fusion Engineering and Design, 2013, 88.6-8: 1078-1081.
- [41.] HARRINGTON, C. Dynamic modelling of balance of plant systems for a pulsed DEMO power plant. Fusion Engineering and Design, 2015, 98: 2147-2151.

- [42.] DEMO1 – pulsed power plant with conservative technology, PROCESS 382 : Run on Thu Apr 16 16:10:11
- [43.] BST 2015 by Richard Kemp Reactor concept design: Pulsed tokamak model, (c) CCFE; Available on: <http://www.ccf.ac.uk/powerplants.aspx>
- [44.] Sattin, F. et al., Difficulties and solutions for estimating transport by perturbative experiments, *Plas. Phys. Contr. Fusion* 56 (2014) 114008
- [45.] Bubelis, E. et al., Final Report on Deliverable Conceptual Design Definition for an Intermediate Cooling Loop Configuration and Coolant, 2014, EFDA_D_2HDVN9
- [46.] Vincenzi, P. et al., EU DEMO transient phases: main constraints and heating mix studies for ramp-up and rampdown, 2016, 29th SOFT, P4.19.
- [47.] W.R. Spears, The SCAN-2 cost model, EUR-FU/XII- 80/86/62, 1986.
- [48.] R. Storn, K. Price, Differential Evolution – A Simple and Efficient Heuristic for global Optimization over Continuous Spaces, *Journal of Global Optimization* 11 (1997) 341-359
- [49.] Projected Costs of Generating Electricity, 2010 Edition, OECD Publications, Paris, 2010.
- [50.] D. Maisonnier, I. Cook, P. Sardain, L. Boccaccini, E. Bogusch, K. Broden, et al., The European power plant conceptual study, *Fusion Engineering and Design* 75–79 (2005) 1173–1179.
- [51.] F. Najmabadi, R.W. Conn, The ARIES team, The ARIES-III D-3He Tokamak Reactor Study – Final Report, Report UCLA-PPG-1384, University of California, Los Angeles, 1992.
- [52.] W.R. Spears, The SCAN-2 cost model, EUR-FU/XII-80/86/62, 1986.
- [53.] HAN, W. E., et al. Start-up requirements and current-drive issues for a pulsed DEMO, and potential implications for power output to the grid. *Fusion Engineering and Design*, 2013, 88.6-8: 994-997.
- [54.] LI-PUMA, A., et al. Consistent integration in preparing the helium cooled lithium lead DEMO-2007 reactor. *Fusion Engineering and Design*, 2009, 84.7-11: 1197-1205.

- [55.] [IEA, 2010] Philibert, C., Technology roadmap: concentrating solar power, OECD/IEA, 2010.
- [56.] DUNN, William L.; SHULTIS, J. Kenneth. *Exploring monte carlo methods*. Elsevier, 2011.
- [57.] BUDISCHAK, Cory, et al. Cost-minimized combinations of wind power, solar power and electrochemical storage, powering the grid up to 99.9% of the time. *Journal of Power Sources*, 2013, 225: 60-74.
- [58.] IBRAHIM, Hussein; ILINCA, Adrian; PERRON, Jean. Energy storage systems—characteristics and comparisons. *Renewable and sustainable energy reviews*, 2008, 12.5: 1221-1250.
- [59.] BUSTREO, Chiara, et al. Energy and environmental observatory. The Italian National Energy Strategy: a critical view of the power sector. *ECONOMICS AND POLICY OF ENERGY AND THE ENVIRONMENT*, 2013.
- [60.] ARTIOLI, C., et al. Una mappa delle emissioni specifiche e del costo medio di generazione di diversi mix elettrici. Report RdS/2013/062, Ricerca di Sistema Elettrico, 2013.
- [61.] CABAL, H., et al. Fusion power in a future low carbon global electricity system. *Energy Strategy Reviews*, 2017, 15: 1-8.
- [62.] VITHAYASRICHAREON, Peerapat; MACGILL, Iain F. A Monte Carlo based decision-support tool for assessing generation portfolios in future carbon constrained electricity industries. *Energy policy*, 2012, 41: 374-392.
- [63.] HONG, Sanghyun; QVIST, Staffan; BROOK, Barry W. Economic and environmental costs of replacing nuclear fission with solar and wind energy in Sweden. *Energy Policy*, 2018, 112: 56-66.
- [64.] HEIDE, Dominik, et al. Reduced storage and balancing needs in a fully renewable European power system with excess wind and solar power generation. *Renewable Energy*, 2011, 36.9: 2515-2523.

- [65.] FOXON, Timothy J. Transition pathways for a UK low carbon electricity future. *Energy Policy*, 2013, 52: 10-24.
- [66.] MARSEGUERRA, Marzio; ZIO, Enrico. Algoritmi Genetici e Monte Carlo: un Connubio promettente per l'Ottimizzazione di Progetto e Gestione Logistica d'Impianto. In: *Atti del Convegno Nazionale per la Valutazione e Gestione Del Rischio Negli Insediamenti Civili ed Industriali*, 24-26 ottobre 2000. 2000. p. 1-1.
- [67.] CANTONI, Matteo; MARSEGUERRA, Marzio; ZIO, Enrico. Genetic algorithms and Monte Carlo simulation for optimal plant design. *Reliability Engineering & System Safety*, 2000, 68.1: 29-38.
- [68.] EUROPEA, Commissione. Comunicazione della Commissione al Parlamento Europeo, al Consiglio, al Comitato economico e sociale europeo e al Comitato delle Regioni. *Tabella di marcia verso un'Europa efficiente nell'impiego delle risorse*, COM (2011), 2011, 571.
- [69.] CHIODI, Alessandro, et al. Modelling Electricity Generation-Comparing Results: From a Power Systems Model and an Energy Systems Model. 2014.
- [70.] BRADSHAW, Alexander Marian; HAMACHER, Thomas; FISCHER, Ulrich. Is nuclear fusion a sustainable energy form?. *Fusion Engineering and Design*, 2011, 86.9-11: 2770-2773.
- [71.] HAMACHER, Thomas, et al. Nuclear fusion and renewable energy forms: Are they compatible?. *Fusion Engineering and Design*, 2013, 88.6-8: 657-660.
- [72.] TAKEDA, Shutaro, et al. Limitation of fusion power plant installation on future power grids under the effect of renewable and nuclear power sources. *Fusion Engineering and Design*, 2016, 109: 1754-1758.
- [73.] CHUYANOV, V. A.; GRYAZNEVICH, M. P. Modular fusion power plant. *Fusion Engineering and Design*, 2017, 122: 238-252.

- [74.] CAU, Giorgio; COCCO, Daniele; TOLA, Vittorio. Analisi dell'integrazione di impianti a vapore Ultra Supercritici (USC) dotati di tecnologia CCS e sistemi solari a concentrazione. 2014.
- [75.] MARCHITELLI, VIVIANA. Valutazione tecnico-economica sull'applicazione delle tecnologie CCS (Carbon Capture and Storage) ad impianti termoelettrici a carbone. 2012.
- [76.] BRADBURY, Kyle. Energy storage technology review. *Duke University*, 2010, 1-34.
- [77.] PARLAMENTARE, Audizione. Strategia Energetica Nazionale 2017.
- [78.] "SEN 2017 – Documento di consultazione", 12nd June 2017
- [79.] CARLSSON, J., et al. ETRI 2014-Energy technology reference indicator projections for 2010-2050. *European Commission, Joint Research Centre, Institute for Energy and Transport, Luxembourg: Publications Office of the European Union*, 2014.
- [80.] MARCHESI, R., et al. Costi di produzione di energia elettrica da fonti rinnovabili. report published by Energy Department of Polytechnic of Milan and commissioned by AEEG Italian Authority for electricity, gas and water system, 2010.
- [81.] SULL'ENERGIA, RIFLESSIONI. Energia elettrica, anatomia dei costi. 2014.
- [82.] <http://www.irena.org/>, 2018
- [83.] <http://www.irena.org/publications%20>, 2018
- [84.] <http://www.world-nuclear.org/information-library/economic-aspects/economics-of-nuclear-power.aspx>, 2018
- [85.] <https://www.entsoe.eu/data/data-portal/>, 2018
- [86.] <https://transparency.entsoe.eu/>, 2018
- [87.] <https://data.open-power-system-data.org/>, 2018
- [88.] https://data.open-power-system-data.org/time_series/2018-03-13/, 2018
- [89.] <https://www.pvaustria.at/daten-fakten/>, 2018
- [90.] <http://publications.europa.eu/code/it/it-370100.htm>, 2018
- [91.] <https://www.terna.it/>, 2018
- [92.] <https://www.terna.it/it-it/sistemaelettrico/statisticheeprevisioni/datistatistici.aspx>, 2018

- [93.] <https://www.terna.it/it-it/sistemaelettrico/transparencyreport/load.aspx>, 2018
- [94.] <https://www.gse.it/>, 2018
- [95.] <http://www.rse-web.it/home.page>, 2018
- [96.] http://www.rse-web.it/temi.page?RSE_originalURI=/temi/sottotema/documenti/4&objId=1&typeDesc=Rapporto&RSE_manipulatePath=yes&docIdType=1&resultList=yes&country=ita, 2018
- [97.] <http://www.rse-web.it/colloquia/Decarbonizzazione-dell-rsquoeconomia-italiana--ndash-Scenari.page>, 2018
- [98.] <http://minihydro.rse-web.it/Links/Links.asp>, 2018
- [99.] <https://iea-etsap.org/>, 2018
- [100.] <https://www.gov.uk/government/publications/the-carbon-plan-reducing-greenhouse-gas-emissions--2>, 2018
- [101.] <https://www.lazard.com/>, 2018
- [102.] <https://www.lazard.com/media/2391/lazards-levelized-cost-of-storage-analysis-10.pdf>, 2018
- [103.] <https://www.lazard.com/perspective/levelized-cost-of-storage-analysis-20/>, 2018
- [104.] <https://www.qualenergia.it/articoli/20150325-batterie-al-lito-calo-prezzi-oltre-le-previsioni-siamo-ai-livelli-previsti-il-2020/>, 2018
- [105.] <http://large.stanford.edu/courses/2014/ph240/galvan-lopez2/>, 2018
- [106.] <https://www.iea.org/>, 2018
- [107.] <https://www.iea.org/statistics/resources/unitconverter/>, 2018
- [108.] <http://report.eni.com/factbook-2013/it/tavole/tabella-di-conversione-dell-energia.html>, 2018
- [109.] <http://www.conversion-website.com/conversions/index.html>, 2018
- [110.] <https://www.unitjuggler.com/convert-energy-from-boe-to-kgSKE.html>, 2018
- [111.] <https://www.indexmundi.com/commodities/glossary/mmbtu>, 2018

- [112.] <https://medium.com/@Jorisvandorp/how-much-would-a-100-nuclear-energy-system-cost-3dd7703dd5d3>, 2018
- [113.] <https://cleantechnica.com/2018/05/16/controllable-renewable-power-plants-are-a-good-alternative-to-new-nuclear-power-in-eastern-europe/>, 2018
- [114.] <http://www.greenreport.it/news/energia/strategia-energetica-nazionale-greenpeace-wwf-bene-chiusura-anticipata-carbone-poca-ambizione-sul-resto/>, 2018
- [115.] <http://www.greenpeace.org/italy/it/System-templates/Search-results/?all=scenari%20energetici>, 2018
- [116.] https://www.analisiaziendale.it/il_costo_medio_ponderato_del_capitale_wacc_200001_5.html, 2018
- [117.] MAGGIO, Daniele. Modelli numerici di simulazione del sistema di accelerazione elettrostatica di fasci di particelle per iniettori di neutri e studi parametrici preliminari. 2015, (<http://tesi.cab.unipd.it/49255/>)
- [118.] BUSTREO, Chiara. The role of fusion in long term scenarios. 2012. (<http://paduaresearch.cab.unipd.it/4927/>)
- [119.] DI VIETRO, Francesco. Un codice per il calcolo stocastico del costo medio di generazione di un kWh in un sistema elettrico. 2016. (<http://tesi.cab.unipd.it/52841/>)
- [120.] DEITEL, Harvey M.; DEITEL, Paul J. C++. *Fondamenti di programmazione*. Maggioli Editore, 2013.
- [121.] DEITEL, Harvey M.; DEITEL, Paul J. C++. *Tecniche avanzate di programmazione* 2° ed. Maggioli Editore, 2014
- [122.] <http://www.cplusplus.com/>, 2018
- [123.] <http://www.dis.uniroma1.it/~liberato/struct/mempunt/index.shtml>, 2018
- [124.] <http://www.bo.cnr.it/corsi-di-informatica/corsoCstandard/Lezioni/24Alldinamica.html>, 2018
- [125.] Master in Calcolo Scientifico. Laboratorio di Visualizzazione. Grafica in Matlab, available at:

<https://docplayer.it/5701250-Master-in-calcolo-scientifico-laboratorio-di-visualizzazione-grafica-in-matlab.html> ,2018

- [126.] Bustreo, C., Maggio, D., Auriemma, F., & Zollino, G. (2017). Economic assessment of different operational reactor cycle structures in a pulsed DEMO-like power plant. *Fusion Engineering and Design*, 124, 1219-1222.
- [127.] “Long Term Scenarios for Power Generation in Italy”, AIV XXIII Conference, Firenze 5th -7th April 2017.
- [128.] Bustreo, C., Giuliani, U., Maggio, D. & Zollino, G. How fusion power can contribute to a fully decarbonized European power mix after 2050. *Fusion Engineering and Design*, status: submitted

